IRIDIUM CATALYZED BORATION OF DIHYDROISOQUINOLINE DERIVATIVES

A Thesis Submitted to the
Graduate School of Engineering and Sciences of
İzmir Institute of Technology
in Partial Fulfillment of the Requirements for the Degree of

MASTER OF SCIENCE

in Chemistry

by
Ece YAZICI

July 2022
İZMİR

ACKNOWLEDGEMENTS

During my MSc studies, there are many people to thank. First of all, I would like to thank my advisor Prof. Dr. Levent ARTOK. This thesis could not have been written without him who not only served as my supervisor but also showed encouragement and challenged me not only throughout this study but also in my life. He patiently guided me through the evaluation period of the thesis, never accepting less than my best efforts.

I also would like to thank Dr. Melih Kuş as a mentor for sharing all this knowledge with me and improving my chemistry skills.

I am expressing my warmest thanks to all the laboratory members of the Artok research group, Yasemin BİLGİ, Ferit BEGAR, Nedim Buğra GÖDE, Gamze EKİYORUM, Cenk OMUR, Kardelen AYTEKİN, Yağmur Damla AYDEMİR who helped me with my works as my colleagues and friends. I would like to extend special thanks to Yasemin BİLGİ for her support, help and friendship in all matters during my thesis studies.

I would thank Prof. Dr. Canan VARLIKLI for Glovebox equipment and also Prof. Dr. Durmuş ÖZDEMİR for GC analysis.

Special thanks to Dr. Onur BÜYÜKÇAKIR and Prof. Dr. Derya GÜLCEMAL participating as committee member.

I would like to express my thanks to best friends Melis YALÇIN, Kısmet Tuğçe ERDEMLİ, Mustafa ERDOĞMUŞ and Ahmet Salih ÜNAL. They have always been by my side whenever I needed them. I would especially like to thank, Mehmet Anıl ARAPOĞLU for loving me unconditionally and for his everlasting encouragement.

Finally, I am deeply appreciated to my mother Saniye YAZICI and my father Osman YAZICI and my brother Erhan YAZICI for their continuous support, encouragement and prayers throughout my entire life. I would like to thank my little nephews, Cihan YAZICI and Osman YAZICI for being my motivation source.

At last, I would like to thank The Scientific and Technological Research Council of Turkey (TUBITAK-218Z075), TÜBİTAK (121Z535) and TENMAK Boron Research Institute (BOREN-2019-31-06-95-007) for financial support.

ABSTRACT

IRIDIUM CATALYZED BORATION OF DIHYDROISOQUINOLINE DERIVATIVES

Transition metal catalyzed borylation reactions have an important place in organometallic chemistry. In recent years, these reactions have been extensively investigated and have become a versatile tool in the synthesis of new organic materials. C-H bonds can be easily transformed into C-B bonds by borylation reactions.

In particular, iridium-catalyzed borylation includes significant advances such as mild reaction conditions, additive-free, high efficiency and being in a single step. In this thesis, the borylation of dihydroisoquinolines with a wide range of biological properties was performed for the first time. Investigating the extent of the reaction has led to the development of optimization studies. Besides, the effects of steric and electronic factors on selectivity are also shown.

In this new methodology, C3-borylated products with high regioselectivity and yield were formed with the directing effect of the acyl group. The use of $AsPh_3$ as a ligand is critical to the product selectivity of the method. When the reagent scope was investigated, it was determined that the functional group tolerance of the reactions was quite high.

Finally, borylated dihydroisoquinolines have been converted into various intermediates by application studies.

ÖZET

DİHİDROİZOKİNOLİN TÜREVLERİNİN İRİDYUM KATALİZLİ BORASYONU

Geçiş metali katalizli borilasyon reaksiyonları organometalik kimyada önemli bir yere sahiptir. Son yıllarda, bu reaksiyonlar kapsamlı bir şekilde araştırılmış ve yeni organik malzemelerin sentezinde çok yönlü bir araç haline gelmiştir. C-H bağları, borilasyon reaksiyonları ile kolayca C-B bağlarına dönüştürülebilmektedir.

Özellikle iridyum katalizli borilasyon, ılıman reaksiyon koşulları, katkısız, yüksek verimli ve tek adımda olması gibi önemli gelişmeler içermektedir. Bu tezde ilk kez geniş biyolojik özelliklere sahip dihidroizokinolinlerin borilasyonu gerçekleştirilmiştir. Reaksiyonun kapsamının araştırılması optimizasyon çalışmalarının geliştirilmesine yol açmıştır. Ayrıca sterik ve elektronik faktörlerin seçicilik üzerindeki etkileri de gösterilmiştir.

Bu yeni metodolojide açil grubunun yönlendirici etkisi ile regio seçimli ve yüksek verimde C3-borillenmiş ürünler oluşturulmuştur. $AsPh_3$ bileşiğinin bir ligand olarak kullanılması, yöntemin ürün seçimliliği açısından kritik öneme sahiptir. Reaktif kapsamı araştırıldığında, reaksiyonların fonksiyonel grup toleransının oldukça yüksek olduğu belirlenmiştir.

Son olarak, borillenmiş dihidroizokinolinlerin uygulama çalışmaları ile çeşitli ara ürünlere dönüştürülmüştür.

TABLE OF CONTENTS

LIST OF FIGURES

Figure **Page**

Figure **Page**

LIST OF TABLES

Figure **Page**

LIST OF ABBREVIATIONS

Ac	Acetyl	MTBE	Methyl tertiary-butyl ether
N.D.	Not determined	NMR	Nuclear Magnetic Resonance
$AsPh_3$	Triphenylarsine	NOE	Nuclear Overhauser Effect
BOC	Di-tert-butyl dicarbonate	NOESY	Nuclear Overhauser Spectroscopy
Bpin	Bis(pinacolato)diboron	*o*	Ortho
COSY	Correlated Spectroscopy	ON	Overnight
DCM	Dichloromethane	*p*	Para
DDQ	2,3-Dichloro-5,6-dicyano-dicyano-1,4-benzoquinone	Piv	Pivaloyl chloride
Dtbpy	4,4'-Di-tert-butyl-2,2'-bipyridine	PPh_3	Triphenylphosphine
EtOAc	Ethyl acetate	Ppm	parts per million
Eq	Equivalent	RT	Room Temperature
GC	Gas Chromatography	T	Time
g	Gram	THF	Tetrahydrofuran
HBpin	Pinacolborane	TLC	Thin Layer Chromatography
HMBC	Heteronuclear Multiple Bond Correlation	µL	Microliter
h	Hour		
Me	Methyl		
mg	Milligrams		
min	Minute		
mL	Milliliter		
mmol	Millimoles		
MS	Mass Spectrometry		

CHAPTER 1

INTRODUCTION

Isoquinoline is a heterocyclic aromatic compound also known as the structural isomer of quinoline, formed by joining a benzene ring to a pyridine ring. It was discovered in bone tissue and isolated as the sulfate salt from coal-tar by Hoogewerf and van Dorp in 1885.[1] Isoquinoline and its derivatives are the primary organic motifs present in different structural diversity in natural alkaloid structures (Figure 1.1). Among the various biological activities of these compounds, there are those with antimalarial, anti-HIV, and antileukemic effects.[2] In the industrial field, isoquinoline is used as a chiral ligand for metal-catalyzed syntheses.[3-5]

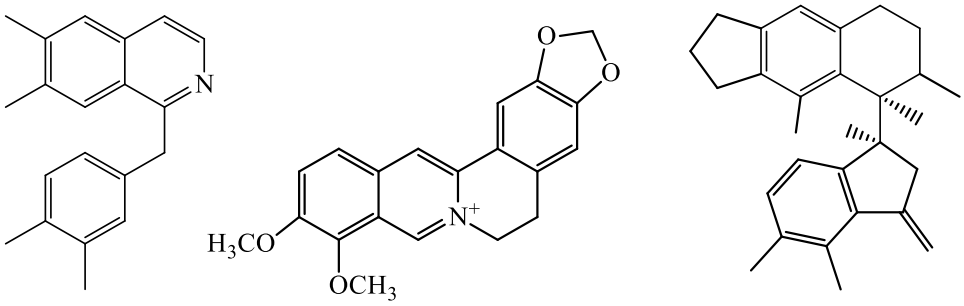

Papaverine (antispasmodic drug) | Berberine (antidiabetic) | Noscapine (antitussive effect)

Figure 1.1. Biologically active natural isoquinoline alkaloids.

In modern organic chemistry, boron is significant for synthesis routes and functional materials.[6-8] Organoboron structures containing at least one carbon-boron bond are classified as boranes, borinic acids and esters, boronic acids and esters, boronamides, boryl anions, and borate anions (Figure 1.2). Boronic acids, borate esters, and trifluoroborate salts are used as essential intermediates in various cross-coupling reactions.[9] The addition of convertible functional groups to organoboron compounds leads to the development of new stereoselective methodologies.[10]

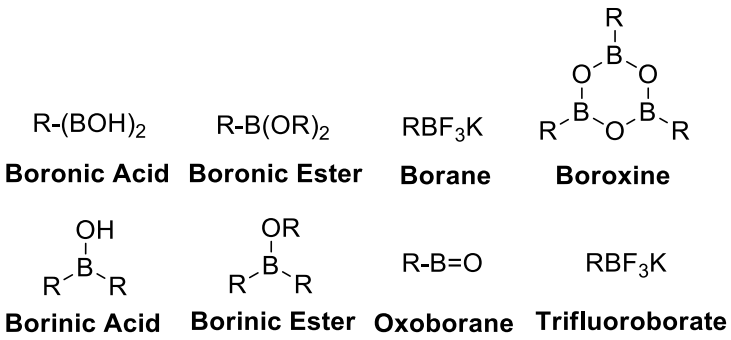

Figure 1.2. Organoboron derivatives.

The metal-catalyzed C-H borylation reaction is the formation of organoboron structures by direct conversion a C-H bond to a C-B bond without substrate pre-activation.[11] Boronic acid and boronic esters are boryl groups that are usually added to organic compounds by borylation processes.[12] Iridium-catalyzed borylation processes have been studied in recent years. Effective techniques have been created for the functionalization of C-H bonds. This approach may be more helpful than typical borylation procedures, as it uses affordable and abundant hydrocarbon starting material, restricts pre-functionalized organic molecules, and reduces toxic by-products.[13, 14] The regioselectivity of heteroarene C-H borylation is hard to predict and interpret. Heteroarene borylation can be controlled by steric factors, but its regioselectivity is difficult to interpret.[15]

In this thesis, the synthesis of boron-functionalized dihydroisoquinoline compounds is aimed. Selective borylation of electron-deficient heterocycles such as quinoline has been studied in the literature, but there are no studies on dihydroisoquinolines. This study presented the iridium-catalyzed regioselective C-3-borylation of dihydroisoquinoline and its derivatives. The developed strategy can be used as a general method for the borylation of cyclic and heterocyclic structures.

CHAPTER 2

LITERATURE WORKS

2.1. C-H Borylation

Iridium-catalyzed C–H borylation of arenes has become a popular method for functionalizing arenes because of its ability to generate versatile aryl organoboronate esters intermediate without using the reactive groups.[16] Understanding how heteroarenes are borylated could lead to a more efficient derivatization of more complex and prominent compounds and natural products. Under mild circumstances, Ishiyama, Miyaura, and Hartwig[17, 18], Smith[19], and Marder[20], and their colleagues showed that an Ir-complex could be used to borylate aromatic C-H bonds (Figure 2.1).

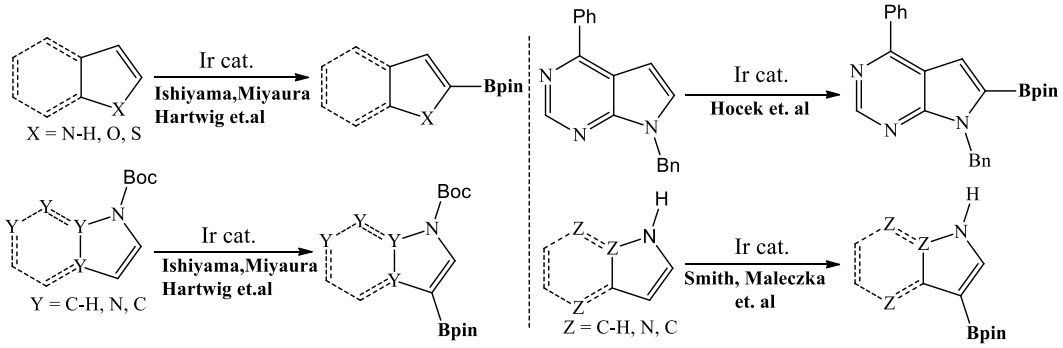

Figure 2.1. Iridium-catalyzed borylation of heteroarene examples.

The first reported examples of catalytic C-H borylation of aromatic structures [Cp*Ir(PMe_3)(H)(Bpin)] (Figure 2.2).[21] However, since this process has drawbacks such as elevated temperatures, high catalyst loadings, long reaction times, and law chemical selectivities, subsequent studies have been conducted to solve these problems.

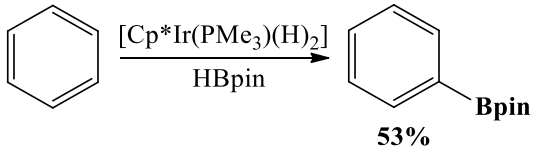

Figure 2.2. First catalytic borylation.

In 2002, Smith and colleagues avoided selectivity issues while producing in situ phosphine-ligated iridium complexes that could catalyze borylation reactions under milder conditions (Figure 2.3a). This improved method eliminated the need for boryl complexes, which are expensive and difficult to synthesize. Application studies of this reaction are showed in the first reported one-pot borylation/Suzuki-Miyaura cross-coupling protocol (Figure 2.3b).[14]

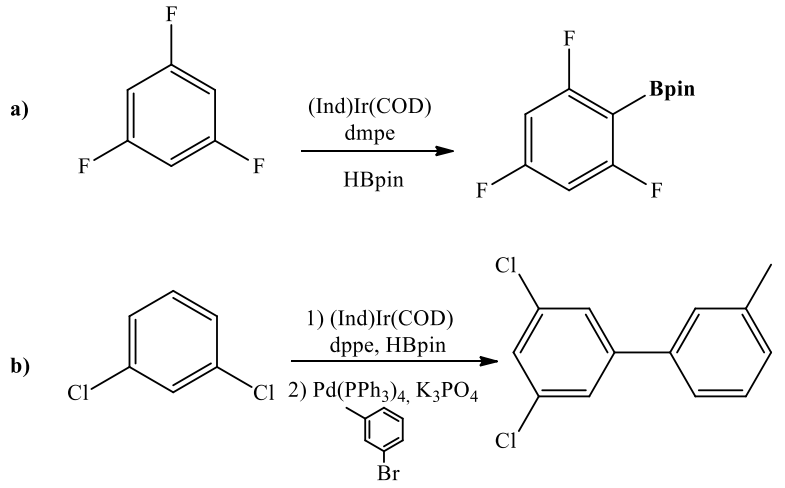

Figure 2.3. Phosphine-ligated Ir complex catalyzed borylation.

Hartwig and colleagues reported borylation reactions with higher turnover numbers than before observed with in situ generated bipyridine-ligated iridium complexes. The same group investigated that the most effective iridium catalyst combinations are alkoxy-iridium complex and bipyridine ligands containing electron-donating substituents (Figure 2.4a). This process is the first reported aromatic C-H borylation performed at room temperature. (Figure 2.4b).[22]

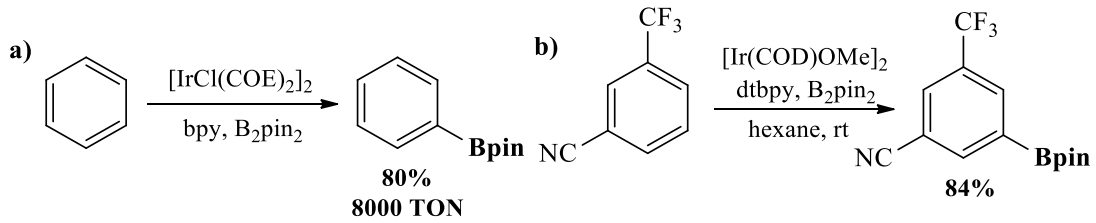

Figure 2.4. Bipyridine-ligated Ir complex catalyzed borylation.

An exciting aspect of iridium-catalyzed C-H borylation is the experimental simplicity of pre-mixing the pre-catalyst, ligand, and bis-boryl reagent that produces the active catalyst in situ. The combination of $[Ir(COD)OMe]_2$ and dtbpy is still the most

used catalytic system. The latest findings of Smith, Hartwig, and their related groups show that high reactivity is achieved with phenanthroline-based ligands (Figure 2.5).[23, 24]

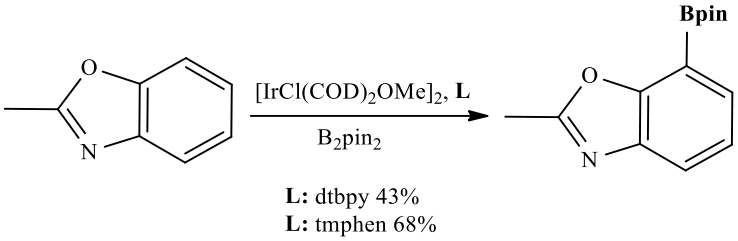

Figure 2.5. Comparison of Me_4Phen and dtbpy ligands.

2.2. Mechanistic Studies

Based on the previous information from the redox chemistry of iridium, the Ir(I) / Ir(III) or Ir(III) / Ir(V) cycles were considered. It was suggested on the basis of computational research conducted by Sakaki and his colleagues that, the active catalyst is Ir(III).[25] Also, reactions involving a preformed Ir(III) trisboryl complex have been shown to have excellent catalytic activity.[26] The general catalytic cycle is shown below (Figure 2.6). The mixture of pre-catalyst, ligand, boron reagent, and solvent form the 16-electron trisboryl Ir (III)/bpy intermediate. During the induction period, the COD is reduced to the COE ligand and the boron reagent provides oxidation of the Ir(I) pre-catalyst. Thus, the hexacoordinate Ir (III) complex **A** carries two types of ancillary donors. In addition, induction time is necessary for the reduction of COD to COE. This period is eliminated by the addition of COE-bearing pre-catalysts and a catalytic amount of HBpin. The COE leaves the structure, forming the active pentacoordinate Ir(III) complex **B**, which contains a vacant coordination region. Arene joins the active complex via rate-limiting oxidative addition. Thus, it forms a sterically crowded heptacoordinate Ir(V) intermediate **C**. This intermediate structure undergoes reductive elimination because of the small activation energy barrier to create aryl boron and Ir (III) bisboryl monohydride **D**. Oxidative addition of B_2pin_2 or HBpin and reductive elimination of HBpin or H_2 takes place, regenerating form **B** for the next catalytic cycle. Thus, the catalytic cycle is completed.

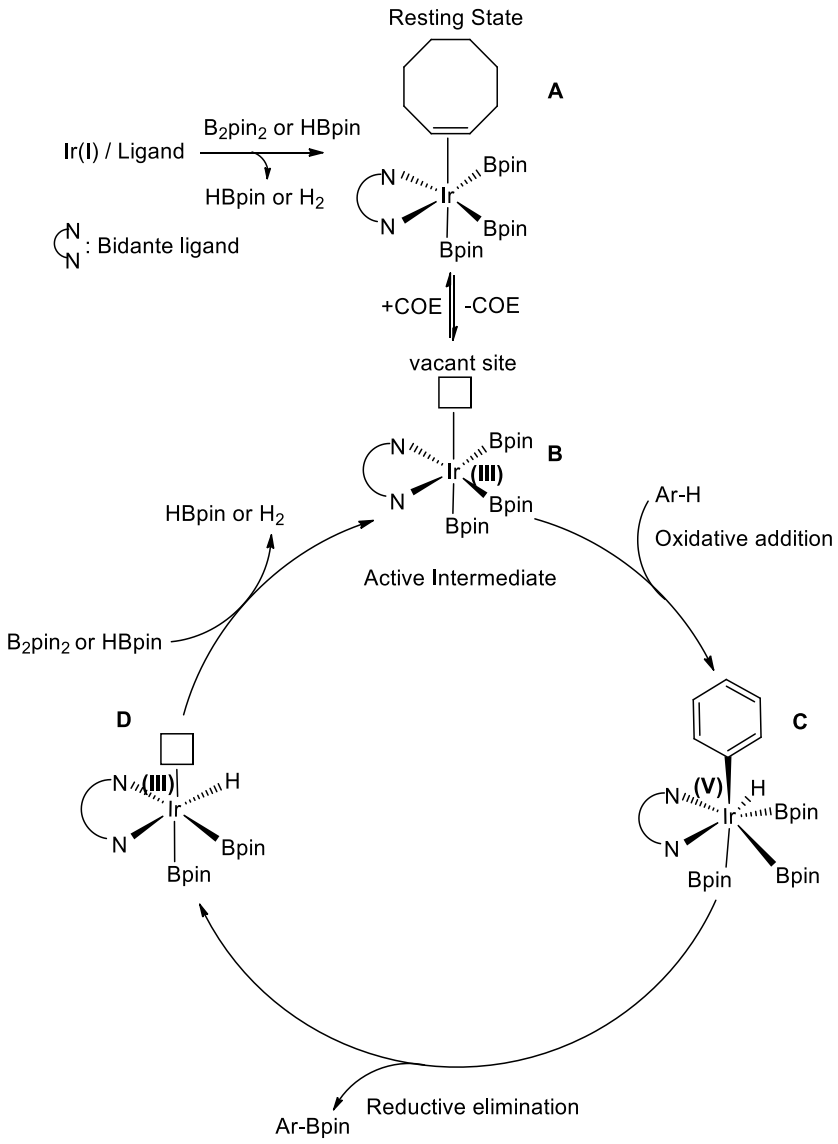

Figure 2.6. Catalytic cycle.

2.3. Scope and Regiochemistry

The reaction displays good selectivity for aromatic C-H bonds. Groups such as nitrile, silyl, ketone, amide, ester, amine, and some alcohols are usually well-tolerated, while nitro, sulfonyl, alkenes, alkynes, and enolizable protons could be problematic. The reaction can be carried out in various solvents, even though polar solvents have an inhibitory effect. In Ir-catalyzed C-H borylation, intrinsic selectivity depends on the steric or electronic properties.

2.3.1. Intrinsic Regioselectivity

2.3.1.1. Steric Regioselectivity

Many carbocyclic sites are borylated by steric regiocontrol because of the crowded structure of the active catalyst **B**. Substituents have a profound effect on the regioselectivity of borylation reactions, but they also have a powerful impact on the reactivity of substrates through steric and electronic effects. Borylation of symmetrical 1,2-disubstituted and 1,3-disubstituted arenes proceeds via activation of uncongested C-H bonds and yields a single product (Figure 2.7a, 2.7b). This is because the cleavage of the C-H bond from the *ortho* position is disfavored for moderate or large-sized substituents. If the accessible positions are provided or substituents are small, *ortho* borylation could be possible (Figure 2.7c, 2.7d).[27]

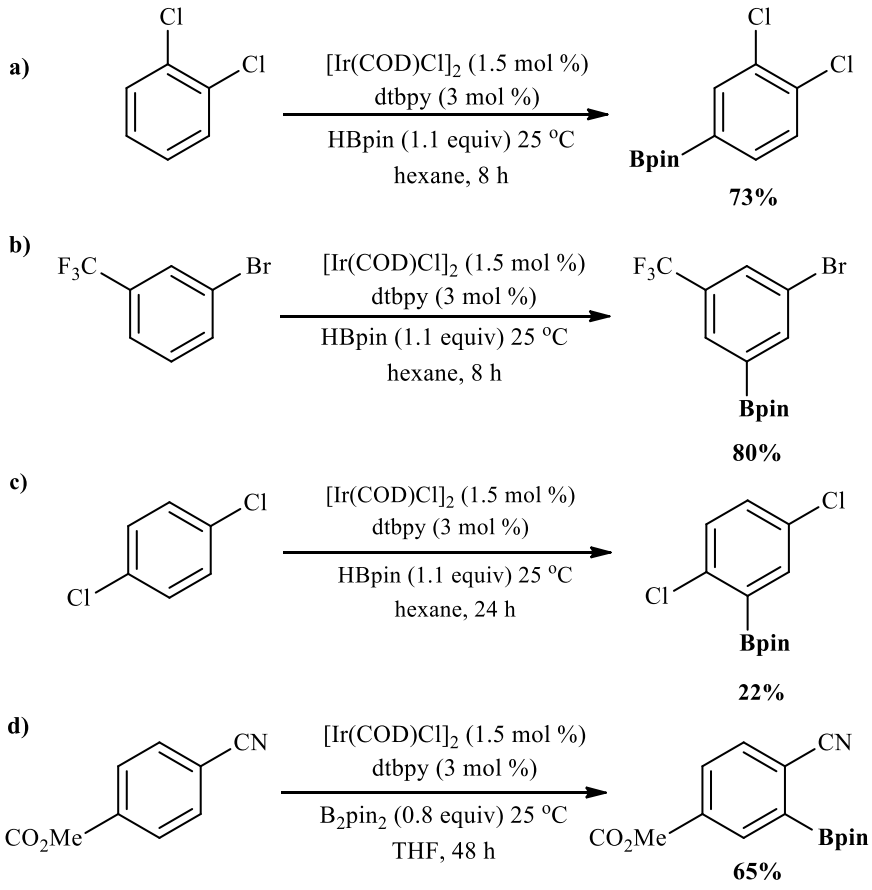

Figure 2.7. Steric selectivity of arenes.

2.3.1.2. Electronic Regioselectivity

When the steric factors are minor, the effect of the electronic factor gains importance. In such examples, such as for benzodioxol, is the more hindered *ortho* position is borylated (Figure 2.8a). At lower temperatures, electronic selectivity becomes more prominent. In a study, 1,2-dibustituted arenes gives *ortho* and *meta* borylation (Figure 2.8b).[28] Electronic selectivity is especially observed in the borylation of heteroaromatic substrates.

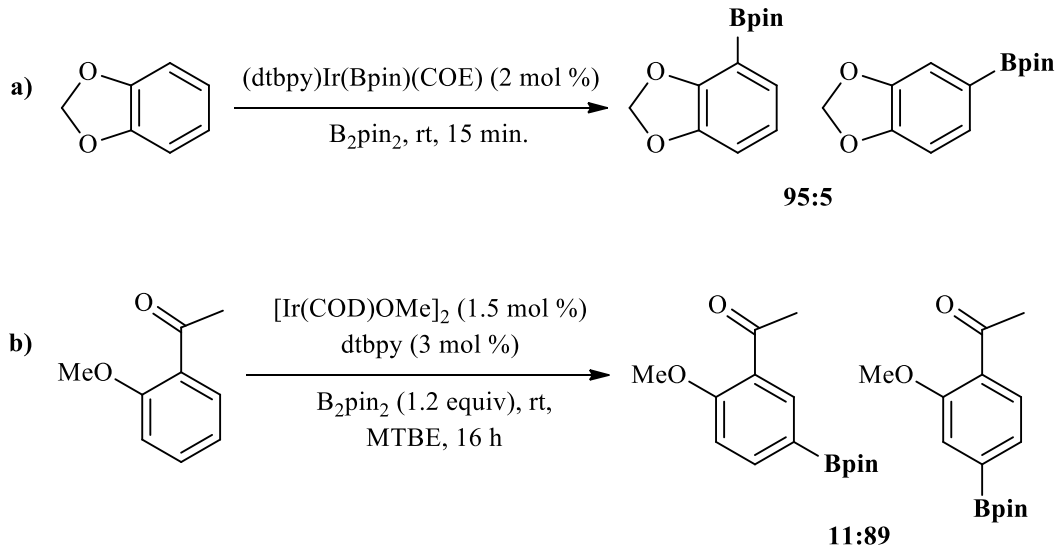

Figure 2.8. Electronic selectivity of arenes.

2.3.2. Directed Borylation

Directed borylation via C-H activation was first developed in arenes and heteroarenes. The Ir complex provides borylation by directing groups within the coordination sphere through chelation control. The systems created for specific regioselectivity have changed the intrinsic selectivity of the catalyst. Three types of approaches have been developed for both the inner and outer spheres.

2.3.2.1. Inner-Sphere-Directed Borylation

Inner sphere directed borylation refers to the interaction of the Ir metal center with a substrate containing a directing group (Figure 2.9). Activation is achieved by directing, resulting in regioselective *ortho* borylation.

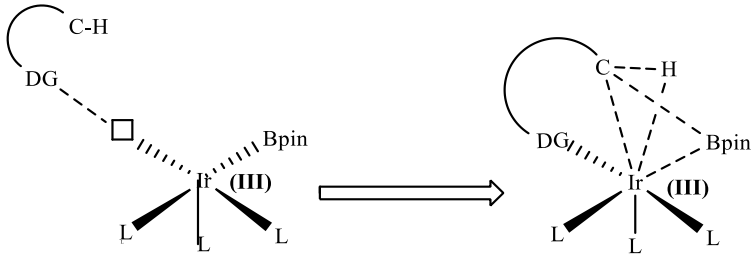

Figure 2.9. Inner-Sphere directed borylation concept.

Inner sphere directed borylations are suitable for substrates with electron-donating or electron-withdrawing functional groups. In addition, it tolerates the use of methyl, ethyl, isopropyl, and *tert*-butyl esters as directing groups. Ishiyama et al. developed a catalytic system comprise $[Ir(\mu\text{-OMe})(COD)]_2$ as the iridium source, and an electron-poor phosphine such as $P[3,5\text{-}(CF_3)_2C_6H_3]_3$ as the ligand. This method was first applied for *ortho*-regioselective borylation of benzoates, amides, carbamates, etc. by catalyzing the site-selective borylation of substrates with oxygen-based directing groups (Figure 2.10).[29] The catalyst activity increased when $AsPh_3$ was used as the ligand, and a yield of over 100% was observed compared to the B_2Pin_2 reagent (Figure 2.10b).

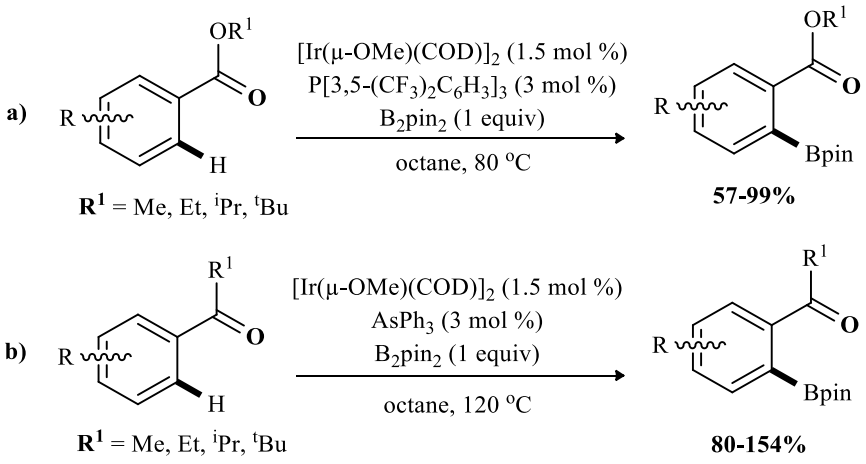

Figure 2.10. Borylations with oxygen-based directing groups.

Sawamura et al. developed a novel approach for site-selective borylation. In this strategy, Silica-SMAP-Ir (solid-supported monophosphine-Ir system) was used as a catalyst for selectivity. This reaction was suitable for functionalized arenes with different oxygenated directing groups, such as benzoates. In most cases, highly efficient ortho-regioselective products have been obtained (Figure 2.11).[30]

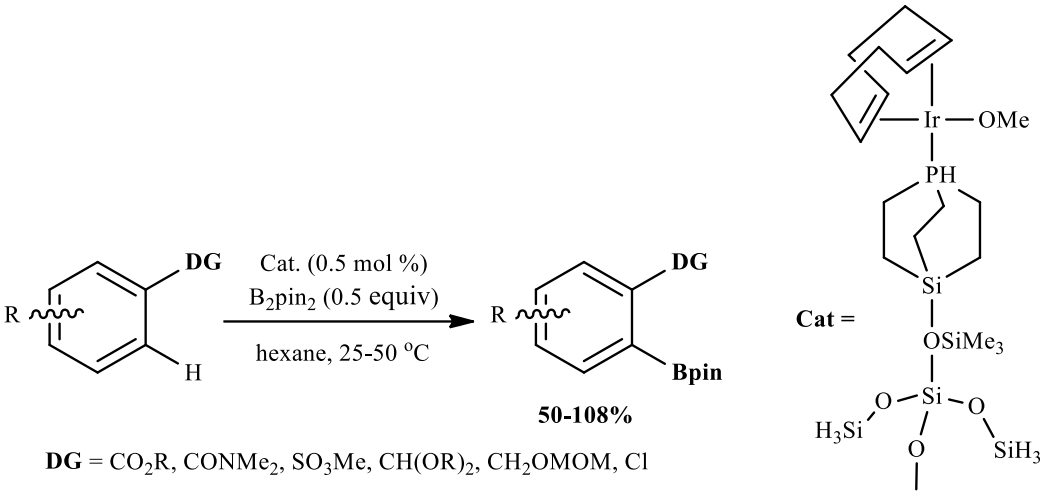

Figure 2.11. Borylations with Silica-SMAP-Ir catalyst.

2.3.2.2. Relay-Directed Borylation

The relay direction is the subclass of the directed borylation, in which substrates containing Si-H bonds are used.[31, 32] Site-selective Ir (III)-catalyzed borylation of arenes is based on the use of silanes as traceless directing groups. (Figure 2.12). A substrate containing binding group coordinates the Ir center and activation is achieved.

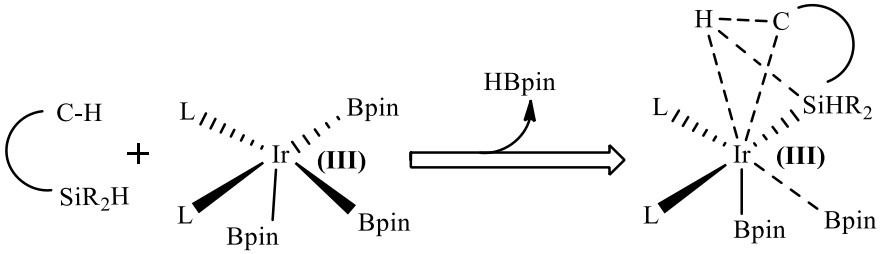

Figure 2. 12. Relay-directed borylation concept.

Indoles are borylated in the most reactive position (C-2) by direct borylation[33], while the regioselective position 7 is borylated by the silyl-oriented method (Figure 2.13).[34]

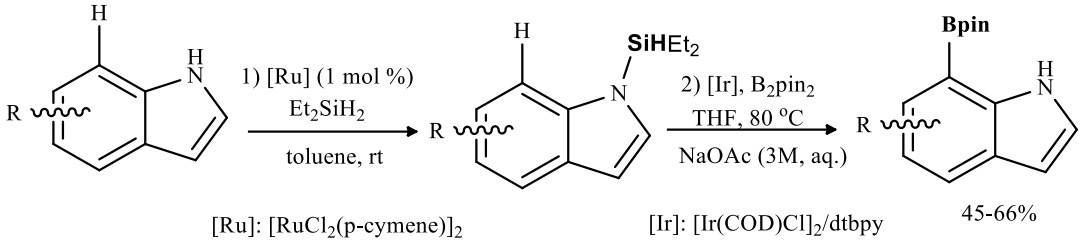

Figure 2.13. Relay-directed borylation of indole.

2.3.2.3. Outer-Sphere-Directed Borylation

Outer sphere-directed borylation is a process where the interaction of a catalytically active ligand with a substrate leads to regioselective C-H activation. This method promotes *ortho* and *meta* borylation. The first strategy comprises the development of borylation procedures, which are provided by the coordination of more classical directing groups to the Ir catalyst. In this situation, ligand modification is essential for facilitating the creation of a vacant free coordination space in the catalyst substrate complex (Figure 2.14).

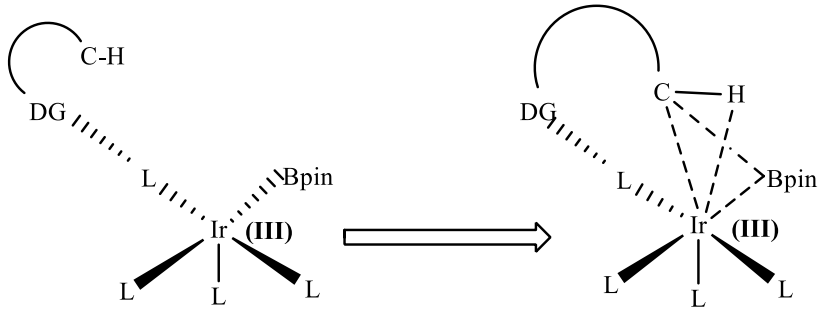

Figure 2.14. Relay-directed borylation of indole.

In the borylation of mono-protected anilines, *ortho* selective products are formed because of the directing effect of acidic N-H groups (Figure 2.15).[35]

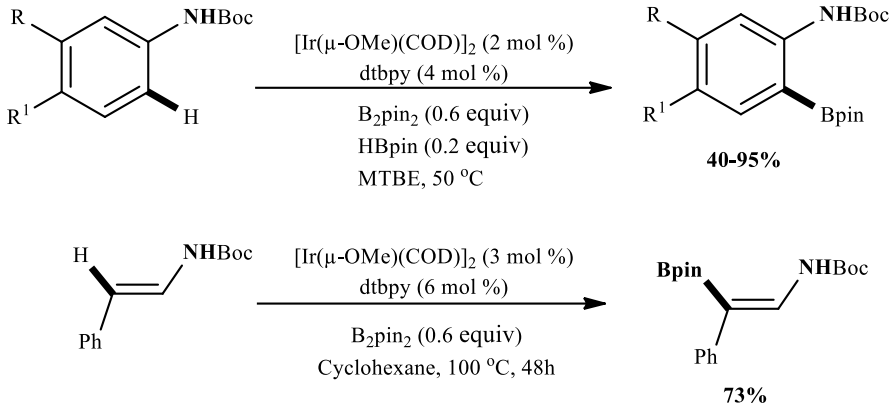

Figure 2.15. Borylation of monoprotected anilines.

In recent years, methods including hydrogen bond recognition between aromatic amides and pendant urea ligand have been developed and *meta*-selectivity has been increased (Figure 2.16).[36]

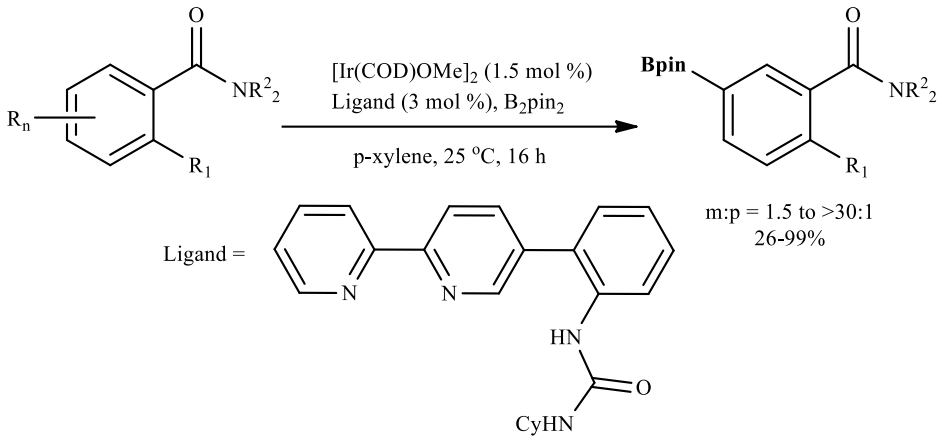

Figure 2.16. Borylation of aryl amide.

2.4. Borylation of Arenes with One Heteroatom

2.4.1. Five-Membered Heteroarenes

Pyrroles, furans, and thiophenes react faster compared to electron-rich carbocyclic arenes. They provide a mixture of mono and bisborylated products even in

the presence of 10 equivalent arenes (Figure 2.17a).[33] An excess amount of arene usage leads high selectivity for the monoboryl product. However, the sulfur atom in thiophene has an inhibitory coordination effect on the catalyst. This situation causes low efficiency.

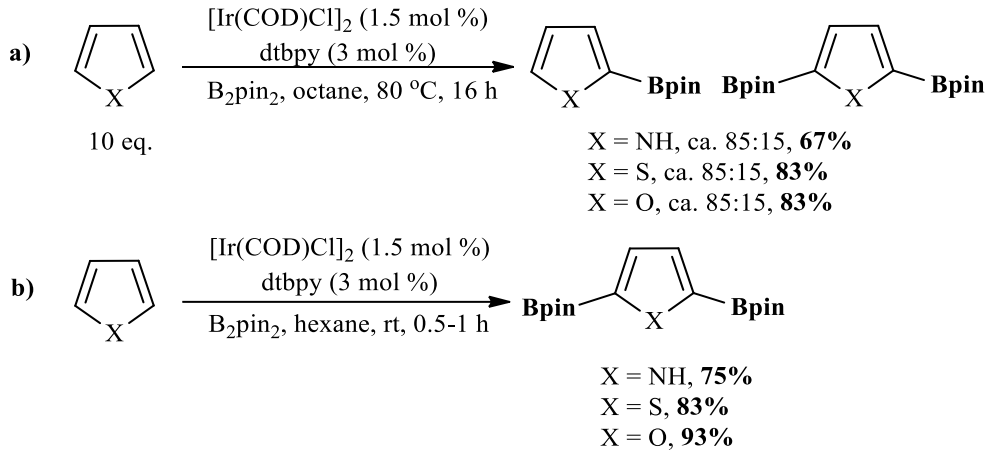

Figure 2.17. C-H borylations of pyrrole, thiophene, and furan.

Since the acidity of C-H increases in connection with the adjacent heteroatom, borylation preferably occurs at the alpha position (C-2 and C-5). When similar conditions are applied at room temperature, furan shows higher selectivity compared to other heterocyclic structures. (Figure 2.17b).[37]

The presence of a carbocyclic ring in heterocyclic structures reveals the potential for borylation at more than one site. However, in structures such as indole, benzothiophene, and benzofuran, borylation occurs prominently in the heterocyclic ring. Borylation takes place selectively at the alpha position at elevated temperatures in case of excess heterocycles. A similar situation is observed in benzofused structures. (Figure 2.18).[22] Bisborylation has been observed in two carbons close to nitrogen when excess indole is used.

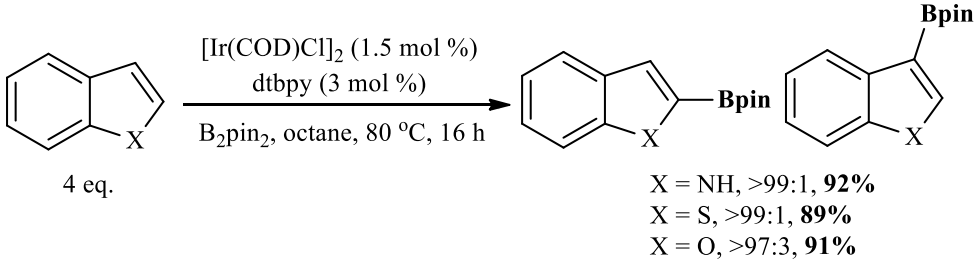

Figure 2.18. C-H borylations of indole, benzothiophene, and benzofuran.

Since the heterocyclic part of the two substituted indoles is sterically crowded, it is borylated at C-7 (Figure 2.19a).[38] When using another substituted indole, borylation occurs first at C-7. Then, due to the *para*-directing effect of the Bpin group, the second borylation takes place at C-4 (Figure 2.19b).[39] This study shows that the borylation of benzofused heterocycles and their monocyclic forms with high reactivity can be achieved with different catalysts, ligands, and reagents other than standard borylation methods.

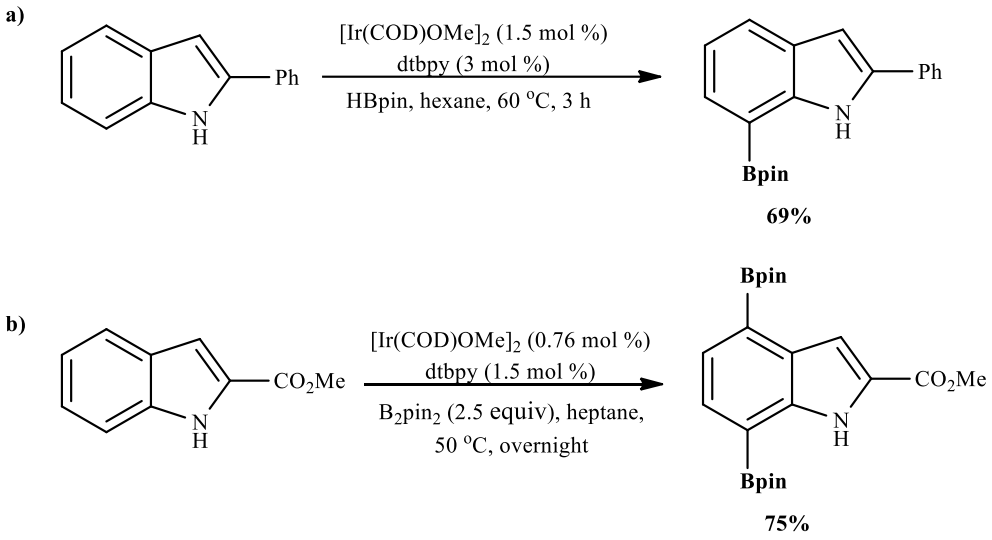

Figure 2.19. C-H borylations of indole.

Similarly, in N-substituted carbonyl derivatives of the carbazole structure, the relay direction effect occurs using Silica-SMAP, and efficient C-1 borylation occurs by providing regiocontrol. This system could also be an alternative method of regiocontrol in other polycyclic heterocyclic structures (Figure 2.20).[40]

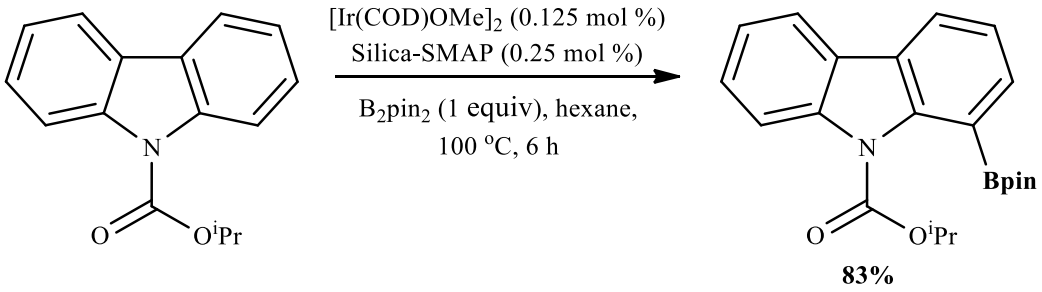

Figure 2.20. C-H borylations of N-substituted indole.

2.4.2. Borylation of Six-Membered Heteroarenes

Heteroarenes containing basic azinyl nitrogen atoms has a distinct challenge in borylation chemistry. Borylation is electronically disfavoured by the alpha position of the azinyl N atom. During C-H activation, a negative charge develops on the alpha carbon atom. A dipolar repulsion occurs between this charge and the azinyl lone pair. The electron density in nitrogen and the steric restrictions on the rest of the molecule affect the degree to which alpha borylation occurs.

For example, 2,3-disubstituted pyridines were sterically borylated at C-5 with high efficiency. However, when using more powerful electron-deficient substituents, the effectiveness of alpha azinyl borylation is enhanced. (Figure 2.21a). Similar trends are observed in 2,4 substituted pyridines. The inhibitory effect of azinyl nitrogen provides C-5 borylation. This condition ensures that the bulk of the C-4 substituent can be tolerated. Even though pyridine is electron deficient, borylation is selective for C-2 even at ambient temperature. Against this, more stringent conditions are[41] required for the C5 selectivity of electron-rich and sterically congested pyridine to increase. (Figure 2.21b).[42]

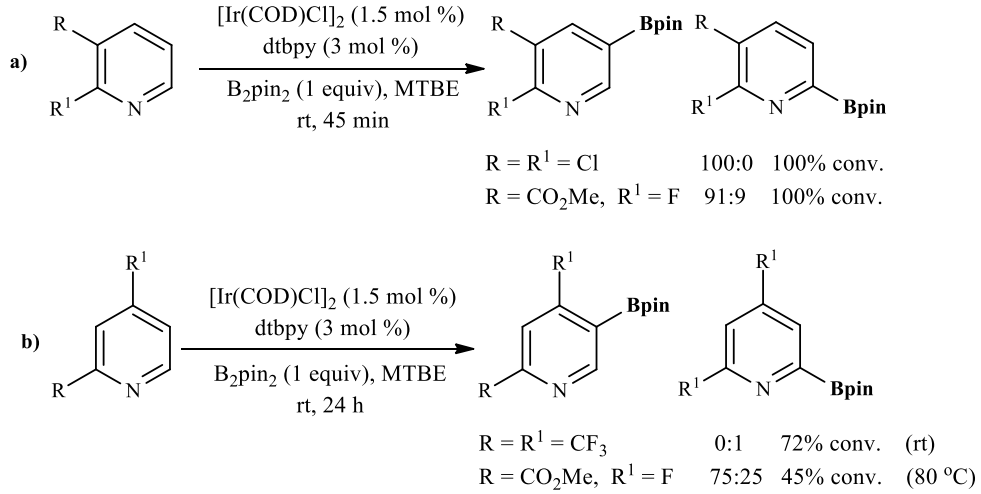

Figure 2.21. C-H borylations of substituted pyridine.

Outer sphere directing effects are used to override this type of selectivity. This effect facilitates *ortho*-selective borylation in situ in 2-substituted aminopyridines (Figure 2.22).[32]

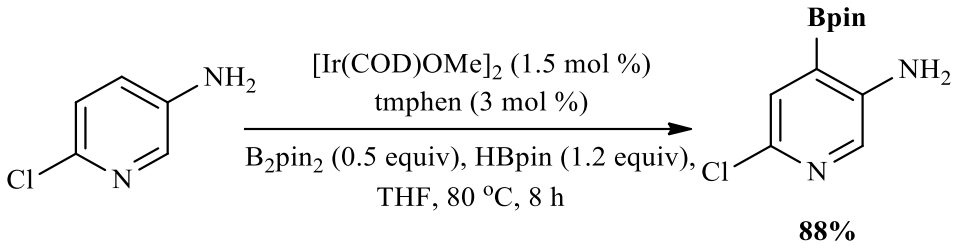

Figure 2.22. Outer-sphere directed C-H borylations of aminopyridine.

In inner sphere systems, azinyl nitrogen coordinates directly to the Ir metal center. Selective borylation occurs because the directing group is present in the structure. Nakao used bulky aluminum Lewis acids that block access to the *meta* position, taking advantage of the coordination ability of azinyl nitrogen to direct the borylation to C-4 (Figure 2.23).[43]

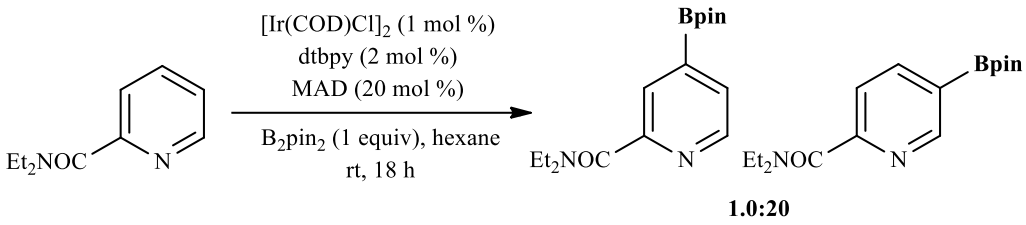

Figure 2.23. C-H borylations of N-diethylpicolinamide

Benzofused structures containing a heteroatom such as a quinoline are the most active substrates for C-H borylation. According to the studies by Miyaura et al., the C-H bond at C-5 of quinoline shows a sterically inhibitory effect. The lone pair on nitrogen prevents activation at C-2. As a result, monoborylation occurs at C-3 with a yield of 84% (Figure 2.24).[33]

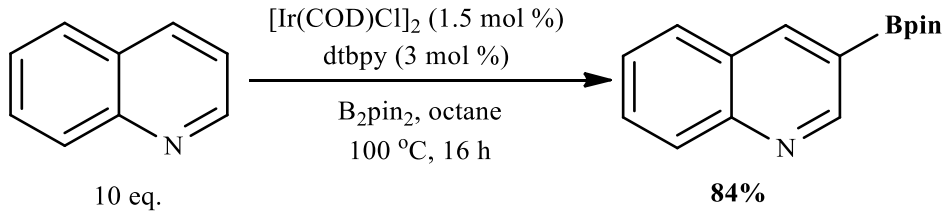

Figure 2.24. C-H borylations of quinoline.

In the presence of excess boron, two bis boryl products are formed (Figure 2.25a). When disubstituted quinolines are used as the reactant, borylation occurs only at the C-4 position. Positions C-3, C-5, and C-7 have steric hindrances. C-8 is not reactive because peri hydrogen prevents catalyst inhibiting bindings (Figure 2.25b).[44] Selectivity depends on the R groups in the quinoline structure. Electron-withdrawing groups increase the C-5 selectivity (Figure 2.25c).

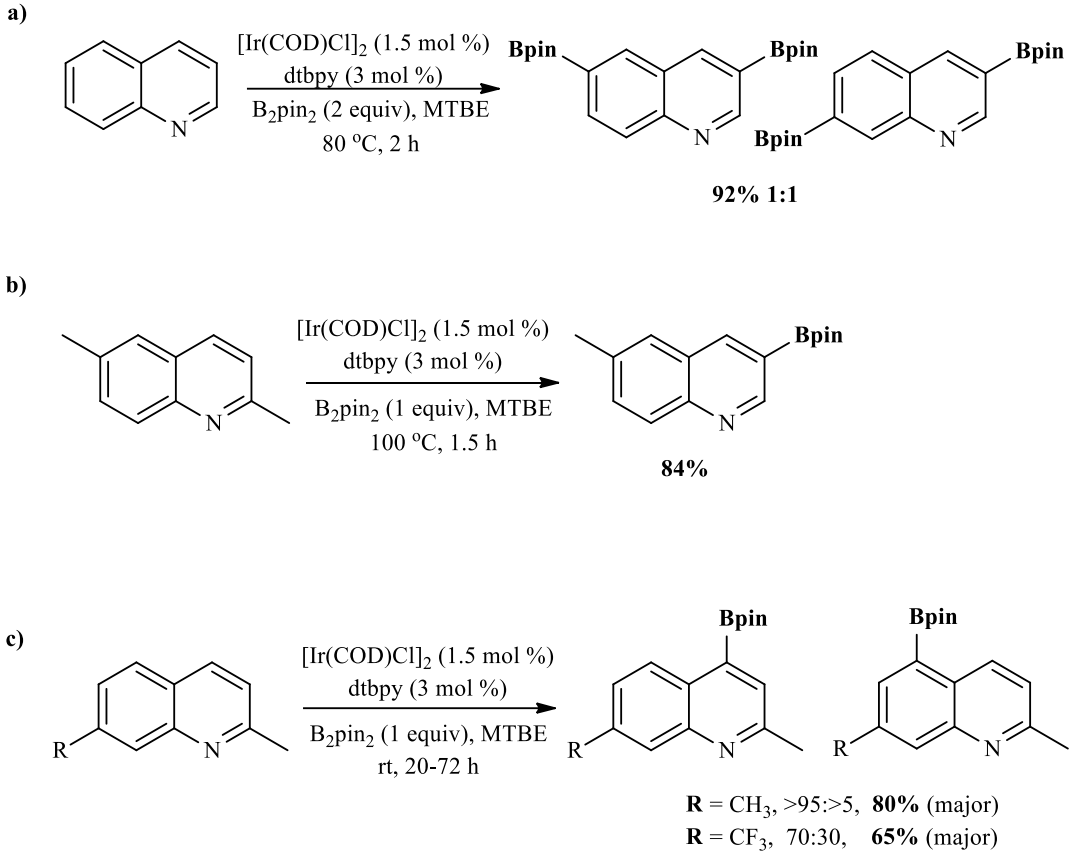

Figure 2.25. C-H borylations of quinoline and derivatives.

In a study published in 2009, the reaction time of quinoline was shortened using microwave irradiation and carried out in minutes at 80 °C. The reaction efficiency was improved when MTBE was used as a solvent. Thus, the need for solvents with a high boiling point is eliminated (Figure 2.26).[45]

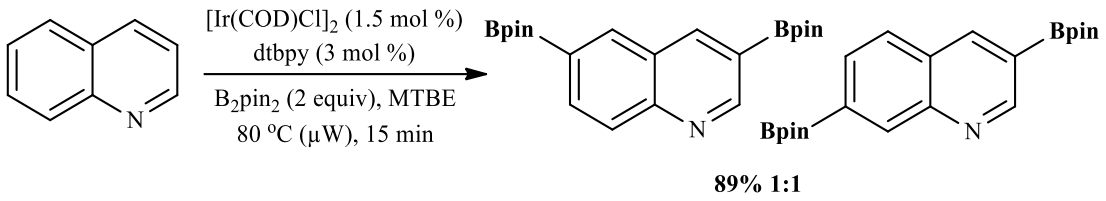

Figure 2.26. C-H borylations of quinoline.

In selective borylation of C-8, a silica-supported monophosphite ligand was used instead of dtbpy, which is often used in borylation experiments. This system provides high regioselectivity even with congested structures (Figure 2.27).[46]

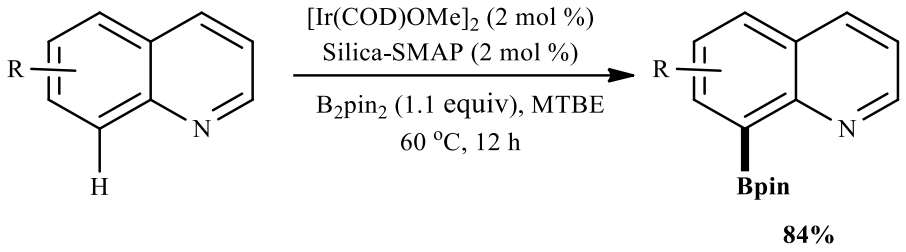

Figure 2.27. C-8 borylations of quinoline by Silica-SMAP/Ir complex.

As another example of ligand type used in borylation, hemilable ligands in the borylation of 1-aryl isoquinolines provided direct *ortho*-selectivity (Figure 2.28).[47]

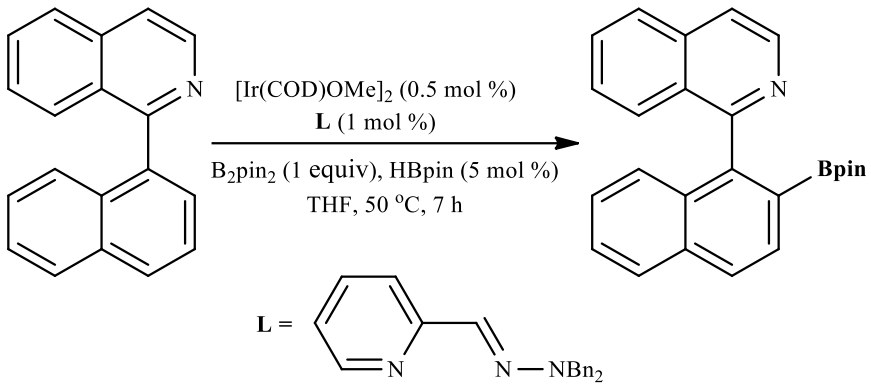

Figure 2.28. C-H borylations of 1-aryl isoquinoline with hemilable ligand.

Transition metal catalyzed (Pd, Rh, Ir, Cu, and Co) C-H activation reactions are practical way for direct arylation.[48-51] Dihydroisoquinolines form strategic molecules synthetically, as they are precursors of both isoquinolines and tetrahydroisoquinolines.[52-56] Due to the low reactivity of dihydroisoquinolines, reports

of C-H functionalization are very limited.[57, 58] Groups such as N-oxides, acyl groups or tethers are used to direct regioselectivity.[59-63]

Kapur et al. first demonstrated Ru-catalyzed, acyl-directed regioselective C(3)-H alkylation of N-acetyl-1,2-dihydroisoquinolines with α-diazomalonates.[64, 65] The catalytic system formed by metal carbene migration insertion works efficiently over a wide range of substrates.

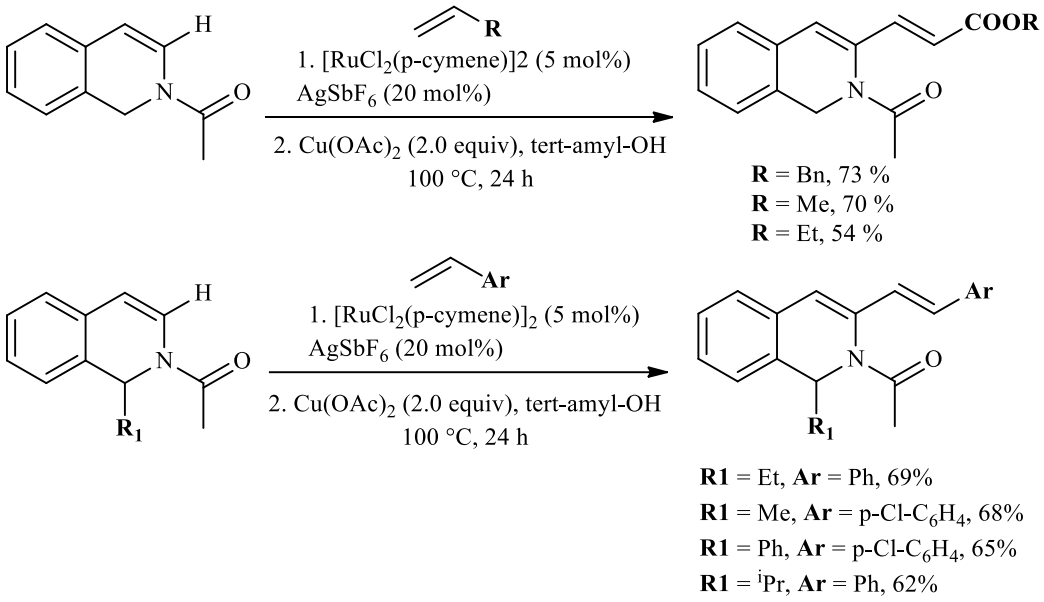

Figure 2.29. Ru-catalyzed C(3)-H alkylation of N-acetyl-1,2-dihydroisoquinolines.

In 2014, a new palladium-catalyzed methodology has been developed for the regioselective C-4 arylation of 1,2-dihydroisoquinolines.[66] The reaction proceeds via heteroatom-guided electrophilic palladation.

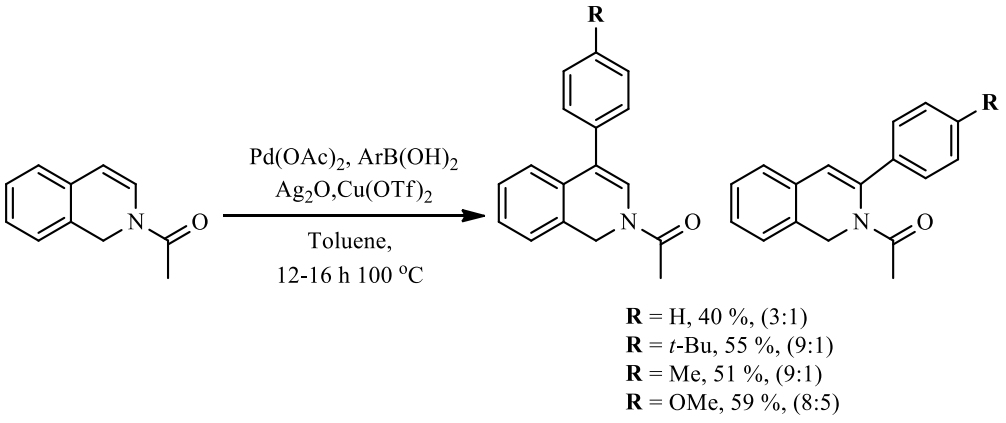

Figure 2.30. Pd-catalyzed C(4)-H alkylation of N-acetyl-1,2-dihydroisoquinolines.

In another study, Pd-catalyzed C-H activation was used for acetoxylation/alkoxylation of 1-phenyl-3,4-dihydroisoquinoline. In this strategy, Ac_2O acts as an acetoxylating agent, $PhI(OAc)_2$ acts as a terminal oxidant, and the desired product is obtained with high efficiency.[67]

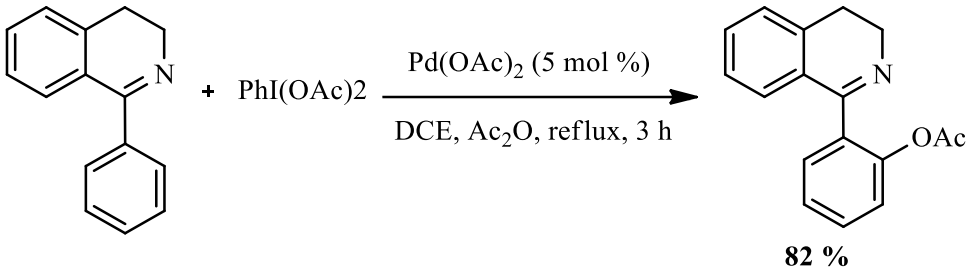

Figure 2.31. Acetoxylation of 1-phenyl-3,4-dihydroisoquinoline.

Inspired by these studies, the imine group of dihydroisoquinoline was used as the directing group to ensure C-H activation, and the [4+2] annulation tetracyclic isoquinolinium salt was formed. 1-phenyl-3,4-dihydroisoquinolines have been quickly and effectively converted to quaternary ammonium salts of dihydroisoquinoline compounds by Rh-catalyzed C-H activation.[68]

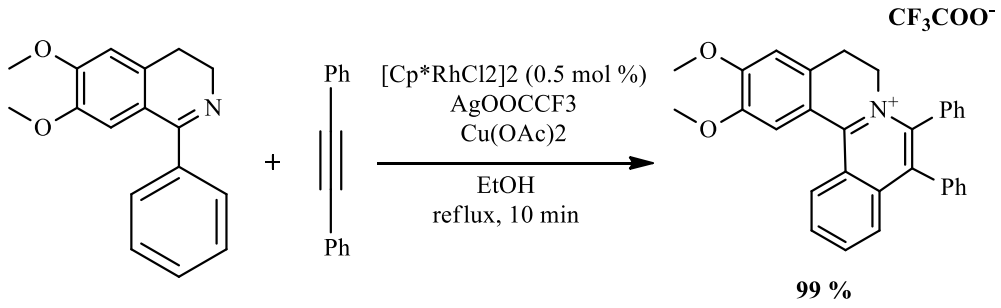

Figure 2.32. Imine-directed Rh- catalyzed C–H activation.

Iridium-catalyzed C-H borylation is a method that is still being developed. Steric and electronic effects govern the formation of selective organoboron structures. Since the least sterically hindered sites are more accessible, the crowded catalyst structure is more eligible to borylate such sites via coordinative pathways. The contribution of electronic effects to the result is usually observed at low temperatures. These effects remain less available compared to steric effects. Selective borylation of congested structures could be achieved by the electronic effect of substitute groups or by the directing effect of various catalyst ligand complexes.

CHAPTER 3

EXPERIMENTAL

3.1. General Information

MTBE and THF solvents were freshly distilled from $LiAlH_4$ under nitrogen gas. DME, Decane, and Dioxane were purified from benzophenone-ketyl under nitrogen gas prior to use. Distilled dioxane is stored on a 4Å molecular sieve in the dark. DCM, EtOH, Acetonitrile, and Chloroform were dried over 3Å molecular sieve which was kept in a 400 °C ash furnace for 24 hours and cooled under nitrogen gas. Solvents are used after at least 24 hours of storage over the sieve. Reactions were prepared in a LC Technology Solutions Inc. Glovebox System under N_2. The synthesized reagents and products were purified over columns containing silica gel with a size of 200-400 mesh or neutral alumina with a size of >200 mesh. Melting Points were determined using an Electrothermal Melting Point Apparatus 9200.

3.2. Synthesis of Iridium Complexes

3.2.1. Synthesis of $[Ir(COD)Cl]_2$

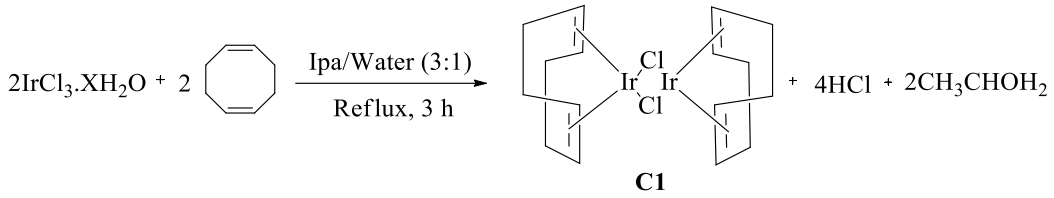

C1

Figure 3.1. Preparation of C1.

$IrCl_3 \cdot XH_2O$ (2.0 g) is added into a 50-mL two-necked, round-bottomed flask charged with 1-propanol (30 mL) and water at a 3/1 ratio. 1,5-Cyclooctadiene (4 mL) is dropwise added to the solution. The resulting solution is stirred in the air for 5 min. Then one neck of the flask is equipped with a water condenser, the other neck is connected to nitrogen gas. The resulting mixture is refluxed with vigorous stirring at 90 °C for 3 h, during which yellow-red solid particles are formed. After cooling the suspension to room temperature, it is concentrated, filtered, and washed with a small amount of cold methanol to remove unreacted 1,5-cyclooctadiene, and dried under vacuum for 24 hours to afford **C1** (red solid, yield: 1.16 g, 58%).[69]

3.2.2. Synthesis of $[Ir(COD)OMe]_2$

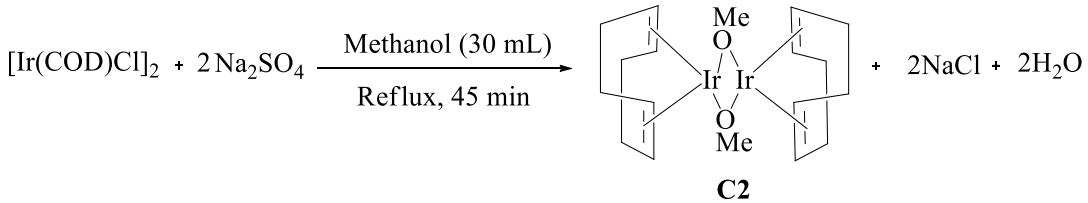

C2

Figure 3.2. Preparation of C2.

An excess of anhydrous Na_2CO_3 (1.20 g) is added into a 100-mL two-necked, round-bottomed flask charged with methanol (30 mL), and $[Ir(COD)Cl]_2$ (1.20 g) under

nitrogen atmosphere. The resulting solution is refluxed with vigorous stirring at 60 °C for 45 min without boiling to prevent partial decomposition. Heating is stopped when the yellow particles turn brown. After cooling the suspension to room temperature, it is filtered and washed with water (6*5 mL) and a small amount of cold methanol under nitrogen atmosphere to get a yellow precipitate. Finally, it is dried under vacuum for 24 hours and stored in an inert atmosphere to afford **C2** (yellow solid, yield: 1.13 g, 97%).[69]

3.3. Synthesis of Substrates

3.3.1. Synthesis of N-Acyl-1,2-Dihydroisoquinoline and Its Derivatives

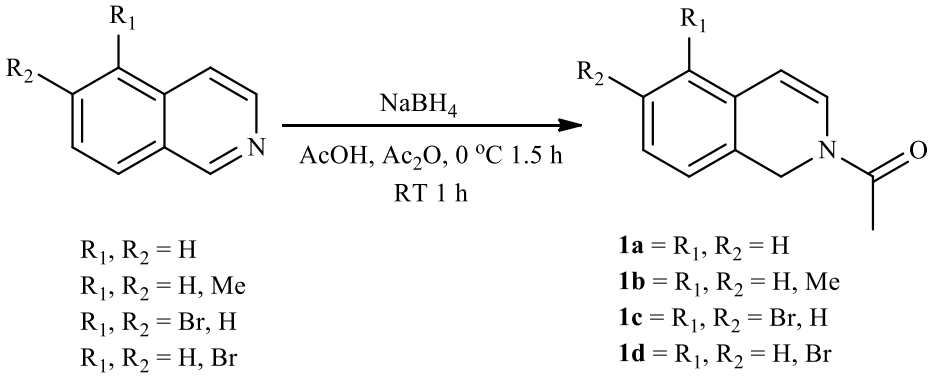

Figure 3.3. Synthesis of N-acyl-1,2-dihydroisoquinoline and its derivatives.

Sodium borohydride (40 mmol, 4 equiv) is slowly added to a mixture of anhydride (53 mmol, 5.3 equiv), acetic acid (15 mL), and isoquinoline derivative (10 mmol) under nitrogen gas at 0 °C over 1.5 hours. After the addition is done, the mixture is stirred for another 1 hour at room temperature. The progress of the reaction is controlled by TLC. Then it is diluted with water (100 mL) and neutralized with sodium carbonate[70] solution. After extraction with EtOAc, it is dried on Na_2SO_4, filtered, and concentrated under reduced pressure. The crude mixture is purified from neutral alumina column chromatography with DCM, afforded **1a** (yellow oil, yield: 1.22 g, 70%), **1b** (pale-yellow gel, yield: 3.96 g, 66%), **1c** (yellow solid, yield: 5.72 g, 75%), **1d**

(light brown solid, yield: 1.86 g, 85%)[71], then used immediately or stored at -30 °C under inert atmosphere to evoid decomposition.

3.3.2 Synthesis of *tert*-butyl isoquinoline-2(1H)-carboxylate

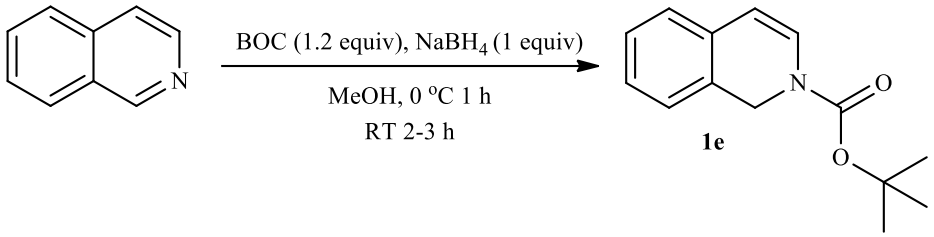

Figure 3.4. Synthesis of 1e.

The solution of isoquinoline (10 mmol, 1.17 mL) in MeOH (15 mL) is cooled down to 0 °C under a nitrogen atmosphere. Then, $NaBH_4$ (10 mmol, 380 mg) is added in portions over 1 h. The mixture is then warmed up to room temperature and stirred for 2-3 hours. The reaction process is controlled by TLC. After the reaction is completed, the solution is quenched with H_2O and extracted with EtOAc, dried with $NaSO_4$, and evaporated under reduced pressure. The residue is purified by silica gel column chromatography (Hexane/EtOAc = 25/1, light-yellow oil, yield: 774 mg, 60%) to afford **1e** and then used immediately.[41]

3.3.3. Synthesis of 1-(Isoquinolin-2(1H)-yl)-2,2-dimethylpropan-1-one

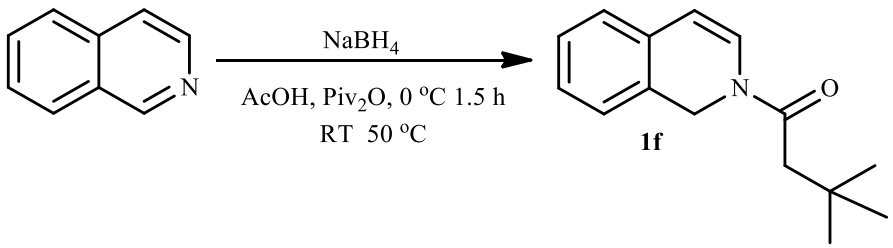

Figure 3.5. Synthesis of 1f.

Sodium borohydride (40 mmol, 4 equiv) is slowly added to a mixture of pivalic anhydride (53 mmol, 5.3 equiv), acetic acid (15 mL), and isoquinoline derivative (10 mmol) under nitrogen gas at 0 °C over 1.5 hours. After the addition is done, the mixture is stirred for another 1 hour at 50 °C. The progress of the reaction is controlled by TLC. It is diluted with water (100 mL) and neutralized with sodium carbonate[70] solution. Then following the extraction with EtOAc, it is dried on Na_2SO_4, filtered, and concentrated under reduced pressure. The crude mixture is purified from silica gel column chromatography to afford **1f** (Hexane/EtOAc = 5/1, orange oil, yield: 150 mg, 10%).[71]

3.4. General Procedure of Borylation Reaction

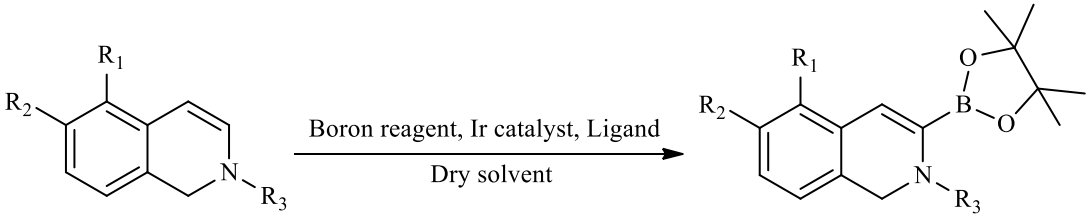

1a = R_1,R_2, R_3 = H, H, Ac
1b = R_1,R_2, R_3 = H, Me, Ac
1c = R_1,R_2, R_3 = Br, H, Ac
1d = R_1,R_2, R_3 = H, Br, Ac
1f = R_1,R_2, R_3 = H, H, Piv

2a = R_1,R_2, R_3 = H, H, Ac
2b = R_1,R_2, R_3 = H, Me, Ac
2c = R_1,R_2, R_3 = Br, H, Ac
2d = R_1,R_2, R_3 = H, Br, Ac

Figure 3.6. Synthesis of organoboranes.

3.4.1. Method Without Pre-Activation

B_2pin_2, Ir complex, ligand, reactant and the dry solvent are added to a 5 mL thick-wall-sealed cap glass tube in a glovebox because of the air sensitivity of the iridium catalyst. Then, sealed and taken out of the glove box. The reaction mixture is stirred magnetically in a preheated oil bath for a period of time. At the end of the reaction, the mixture is cooled to room temperature, then analyzed by Gc.

3.4.2. Method With Pre-Activation

B_2pin_2, Ir complex, and the ligand are added to a 5 mL thick-wall-sealed cap glass tube in a glovebox because of the air sensitivity of the iridium catalyst. Half of the dry solvent to be used in the experiment is added. The mixture is stirred for 2 minutes at room temperature for pre-activation. Then, the reactant and the remaining solvent are added, sealed and taken out of the glove box. The reaction mixture is stirred magnetically in a preheated oil bath for a period of time. At the end of the reaction, the mixture is cooled to room temperature, then an internal standard is added. Conversion and yield calculations were performed with an internal standard on NMR. The crude mixture is purified from silica gel column chromatography, to afford **2a, 2b, 2c, 2d** (EtOAc/MeOH = 5/1).

3.5. Oxidation of 2a with Oxone

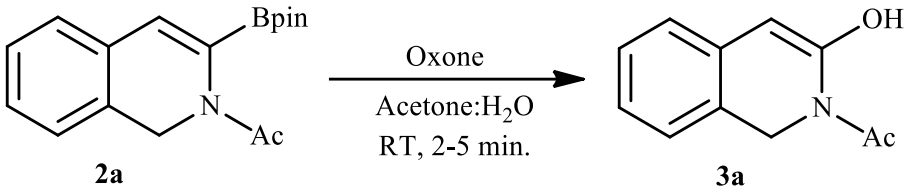

Figure 3.7. The oxidation reaction of 2a.

To a mixture of **2a** (28.7 mg, 0,01 mmol) and acetone (50 µL, 0.2 M) in a 50 mL round-bottom flask oxone (50 µL of a 0.2 M solution in H_2O, 1 equiv) is added in one portion. The reaction mixture is stirred at room temperature until the completion of the reaction (~2 min). H_2O (5.5 µL) and HCl (0.1 M, 10.3 µL) are added to the crude mixture, successively, extracted with DCM, dried over Na_2SO_4, and concentrated under reduced pressure.[70] Then the resulting mixture is purified by a short pad of silica gel column chromatography with DCM as eluent, to afford **3a** (Hexane/EtOAc = 1/1, white solid, yield: 2.87 mg, 10%).[72]

3.6. Suzuki Reactions of 2a

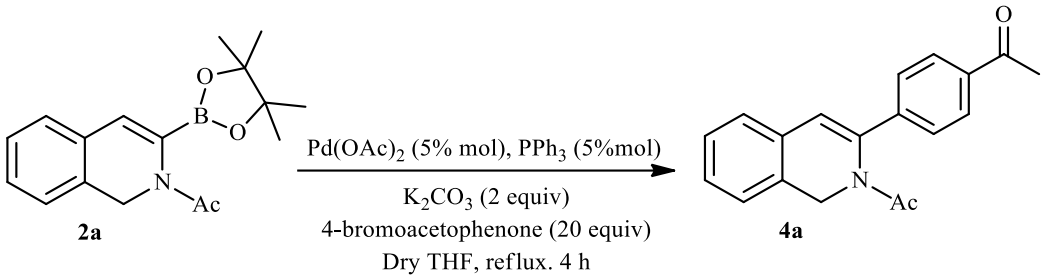

Figure 3.8. Suzuki reaction of 2a.

$Pd(OAc)_2$ (3.3 mg, 0.015 mmol) and PPh_3 (3.8 mg, 0.015mmol) are added into the 10 mL round-bottom flask containing 0.2 mL of THF. Then, **2a** (51.8 mg, 0.3 mmol), K_2CO_3 (82.8 mg, 0.6 mmol) and 4-bromoacetophenone (59.6 mg, 0.3 mmol) with dry THF (0.7 mL) are added under nitrogen atmosphere, stirred under reflux system. The crude mixture is quenched with NH_4Cl, extracted with EtOAc, dried over Na_2SO_4, and concentrated under vacuum.[70] The coupling product **4a** is purified by silica gel chromatography (Hexane/EtOAc = 2/1, yellow oil, yield: 45.4 mg, 52%).[73]

3.7. Oxidation with DDQ

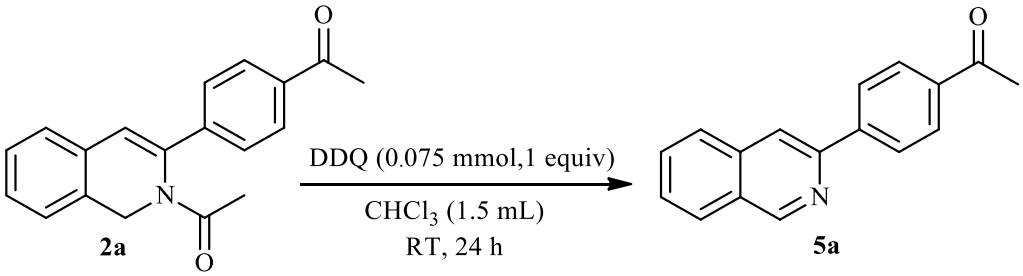

Figure 3.9. Oxidation of 2a.

To a Schlenk tube (4 mL) containing **2a** (21.8 mg, 0.075 mmol) and DDQ (17 mg, 0.075 mmol) is added $CHCl_3$ (1.5 mL) and stirred at room temperature for 24 h. The resulting mixture is extracted by EtOAc, dried with Na_2SO_4, and concentrated

under vacuum. The oxidized product **5a** is purified by silica gel chromatography (Hexane/EtOAc = 2/1, red solid, yield: 8.90 mg, 48%).[74]

3.8. Characterization Techniques

3.8.1. GC Method

The samples were analyzed by GC/MS (HP GC/MS 6890/5973N on a HP-5MS, 30m, 0.25 mm capillary column, 5% phenylmethoxysiloxane, 95% dimethylpolysiloxane with 0.25μm film thickness) and GC (Shimadzu GC2010 Plus on a 30m, 0.25 mm capillary column (5% dimetylsiloxane, 95% phenyldimethylsiloxane with a 0.25 μm film thickness and FID detector). The GC program was applied during the analysis: the column temperature was 40 °C at the start of the program and it was heated at a rate of 10 °C/min up to 300 °C, then it was kept at this temperature for 15 min.

3.8.2. Calculation of Reactant and Product Amounts on GC

To calculate the amount of reactant and product, the response factor (rf) of each reactant and product was determined. For the determination of the rf, a known amount of the standard compound is dissolved in ethyl acetate together with a known amount of the internal standard and injected into the GC. After the analysis was completed at the set temperature program, the following equation (3.1) was used to determine the rf of the compound.

$$rf = \frac{\text{Internal standard area}}{\text{Compound area}} \times \frac{\text{Compound amount}}{\text{Internal standard amount}} \quad (3.1)$$

Aliquots of the sample taken from the reaction flask which contain trans-stilbene as the internal standard, diluted with ethyl acetate and injected into the GC. The equation (3.2) was used to determine the amounts.

$$\text{Amount of compound} = \frac{\text{Internal standard amount}}{\text{Internal standard area}} \times \text{R.F.} \times \text{Compound area} \quad (3.2)$$

3.8.3. Calculation of Reactant Conversion and Yield on GC

The reactant conversion was calculated using the following equation (3.3): Where $(\text{reactant})_I$ is the weight of reactant at the beginning of the reaction and $(\text{reactant})_t$ is the amount of the reactant at time t.

$$(\text{Reactant Conversion})_t\ \% = \frac{\left((\text{Reactant})_I - (\text{Reactant})_t \right)}{(\text{Reactant})_I} \times 100 \qquad (3.3)$$

Product yield was calculated according to the following equation (3.4):

$$\text{Yield}\% = \frac{(\text{Product mmol})_t}{(\text{Reactant mmol})I} \times 100 \quad (3.4)$$

3.8.4. NMR Method

NMR analyses were recorded by Varian VnmrJ 400 spectrometer in deuterated chloroform. Chemical shifts are reported in ppm downfield from Me_4Si. NMR yields are measured with p-anisaldehyde used as an internal standard. The equation used for the reactant conversion is shown below (3.5): Where $(\text{reactant})_I$ is the mmol of the initial reactant, and $(\text{reactant})_{res}$ is the mmol of the remaining reactant.

$$\text{Reactant Conversion } \% = 100 - \frac{(\text{Reactant mmol})_t}{(\text{Reactant mmol})_I} \times 100 \quad (3.5)$$

The product yield was calculated according to the below equation (3.6):

$$\text{Yield } \% = \frac{\text{Product mmol}}{((\text{Reactant mmol})i - (\text{Reactant mmol})t)} \times 100 \quad (3.6)$$

3.9. Spectral Data for the Prepared Compounds

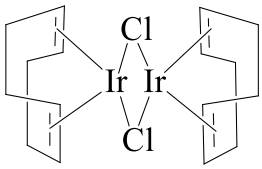

C1

Bis(1,5-cyclooctadiene)diiridium(I) dichloride (C1): ^{1}H NMR (400 MHz, $CDCl_3$) δ: 4.52 – 3.76 (m, 8H, vinylic protons), 2.29 – 2.19 (m, 8H, allylic protons), 1.54 – 1.48 (m, 8H, allylic protons).

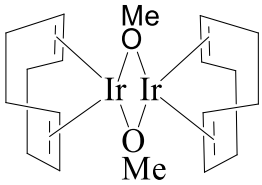

C2

(1,5-Cyclooctadiene)(methoxy)iridium(I) dimer (C2): ^{1}H NMR (400 MHz, $CDCl_3$) δ: 3.59 – 3.44 (m, 8H, vinylic protons), 3.22 (s, 6H, methoxide, 2.20 (m, 8H, allylic protons), 1.35 (m, 8H, allylic protons).

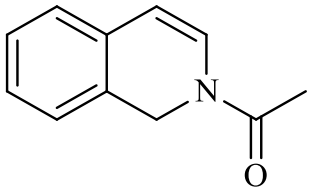

1a

1-(isoquinolin-2(1H)-yl)ethanone (1a): DCM; yellow oil; ^{1}H NMR (400 MHz, $CDCl_3$) δ: 7.16 – 7.10 (m, 2H), 7.06 – 7.03 (m, 1H), 7.00 – 6.95 (m, 1H), 6.61 (d, *J* = 7.8 Hz, 1H), 5.76 (d, *J* = 7.8 Hz, 1H), 4.89 (s, 2H), 2.17 (s, 3H); ^{13}C NMR (100 MHz, $CDCl_3$) δ: 167.9, 130.4, 129.4, 127.6, 127.3, 126.0, 125.9, 124.6, 109.6, 44.3, 21.1; MS (EI, *m/z*): 173 (22, M^+), 130 (100), 103 (18), 77 (22), 63 (6), 51 (8).

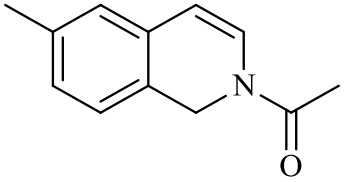

1b

1-(6-methylisoquinolin-2(1H)-yl)ethanone (1b): DCM; yellow solid; ^{1}H NMR (400 MHz, $CDCl_3$) δ: 7.06 – 6.93 (m, 2H), 6.88 (s, 1H), 6.66 (d, *J* = 7.9 Hz, 1H), 5.81 (d, *J* = 7.8 Hz, 1H), 4.92 (s, 2H), 2.32 (s, 3H), 2.23 (s, 3H); ^{13}C NMR (100 MHz, $CDCl_3$) δ: 168.9, 137.7, 130.7, 128.4, 127.0, 126.5, 126.3, 125.8, 110.2, 60.9, 44.6, 21.8.

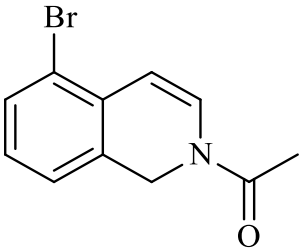

1c

1-(5-bromoisoquinolin-2(1H)-yl)ethanone (1c): DCM; pale-yellow oil; M.P. (°C): 72 - 74 ^{1}H NMR (400 MHz, $CDCl_3$) δ: 7.40 (d, *J* = 7.4 Hz, 1H), 7.06 – 6.93 (m, 2H), 6.74 (d, *J* = 6.9 Hz, 1H), 6.19 (d, *J* = 7.9 Hz, 1H), 4.91 (s, 2H), 2.22 (s, 3H); ^{13}C NMR (100 MHz, $CDCl_3$) δ: 168. 5, 168.5, 131.7, 131.4, 130.2, 128.2, 125.1, 120.2, 108.4, 44.4, 21.2.

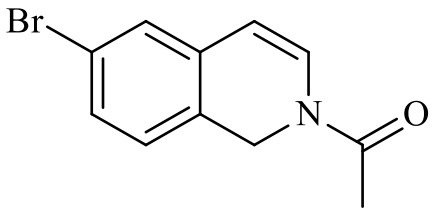

1d

1-(6-bromoisoquinolin-2(1H)-yl)ethanone (1d): DCM; : light-brown solid; M.P. (°C): 50 - 52; ^{1}H NMR (400 MHz, $CDCl_3$) δ: 7.27 – 7.22 (m, 1H), 7.14 (d, *J* = 2.0 Hz, 1H), 6.93 (d, *J* = 8.1 Hz, 1H), 6.67 (d, *J* = 7.9 Hz, 1H), 5.72 (d, *J* = 7.9 Hz, 1H), 4.85 (s, 2H), 2.19 (s, 3H).

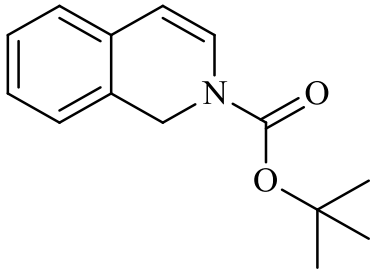

1e

***tert*-butyl isoquinoline-2(1H)-carboxylate (1e):** Hexane/EtOAc; light-yellow oil; ^{1}H NMR (400 MHz, $CDCl_3$) δ: 7.17 – 6.96 (m, 5H), 5.67 (br d, *J* = 7.0 Hz, 1H), 4.79 (s, 2H), 1.51 (s, 9H).

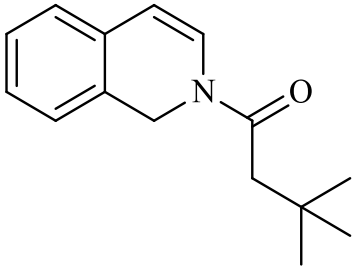

1f

1-(isoquinolin-2(1H)-yl)-3,3-dimethylbutan-1-one (1f): Hexane/EtOAc; orange oil; ^{1}H NMR (400 MHz, $CDCl_3$) δ: 7.16 – 7.10 (m, 2H), 6.61 (d, *J* = 7.8 Hz, 1H), 5.76 (d, *J* = 7.8 Hz, 1H), 4.89 (s, 2H), 2.56 (s, 2H), 1.09 (s, 9H); ^{13}C NMR (100 MHz, $CDCl_3$) δ: 167.9, 130.4, 129.4, 127.6, 127.3, 126.0, 125.9, 124.6, 109.6, 96.1, 49.3, 29.3.

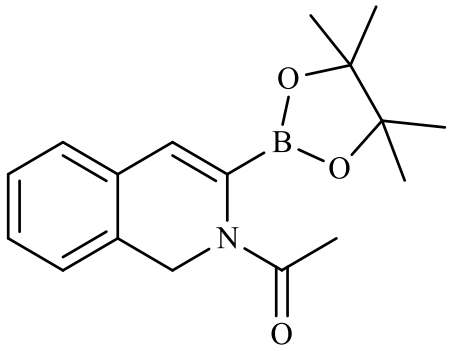

2a

1-(3-(4,4,5,5-tetramethyl-1,3,2-dioxaborolan-2-yl)isoquinolin-2(1H)-yl)ethanone (2a): EtOAc/MeOH; light yellow solid; M.P. (°C): 220-224; ^{1}H NMR (400 MHz, $CDCl_3$) δ: 7.17 (dt, J = 28.3, 7.7 Hz, 2H), 7.06 (d, *J* = 7.7 Hz, 1H), 7.00 (d, J = 7.8 Hz, 1H), 6.17 (s, 1H), 4.89 (s, 2H), 2.32 (s, 3H), 1.30 (s, 12H); ^{13}C NMR (100 MHz, $CDCl_3$) δ: 172.9, 130.2, 128.4, 127.2, 126.4, 125.5, 115.7, 45.6, 29.7, 25.3, 16.7; MS (EI, m/z): 299 (6, M^+), 284 (4), 256 (8), 255 (5), 241 (100), 199 (28), 184 (30), 156 (68), 141 (4), 129 (8), 115 (26), 103 (4), 89 (4), 77 (10), 69 (2) ,59 (2), 55 (6).

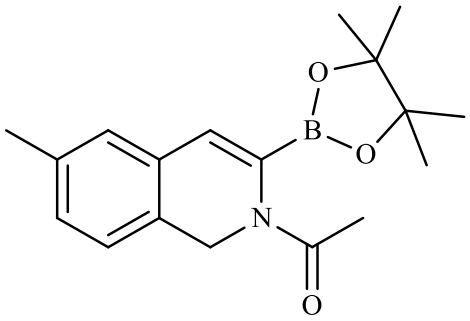

2b

1-(6-methyl-3-(4,4,5,5-tetramethyl-1,3,2-dioxaborolan-2-yl)isoquinolin-2(1H)-yl) ethanone (2b): EtOAc/MeOH; light yellow solid; ^{1}H NMR (400 MHz, $CDCl_3$) δ: 7.00 – 6.91 (m, 1H), 6.84 (s, 1H), 6.62 (d, J = 7.9 Hz, 1H), 5.76 (d, J = 7.8 Hz, 1H), 4.88 (s, 2H), 2.28 (s, 3H), 2.18 (s, 3H); ^{13}C NMR (100 MHz, $CDCl_3$) δ: 168.5, 137.3, 130.2, 127.9 , 127.6, 126.6, 126.0, 125.8, 125.6, 125.3, 109.8, 44.1, 21.3, 21.0; MS (EI, m/z): 377 (10, M^+), 362 (8), 336 (12), 321 (22), 320 (12), 319 (37), 281 (20), 266 (17), 254 (14), 253 (11), 236 (13), 209 (32), 208 (23), 194 (16), 193 (14), 191 (14), 177 (33), 135 (12), 104 (12), 96 (12), 83 (12), 73 (30).

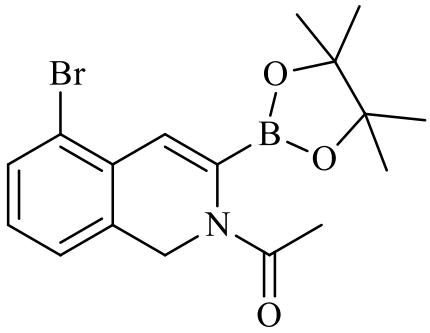

2c

1-(5-bromo-3-(4,4,5,5-tetramethyl-1,3,2-dioxaborolan-2-yl)isoquinolin-2(1H)-yl) ethanone (2c): EtOAc/MeOH; light yellow solid; M.P. (°C): 256.3; ^{1}H NMR (400 MHz, $CDCl_3$) δ: 7.41 (d, J = 7.3 Hz, 1H), 7.02 – 6.87 (m, 2H), 6.53 (s, 1H), 4.85 (s, 2H), 2.31 (s, 3H), 1.29 (s, 12H); ^{13}C NMR (100 MHz, $CDCl_3$) δ: 173.2, 132.8, 131.7, 129.7, 128.5, 127.95, 124.7, 121.9, 113.5, 81.2, 45.5, 25.2, 16.9; MS (EI, m/z): 322 (11, M^+), 321 (33), 320 (18), 319 (37), 318 (17), 267 (10), 262 (11), 253 (10), 236 (10), 235 (10), 234 (10), 209 (18), 208 (9), 207 (100), 191 (14), 177 (14), 155 (12), 135 (16), 96 (16), 73 (13).

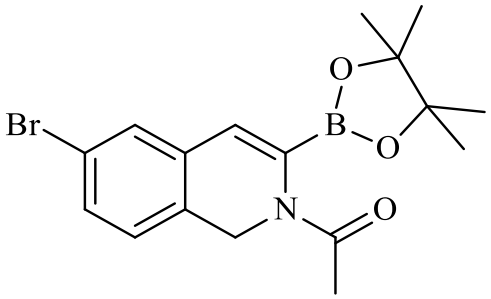

2d

1-(6-bromo-3-(4,4,5,5-tetramethyl-1,3,2-dioxaborolan-2-yl)isoquinolin-2(1H)- yl) ethanone (2d): EtOAc/MeOH; light yellow solid; M.P. (°C): 260-265; ^{1}H NMR (400 MHz, $CDCl_3$) δ: 7.82 (dd, J = 8.9, 1.0 Hz, 1H), 6.99 (dd, J = 8.9, 0.6 Hz, 1H), 6.85 (d, J = 8.0 Hz, 1H), 6.05 (s, 1H), 4.81 (s, 2H), 2.30 (s, 3H), 1.23 (s, 12H); ^{13}C NMR (100 MHz, $CDCl_3$) δ 173.1, 132.8, 129.7, 128.5, 127.9, 124.7, 121.9, 113.6, 113.5, 81.2, 45.5, 25.2.

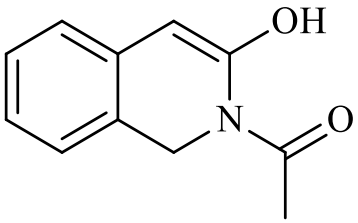

3a

1-(3-hydroxyisoquinolin-2(1H)-yl)ethanone (3a): Hexane/EtOAc; white solid; ^{1}H NMR (400 MHz, $CDCl_3$) δ: 7.36 – 7.05 (m, 4H), 5.25 (s, 1H), 4.87 (s, 2H), 2.12 (s, 3H), 0.84 (s, 1H); ^{13}C NMR (100 MHz, $CDCl_3$) δ: 172.9, 161. 5, 128.1, 127.6, 127.3, 126.5, 125.9, 124.6, 96.1, 44.3, 24.8; MS (EI, m/z): 190 (5, M^+), 189 (40), 148 (3), 147 (34), 146 (100), 128 (3), 119 (16), 118 (47), 117 (6), 92 (3), 91 (32), 90 (40), 89 (26), 84 (4), 77 (4), 65 (8), 64 (4), 63 (9), 51 (5), 49 (4).

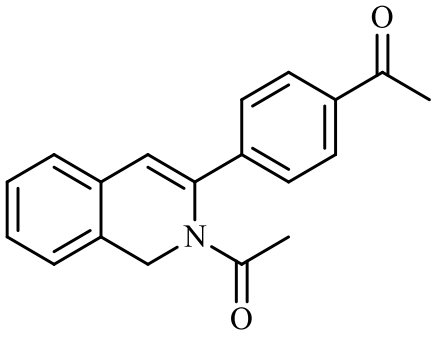

4a

1-(4-(2-acetyl-1,2-dihydroisoquinolin-3-yl)phenyl)ethanone (4a): Hexane/EtOAc; yellow oil; ^{1}H NMR (400 MHz, $CDCl_3$) δ: 7.99 (d, *J* = 8.3 Hz, 1H), 7.62 (d, *J* = 8.3 Hz, 1H), 7.27 – 7.24 (m, 1H), 6.72 (s, 1H), 5.03 (s, 1H), 2.62 (s, 1H), 1.60 (s, 1H); ^{13}C NMR (100 MHz, $CDCl_3$) δ: 197.3, 171.2, 142.2, 138.9, 136.8, 133.4, 131.8, 129.2, 128.4, 127.8, 126.3, 125.8, 125.5, 119.9, 45.9, 26.7, 24.1; MS (EI, *m/z*): 291 (24, M^+), 261 (4), 248 (100), 206 (24), 178 (6), 167 (6), 149 (4), 128 (6), 112 (6), 102 (4), 83 (4), 77(4), 70 (10), 57 (6).

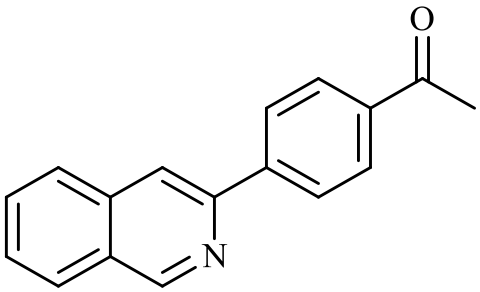

5a

1-(4-(isoquinolin-3-yl)phenyl)ethenone (5a): Hexane/EtOAc; red solid; ^{1}H NMR (400 MHz, $CDCl_3$) δ: 9.35 (s, 1H), 8.22 (d, *J* = 8.6 Hz, 1H), 8.14 (s, 1H), 8.08 (d, *J* = 8.6 Hz, 1H), 8.01 (d, *J* = 8.2 Hz, 1H), 7.90 (d, *J* = 7.9 Hz, 1H), 7.72 (ddd, *J* = 8.2, 6.9, 1.2 Hz, 1H), 7.62 (ddd, *J* = 8.1, 6.9, 1.1 Hz, 1H), 2.65 (s, 1H); ^{13}C NMR (100 MHz, $CDCl_3$) δ: 197.9, 152.6, 149.7, 143.9, 136.7, 136.4, 130.9, 128.9, 128.1, 127.7, 127.6, 127.1, 127.0, 117.6, 26.8; MS (EI, *m/z*): 247(64, M^+), 232 (100), 204 (52), 176 (20), 151 (6), 128 (2), 116 (18), 101 (10), 88 (12), 75 (8), 61 (4), 51 (2).

CHAPTER 4

RESULT AND DISCUSSION

In this study, various parameters for obtaining regioselective organoboron products were examined primarily by using dihydroisoquinoline and its derivatives. Optimization studies were performed with different combinations of boron source, ligand, and solvent under thermal conditions.

Table 4.1. Effects of boron source, ligand, and solvent types on the borylation of 1a.

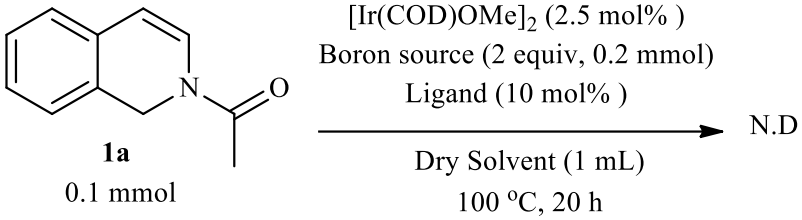

No	Boron	Ligand	Solvent	Conversion%[a]
1	B_2pin_2	dtbpy	MTBE	N.D
2	HBpin	dtbpy	MTBE	N.D
3	HBpin	$AsPh_3$	MTBE	N.D
4	B_2pin_2	$AsPh_3$	Cyclohexane	N.D
5	B_2pin_2	$AsPh_3$	Octane	N.D

a) Determined by GC.

The first trials were conducted to determine the optimum boron source for the borylation reaction of N-acyl-1,2-dihydroisoquinoline with dtbpy in MTBE solvent at 100 °C (Table 4.1, entries 1 and 2). All of these reactions are done without catalyst pre-

activation. Although iridium complexes bearing dtbpy are mostly preferred in aromatic C-H borylation, no organoboron products were formed to determine under these conditions. The relatively strong coordination ability of dtbpy should have inhibited the coordination of carbonyl oxygen in the substrate to the iridium center. On the basis of these results, a soft monodentate ligand, $AsPh_3$ was decided to evaluate, which is effective in the borylation of structures containing carbonyl groups.[33] Unfortunately, in the presence of $AsPh_3$, the use of different boron sources and solvents did not have a positive effect on borylation (Table 4.1, entries 3-5). Performing the reactions at elevated temperatures for a prolong time causes the catalyst to decompose and prevents catalytic activity.

Table 4.2. Effect of pre-stirring on the borylation reaction.

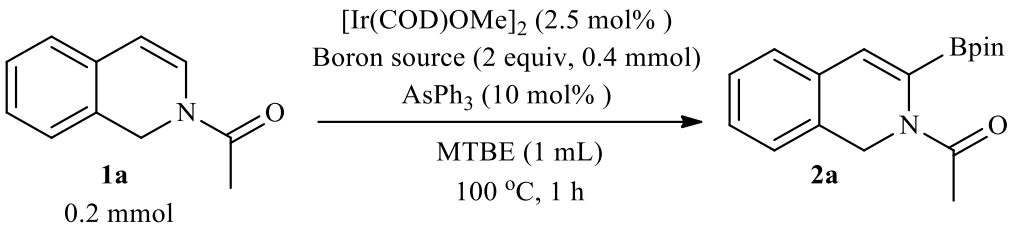

No	Boron	Pre-stirring	Conversion%[a]	Yield%[a]
1	HBpin	-	31	9
2	HBpin	+	23	13
3	B_2pin_2	-	76	53
4	B_2pin_2	+	100	83[b]

a) Calculations are determined by internal standard using p- anisaldehyde on NMR.
b) Isolated yield.

The iridium complex can enter the catalytic cycle in its active form. Ir catalyst, boron, and ligand were mixed in an inert atmosphere in the solvent for two minutes for in situ pre-activation of the complex. The effects of this method on the reaction in the presence of HBpin and B_2pin_2 are shown in Table 4.2. HBPin apparently is not a suitable boron source for the borylation process, because low yields were obtained with this reagent whether pre-stirring is applied or not (Table 4.2, entries 1 and 2). Borylation

reactions were also carried out without pre-mixing where the reactant might coordinate before the catalyst complex reaches its active form. A promising result could be obtained with the use of B_2Pin_2; nevertheless pre-activation process apparently is useful to augment the conversion of **1a** to the desired product **2a** ((Table 4.2, entries 3 and 4). Pre-activation of the catalyst complex accelerated the catalytic cycle and increased the yield of **2a**. The most suitable method for borylation reactions seems to involve catalyst pre-activation step with B_2pin_2.

The mass spectrum of **2a** obtained by GC/MS analysis coincide with the putative borylated structure. The NMR data also shows with certainty that the acyl group attached to nitrogen acts as a director in the carbon-hydrogen activation of the metal.

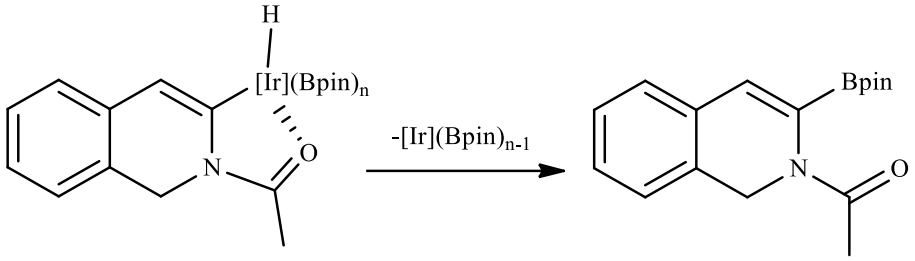

Figure 4.1. Iridium-catalyzed borylation of N-acyl-1,2-dihydroisoquinoline.

NOE and NOESY techniques revealed the interaction of unborylated alkenyl hydrogen H4 and aromatic hydrogen H5, confirming that borylation occurs exclusively from the position 3. The exact structural evidence will be made possible by X-ray analysis.

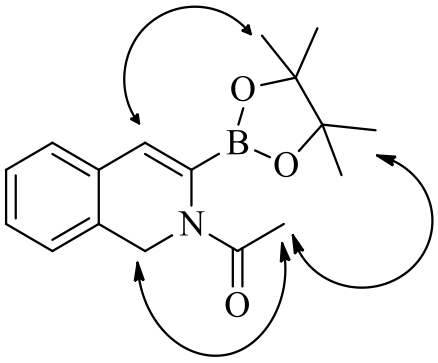

Figure 4.2. NOE study of 2a.

The catalytic cycle proposed is outlined in Figure 4.3.

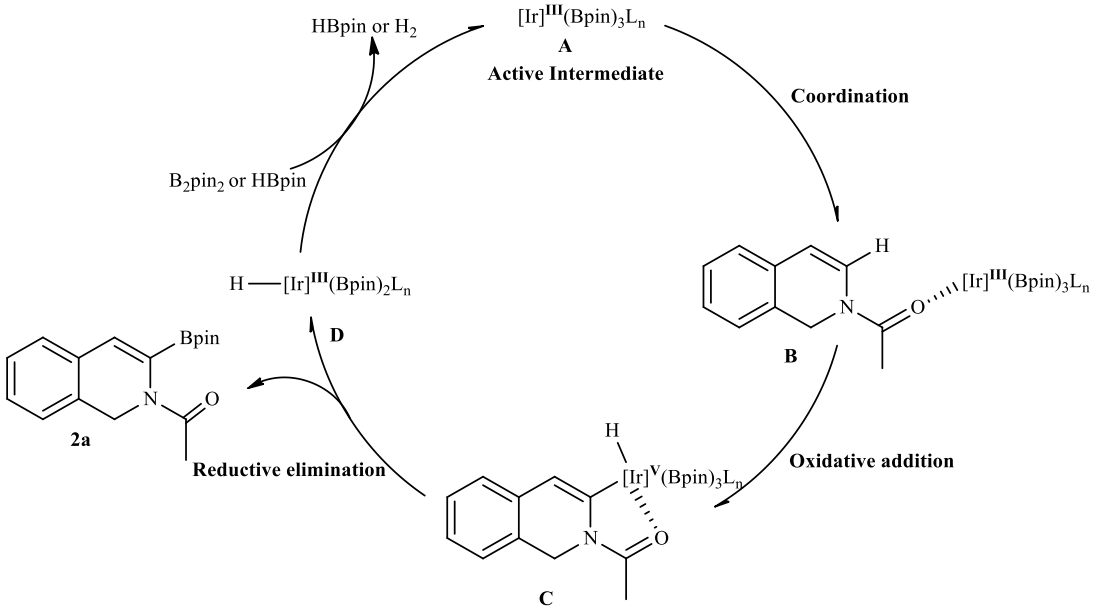

Figure 4.3. Proposed catalytic cycle.

First, the reaction of the Ir (I) complex with B_2Pin_2 and ligand results in the formation of the active tris-boryl Ir (III) complex **A**. The oxygen atom that donates electrons in the ester group coordinates with the metal center of Iridium (**B**). **C** is then obtained by oxidative addition of vinyl C-H bond to **A**. As a result of reductive elimination, Ir-hydride complex **D** and product **2a** are produced. Finally, B_2pin_2 is added oxidatively to **D**, and then the cycle is completed by replenishing **A** and formation of HBpin.

Table 4.3. Optimization of B_2pin_2 amount.

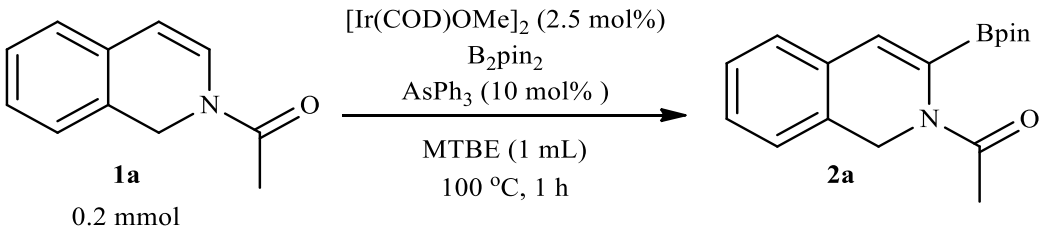

No	B_2pin_2 (equiv)	Conversion%[a]	Yield%[b]
1	1.2	63	10
2	1.5	74	16

(cont. on the next page)

(Con. of. Table 4.3)

3	2	100	83[b]
4	2.5	56	48
5	3	59	58

a) Determined by 1H NMR technique using *p*-anisaldehyde as the internal standard.
b) Isolated yield.

The presence of 1.2 or 1.5 equivalents of boron appears to be ineffective for the yield (Table 4.3, entries 1 and 2). When the ratio was increased to 2 equivalents, the conversion was complete, and the yield increased dramatically to 83% (Table 4.3, entry 3). While the active catalyst reaches maximum capacity in the presence of 2 equivalent of B_2pin_2, further increase of the boron reagent appears to be detrimental for the formation of the product (Table 4.3, entries 4 and 5). Thus, the optimum boron amount for the efficiency of the catalytic activity was determined to be 2 equivalents. The choice of inert solvent is also critical for borylation reactions. The effects of solvent properties on reaction time and yield are shown in Table 4.4.

Table 4.4. Effects of solvent type on N-acyl-1,2-dihydroisoquinoline.

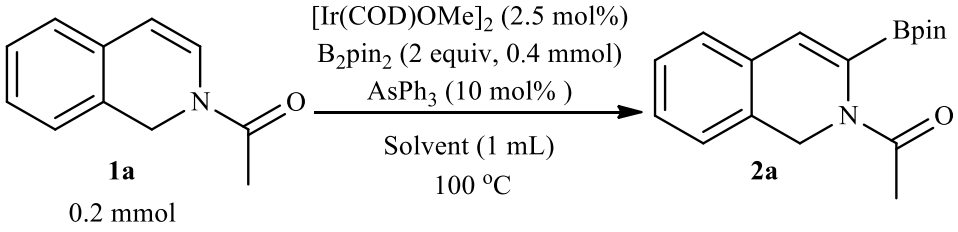

1a
0.2 mmol

2a

No	Solvent	Time, h	Conversion%[a]	Yield%[a]
1	Trifluorobenzene	6	N.D	
2	Diethylene glycol dibutyl ether	6	N.D	
3	Decane	4	45	48
4	Cyclopentylmethylether	4	79	67

(cont. on the next page)

(Con. of. Table 4.4)

5	MTBE	1	100	83[b]
6	THF	4	100	65
7	Dioxane	4	73	58

a) Determined by GC technique using *trans*-stilbene as the internal standard.
a) Isolated yield.

Nonpolar solvents are mostly suitable for Ir-catalyzed C-H borylation reactions[75, 76], but there was a complete loss of reactivity in 1,3,5-trifluorobenzene and diethylene glycol dibutyl ether (Table 4.4, entries 1 and 2). The use of decane slows down the reaction, so a longer reaction time is required for complete conversion (Table 4.4, entry 3).

The catalytic activity of the reaction was promoted with cyclopentyl methyl ether solvent (Table 4.4, entry 4). When the solvent is changed to MTBE, the conversion is completed in just 1 hour and gave rise to the highest product yield (Table 4.4, entry 5). More polar solvents such as THF and dioxane were less effective solvents for the method, affording the desired product relatively in lower yields (Table 4.4, entries 6 and 7)

In the next stage of optimization studies, ligand activity was investigated. The effect of various ligands on the borylation reaction has been evaluated at 100 °C of reaction temperature.

Table 4.5. Ligand effects on borylation reaction.

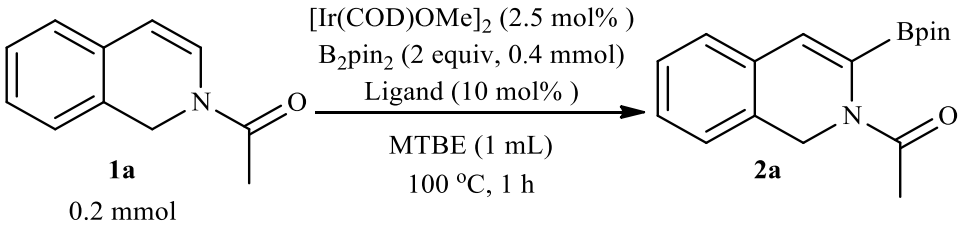

No	Ligand	Conversion%[a]	Yield%[a]
1	Dtbpy (5%)	N.D	

(cont. on the next page)

(Con. of. Table 4.5)

2	PPh_3	N.D	
3	Tris-4-trifluoromethylphenylphosphine	N.D	
4	tris(3,5-bis(trifluoromethyl)phenyl)phosphine	100	25
5	$SbPh_3$	63	57
6	$AsPh_3$	100	83[b]

a) Determined by ^{1}H NMR technique using *p*-anisaldehyde as the internal standard.
b) Isolated yield

Initially, the iridium complex carrying the bidentate dtbpy ligand was used, but no borylated product was formed (Table 4.5, entry 1). Following these results, the effect of monodentate phosphine ligands was also studied. Large cone angle ligands such as PPh_3 and electronically poor tris-4-trifluoromethylphenylphosphine had no effect on the reaction (Table 4.5, entries 2 and 3).

Complexes carrying the more electron-poor ligand, such as tris(3,5-bis(trifluoromethyl)phenyl)phosphine, achieved complete conversion but showed low selectivity (Table 4.5, entry 4). Therefore, phosphorus-free ligands were investigated. A lower yield was obtained with the extremely soft ligand triphenylstibine than with the $AsPh_3$ ligand (Table 4.5, entries 5 and 6). It has also been shown in the literature that $AsPh_3$ is also a good ligand in iridium-catalyzed *ortho*-borylation acetophenone derivatives.[77, 78]

Therefore, optimization studies were continued with $AsPh_3$. In addition, the effects of iridium complexes, boron, and ligands on the method were also investigated in Table 4.6.

Table 4.6. Effects of iridium complex, boron, and ligand sources.

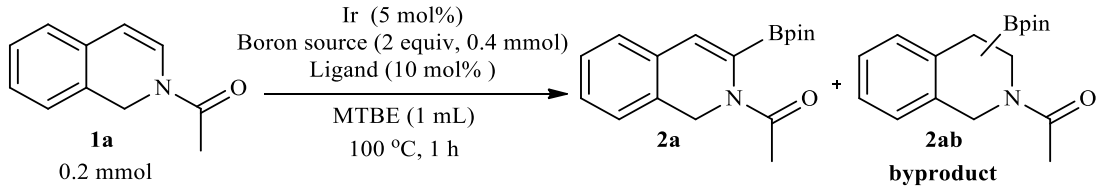

(cont. on the next page)

(Con. of. Table 4.6)

No	Catalyst	Boron	Ligand	Conversion%[a]	Yield%[a]
1	$IrCl_3$	B_2pin_2	$AsPh_3$	N.D	
2	[Ir(COD)(IMes)Cl]	B_2pin_2	$AsPh_3$	N.D	
[b]3	$[Ir(COD)Cl]_2$	B_2pin_2	$AsPh_3$	44	17
4	$[Ir(COD)Cl]_2$	HBpin	$AsPh_3$	N.D	
5	$[Ir(COD)Cl]_2$	B_2pin_2	PPh_3	N.D	
6	$[Ir(COD)Cl]_2$	B_2pin_2	Tris(4-trifluoromethylphenyl)phosphine	N.D	
7	$[Ir(COD)Cl]_2$	B_2pin_2	------	N.D	
8	$[Ir(COD)OMe]_2$	HBpin	------	N.D	
[c]9	$[Ir(COD)OMe]_2$	B_2pin_2	------	90	43

a) Determined by GC technique using *trans*-stilbene as the internal standard.
b) 14% of byproduct was formed.
c) 17% of byproduct was formed.

Ir (III) complexes such as $IrCl_3$ and [Ir(COD)(IMEs)Cl] have shown no catalytic activity (Table 4.6, entries 1-2). When $[Ir(COD)Cl]_2$ is used as a catalyst precursor with B_2pin_2, it results in a slow reaction rate (Table 4.6, entry 3). Besides, the selectivity is low as the byproduct (**2ab**) is formed. When the boron source was changed to HBpin, it did not give any products (Table 4.6, entry 4). Phosphine derivatives as a ligand source also did not give effective results (Table 4.6, entries 5 and 6).

Ligand-free experiments were also performed using $[Ir(COD)Cl]_2$ complex and it was proved that conversion of **1a** would not be possible in the absence of a ligand with this iridium complex (Table 4.6, entry 7). No product formation could be observed in the presence of $[Ir(COD)(OMe)]_2$ complex and HBpin under ligand free conditions (Table 4.6, entry 8). The reaction with B_2pin_2 provides higher activity in the presence of

$[Ir(COD)(OMe)]_2$ under ligand free condition, but also leads to the formation of a reduced product **2ab** (Table 4.6, entry 9).

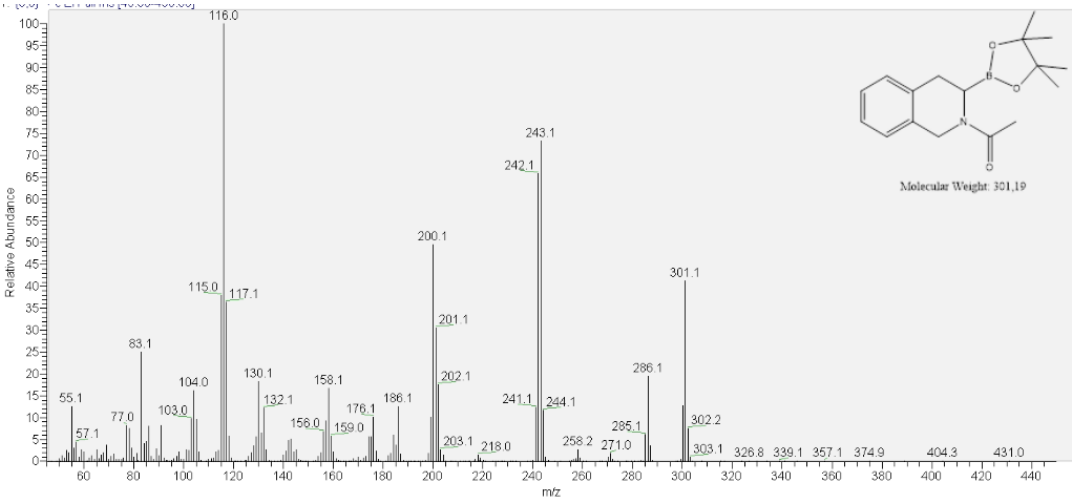

Figure 4.4. GC/MS spectrum of hydrogenated monoborylated by-product.

During the reaction, hydrogenated monoborylated by-product (**2ab**) is formed. This structure has been shown in the GC/MS spectrum (Figure 4.4). However, it could not be isolated by chromatographic methods. In summary, it has been determined that the most effective combination appears to be $[Ir(COD)(OMe)]_2$ /$AsPh_3$ catalyst combination to avoid the formation of by-products and thus, to obtain the desired borylated product.

Table 4.7. Effects of ligand/catalyst ratio.

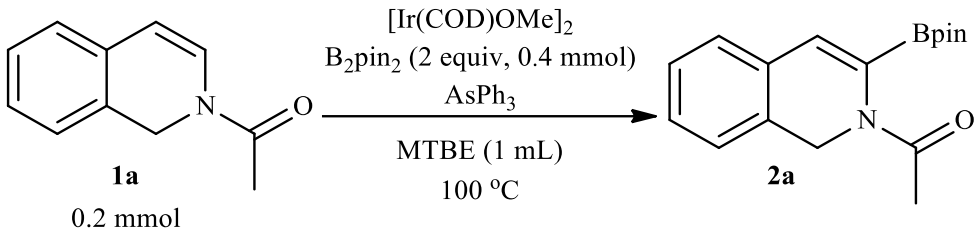

No	Ir%	Asph$_3$%	Time	Conversion%[a]	Yield%[a]
1	1	2	4 h	N.D	
2	1	5	4 h	59	44

(cont. on the next page)

(Con. of. Table 4.7)

3	5	5	1 h 40 min	100	61
4	5	7.5	2 h	100	66
5	5	10	70 min	100	85[b]
6	5	15	1 h 20 min	64	31
7	5	20	3 h	N.D	

a) Determined by ^{1}H NMR technique using *p*-anisaldehyde as the internal standard.
b) Isolated yield

Given the considerations in contamination of the end products and high cost of precious metals and ligands, the use of low concentration of catalysts is desired in industrial applications. Unfortunately, however, a lower catalyst loading could not be afforded by the method (Table 4.7, entries 1 and 2). The ligand to catalyst ratio has a critical role on the borylation activity. With the iridium loading of 5%, the optimum $AsPh_3$:Ir ratio appears to be 2/1 (Table 4.7, entries 3-7).

Table 4.8. Effects of solvent amount.

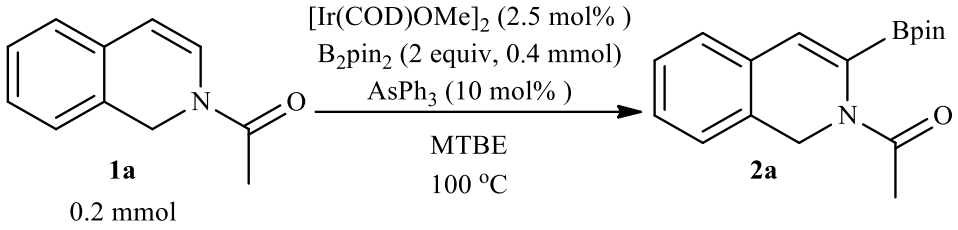

No	MTBE, mL	Time	Conversion%[a]	Yield%[a]
1	0.5	1.5 h	72	34
2	1	70 min	100	85[b]
3	1.5	70 min	75	45

a) Determined by ^{1}H NMR technique using *p*-anisaldehyde as the internal standard.
b) Isolated yield

The optimal amount of solvent for the reaction was also screened. The solubility of reactants is not sufficient within 0.5 mL of MTBE (Table 4.8, entry 1). The reactions carried out in 1 mL of solvent have achieved complete conversion and high selectivity (Table 4.8, entry 2). However, the use of higher volume the solvent (1.5 mL) was detrimental for the process.

Table 4.9. Effect of time and temperature on the borylation reaction.

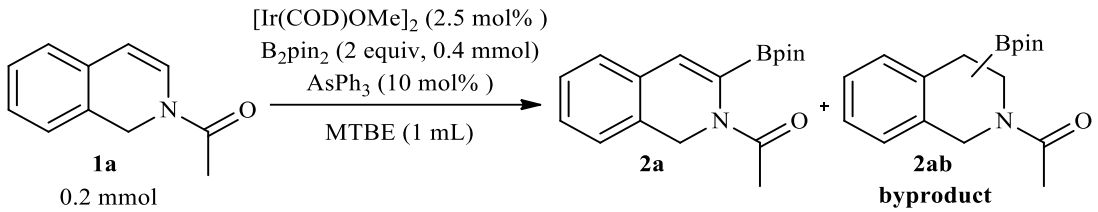

No	Thermal Condition, °C	Time	Conversion%[a]	2a%[a]	2ab%[a]
1	70	4 h	N.D		0
2	80	4 h	N.D		0
3	100	33 min	52	33	0
4	100	70 min	100	85[b]	0
5	100	2 h 40 min	100	47	0
6	110	35 min	52	34	0
7	110	1 h	59	45	6
8	110	4 h	100	42	9
9	120	15 min	71	46	5
10	120	30 min	84	66	6
11	120	1 h	86	57	5
12	120	4 h	100	37	10

a) Determined by ^{1}H NMR technique using *p*-anisaldehyde as the internal standard.
b) Isolated yield

In the last part of the optimization study, the effects of temperature and time on catalytic activity were examined. No catalytic activity is determined at lower 70 and 80 °C (Table 4.9, entries 1 and 2). In the experiments carried out at 100 °C, 70 minutes of the reaction time is needed for complete conversion (Table 4.9, entries 3 and 4), however, when the reaction time is further extended, the yield dramatically decreases. It seems that the borylation product is prone to decomposition under reaction conditions, thus prolonged reaction times gave rise to lower yields (Table 4.9, entry 5). Application of higher reaction temperatures is found to be unsuitable for the process, usually leading to the lower yields (Table 4.9, entries 6-12).

The substrate scope of the method determined for Ir-catalyzed borylation has been investigated on dihydroisoquinoline derivatives containing functional groups with different electronic effects. The functional group tolerance of borylation seems to be generally sufficient.

Table 4.10. Borylation of 1b.

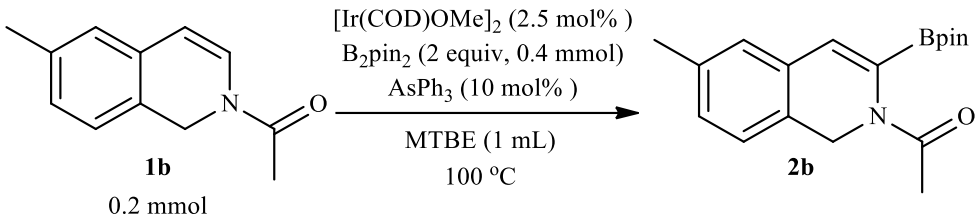

No	Time	Conversion%[a]	Yield%[a]
1	1 h 20 min	63	24
2	2 h 15 min	67	33
2	2 h 30 min	66	33
3	3 h	69	49
5	4 h	100	65[b]

a) Determined by ^{1}H NMR technique using *p*-anisaldehyde as the internal standard.
b) Isolated yield

6-Methyl-substituted dihydroquinoline **1b** is relatively less reactive as compared to its non-substituted counterpart, requiring 4 h of reaction time for complete conversion to furnish the desired borylated product **2b** in a moderate yield (Table 4.10, entries 1-5).

Table 4.11. Borylation of 1c.

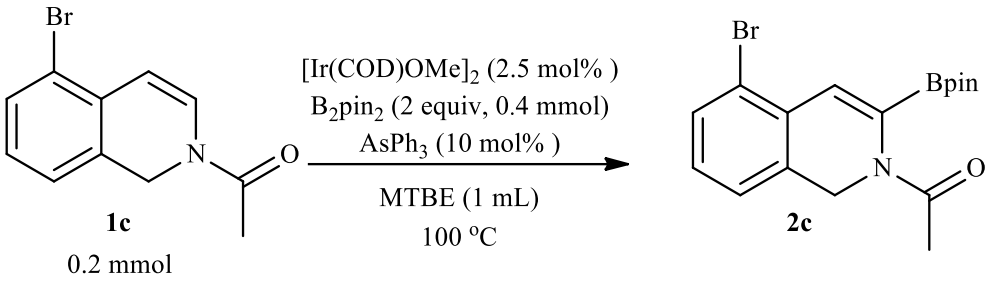

No	Time	Conversion%[a]	Yield%[a]
1	1 h 30 min	47	25
2	3 h 30 min	65	23
3	5 h	73	29[b]
c) 4	1 h 10 min	66	24[b]
d) 5	2 h 15 min	80	28
e) 6	2 h 20 min	N.D	

a) Determined by ^{1}H NMR technique using *p*-anisaldehyde as the internal standard.
b) Isolated yield.
c) 1.5 mL MTBE was used.
d) Ligan/Ir ratio is 1:1.
e) $[Cp^*IrCl_2]_2$ used as a catalyst.

5-Bromo-substituted dihydroquinoline **1c** was even much less reactive toward borylation, maximum 29% yield of **2c** could be obtained and the conversion was incomplete even at prolonged reaction times (Table 4.11, entries 1-3). Diversification of reaction parameters, such as the increase of solvent volume or reducing the ligand to iridium ratio did not have any positive effect on the activity of the substrate **1c** (Table 4.11, entries 4 and 5). Moreover, the conversion **1c** was nil with the use of Ir(III) complex $[Cp^*IrCl_2]_2$ (Table 4.11, entry 6).

Table 4.12. Borylation of 1d.

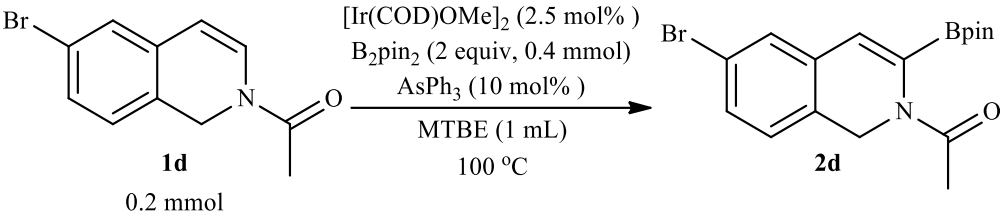

No	Time, h	Conversion%	Yield%[a]
1	6	89	32
[c] 2	3	79	76 [b]

a) Calculations are determined by internal standard using p-anisaldehyde on NMR.
b) Isolated yield.
c) Ligand/Ir ratio is 1:1.

Interestingly, on contrary to the finding with unsubstituted dihydroisoquinoline, $AsPh_3$ to Ir ratio of 1:1 revealed superior activity for the conversion 6-Bromo-substituted dihydroisoquinoline **1d** as compared with 2:1 ratio. (Table 4.12, entries 1 and 2). It seems that less coordinated iridium is more active in C-H activation of electron-poor dihydroisoquinoline substrates.

In conclusion, when optimized conditions applied to dihydroisoquinolines containing electron-donating and withdrawing groups, both substrates afforded the same *3*-selective monoboryl-substituted products selectively. Further research will be carried out on dihydroisoquinolines to widen scope of the method.

Table 4.13. Borylation with different N-protecting groups.

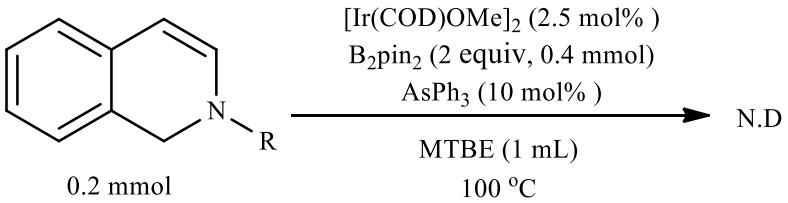

No	R	Yield%[a]
1	Boc	N.D
2	Pivaloyl	N.D

a) Analyzed by GC.

Borylation selectivity should be achieved as a result of the inner sphere direction via coordinative effect of the acyl group bound on the nitrogen. Hence, the reactions were also carried out Boc and Pivaloyl protected dihydroisoquinoline (**1e** and **1f**) also under the optimum conditions so as to determine whether the method would be applicable with different directing groups. However, no catalytic activity was observed in either group (Table 4.13, entries 1 and 2). Sterical congestion might have blocked effective coordination of the carbonyl group with iridium metal core.

Table 4.14. Metal-free borylation with BBr_3.

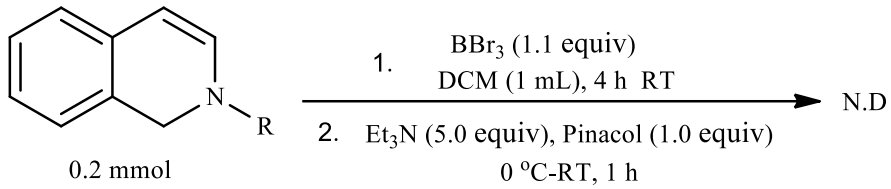

0.2 mmol

No	R	Yield%[a]
1	IsqAc	N.D
2	IsqBoc	N.D
3	IsqPiv	N.D
[b]4	IsqPiv	N.D
[c]5	IsqPiv	N.D

a) Analyzed by GC.
b) Reaction conducted for 16 h.[70]
c) Reaction conditions; BBr_3 (2.5 equiv), DCM, 120 °C, 12 h, then DMAP (4.0 eq.), Pinacol (3.0 eq.), DMF, 120 °C, 2 h.[79]

Due to economic and environmental concerns, metal-free C-H borylation methods have been increasingly more popular.[80-84] It has been reported by a number of groups that acyl groups are also active for selective directed borylation under metal free conditions, provided that a strongly Lewis acidic boron reagent is used, such as BBr_3 and BCl_3. However, all of our trials with BBr_3 under metal free conditions frustratingly failed to produce any borylated product (Table 4.14, entries 1-5).

Organoboranes can be turned into versatile intermediates in the construction of complex molecules with a number of applications.[85-90]

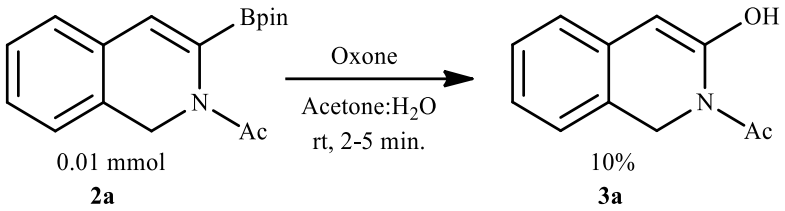

Figure 4.5. Oxidation reaction with oxone.

It is well known that the hydroxyl group is formed by oxidation of the boryl group with Oxone.[72] When the practical method shown in Figure 4.5 is applied to **2a**, the oxidized product **3a** could be obtained only with a 10% yield (Figure 4.5).

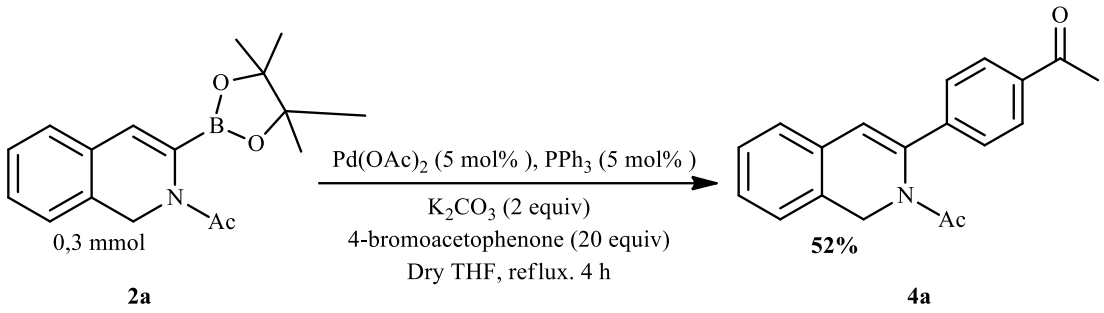

Figure 4.6. Suzuki-Miyaura coupling reaction of 2a.

When the Suzuki-Miyaura coupling reaction applied to **2a** with a Pd catalyst in the presence of aryl halide and a base, however, under an unoptimized condition **4a** coupling product was obtained with a moderate yield (Figure 4.6). Thus, it has been proven that the synthesized borylated dihydroisoquinoline derivatives can be subjected to the Suzuki reaction in the presence of various functional groups.

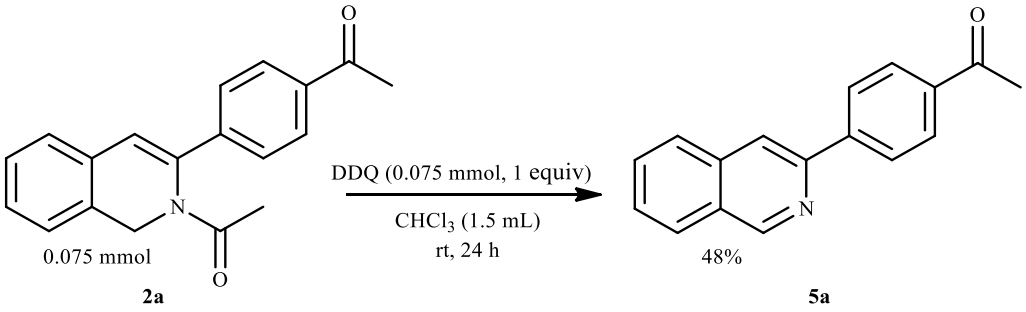

Figure 4.7. Oxidation of 2a with DDQ.

The borylated dihydroisoquinoline or its derivatives can be converted into isoquinoline structures by dehydrogenation.[66, 91] 3-Arylisoquinolines are important because of their prominent biological activity.[92, 93] So, **2a** was converted to 3-arylisoquinoline by reaction with a strong oxidant DDQ at room temperature (Figure 4.6). This method may be practical for the oxidation of substituted dihydroisoquinolines.

CHAPTER 5

CONCLUSION

Organoboranes are the basic building blocks, and their selective production is important for application studies. They have capable of transformation into many functional structures. In this thesis, a new method for iridium-catalyzed borylation of dihydroisoquinolines is presented. It has been found that N-acetyl substituted dihydroisoquinolines undergo borylation selectively on the position of C-3 (Sp^2 C adjacent to the nitrogen atom).

Some factors, such as iridium compounds, boron source, ligand, solvent, time, and temperature, were investigated in the optimization studies. The reactions carried out under thermal conditions are powerful in terms of efficiency and selectivity. The optimal condition involves the use of B_2pin_2 reagent, $[Ir(COD)OMe]_2/AsPh_3$ catalyst combination, and MTBE as the reaction solvent. The optimum reaction temperature is determined to be 100 °C.

During the reaction, iridium should coordinate to the carbonyl group and orients to the adjacent alkenyl carbon-hydrogen bond. Thus, C-3 selective borylated dihydroisoquinoline was achieved by the inner-sphere directing effect of the acyl group. The ligand effect is the key point in these reactions. $AsPh_3$ should bind to the iridium complex with poor coordination ability and provides high selectivity.

This new strategy can be applied to the various dihydroisoquinoline derivatives. The effects of substituent groups with various electronic properties on borylation were observed. Due to the economic and environmental concerns, metal-free borylation reactions with BBr_3 have also been tried but all failed. Finally, the applicability of the borylated products has been shown by simply turning them into their diverse forms. The scope and limits of the method will be continued to be developed.

REFERENCES

1. Kmieciak, A.; Ćwiklińska, M.; Jeżak, K.; Shili, A.; Krzemiński, M. P., Searching for New Biologically Active Compounds Derived from Isoquinoline Alkaloids. Chemistry Proceedings 2021, 3 (1), 97.

2. Gilmore, C. D.; Allan, K. M.; Stoltz, B. M., Orthogonal Synthesis of Indolines and Isoquinolines via Aryne Annulation. Journal of the American Chemical Society 2008, 130 (5), 1558-1559.

3. Tsuboyama, A.; Iwawaki, H.; Furugori, M.; Mukaide, T.; Kamatani, J.; Igawa, S.; Moriyama, T.; Miura, S.; Takiguchi, T.; Okada, S., Homoleptic cyclometalated iridium complexes with highly efficient red phosphorescence and application to organic light-emitting diode. Journal of the American Chemical Society 2003, 125 (42), 12971-12979.

4. Zhao, Q.; Liu, S.; Shi, M.; Wang, C.; Yu, M.; Li, L.; Li, F.; Yi, T.; Huang, C., Series of new cationic iridium (III) complexes with tunable emission wavelength and excited state properties: structures, theoretical calculations, and photophysical and electrochemical properties. Inorganic chemistry 2006, 45 (16), 6152-6160.

5. Zhao, Z.; Yang, X.-H.; Tao, Z.-W.; Xu, H.-R.; Liu, K.; Chen, G.-Y.; Mo, Z.-R.; Wu, S.-X.; Niu, Z.-G.; Li, G.-N., Synthesis and Characterization of High-Efficiency Red Phosphorescent Iridium(III) Complexes with 1-(4-(Trifluoromethyl)phenyl)isoquinoline Ligand. 2019 2019, 66 (4), 9.

6. Ji, L.; Krummenacher, I.; Friedrich, A.; Lorbach, A.; Haehnel, M.; Edkins, K.; Braunschweig, H.; Marder, T. B., Synthesis, Photophysical, and Electrochemical Properties of Pyrenes Substituted with Donors or Acceptors at the 4-or 4, 9-Positions. The Journal of organic chemistry 2018, 83 (7), 3599-3606.

7. Ji, L.; Lorbach, A.; Edkins, R. M.; Marder, T. B., Synthesis and photophysics of a 2, 7-disubstituted donor–acceptor pyrene derivative: An example of the application of sequential Ir-catalyzed C–H borylation and substitution chemistry. The Journal of organic chemistry 2015, 80 (11), 5658-5665.

8. Oda, S.; Ueura, K.; Kawakami, B.; Hatakeyama, T., Multiple Electrophilic C–H Borylation of Arenes Using Boron Triiodide. Organic letters 2020, 22 (2), 700-704.

9. Liu, Z.; Wang, Y.; Chen, Y.; Liu, J.; Fang, Q.; Kleeberg, C.; Marder, T. B., Ir-catalyzed direct borylation at the 4-position of pyrene. The Journal of organic chemistry 2012, 77 (16), 7124-7128.

10. Xu, L.; Wang, G.; Zhang, S.; Wang, H.; Wang, L.; Liu, L.; Jiao, J.; Li, P., Recent advances in catalytic C− H borylation reactions. Tetrahedron 2017, 73 (51), 7123-7157.

11. Hartwig, J. F., Borylation and silylation of C–H bonds: a platform for diverse C–H bond functionalizations. Accounts of chemical research 2012, 45 (6), 864-873.

12. Brown, H. C., Organic syntheses via boranes. Wiley: 1975.

13. Ishiyama, T.; Nobuta, Y.; Hartwig, J. F.; Miyaura, N., Room temperature borylation of arenes and heteroarenes using stoichiometric amounts of pinacolborane catalyzed by iridium complexes in an inert solvent. Chemical communications 2003, (23), 2924-2925.

14. Cho, J.-Y.; Tse, M. K.; Holmes, D.; Maleczka, R. E.; Smith, M. R., Remarkably Selective Iridium Catalysts for the Elaboration of Aromatic C-H Bonds. 2002, 295 (5553), 305-308.

15. Tajuddin, H.; Harrisson, P.; Bitterlich, B.; Collings, J.; Sim, N.; Batsanov, A.; Cheung, M.; Kawamorita, S.; Maxwell, A.; Shukla, L., Chem. Sci. 2012.

16. Mkhalid, I. A.; Barnard, J. H.; Marder, T. B.; Murphy, J. M.; Hartwig, J. F., C− H activation for the construction of C− B bonds. Chemical Reviews 2010, 110 (2), 890-931.

17. Kallepalli, V. A.; Shi, F.; Paul, S.; Onyeozili, E. N.; Maleczka Jr, R. E.; Smith III, M. R., Boc Groups as Protectors and Directors for Ir-Catalyzed C− H Borylation of Heterocycles. The Journal of organic chemistry 2009, 74 (23), 9199-9201.

18. Ishiyama, T.; Miyaura, N., Iridium-catalyzed borylation of arenes and heteroarenes via CH activation. Pure and applied chemistry 2006, 78 (7), 1369-1375.

19. Preshlock, S. M.; Plattner, D. L.; Maligres, P. E.; Krska, S. W.; Maleczka Jr, R. E.; Smith III, M. R., A Traceless Directing Group for C□ H Borylation. Angewandte Chemie International Edition 2013, 52 (49), 12915-12919.

20. Klečka, M.; Pohl, R.; Klepetářová, B.; Hocek, M., Direct C–H borylation and C–H arylation of pyrrolo [2, 3-d] pyrimidines: synthesis of 6, 8-disubstituted 7-deazapurines. Organic & biomolecular chemistry 2009, 7 (5), 866-868.

21. Iverson, C. N.; Smith, M. R., Stoichiometric and catalytic B-C bond formation from unactivated hydrocarbons and boranes. Journal of the American Chemical Society 1999, 121 (33), 7696-7697.

22. Ishiyama, T.; Takagi, J.; Ishida, K.; Miyaura, N.; Anastasi, N. R.; Hartwig, J. F., Mild Iridium-Catalyzed Borylation of Arenes. High Turnover Numbers, Room Temperature Reactions, and Isolation of a Potential Intermediate. Journal of the American Chemical Society 2002, 124 (3), 390-391.

23. Larsen, M. A.; Hartwig, J. F. J. J. O. T. A. C. S., Iridium-catalyzed C–H borylation of heteroarenes: scope, regioselectivity, application to late-stage functionalization, and mechanism. 2014, 136 (11), 4287-4299.

24. Preshlock, S. M.; Ghaffari, B.; Maligres, P. E.; Krska, S. W.; Maleczka Jr, R. E.; Smith III, M. R. J. J. O. T. A. C. S., High-throughput optimization of Ir-catalyzed C–H borylation: a tutorial for practical applications. 2013, 135 (20), 7572-7582.

25. Tamura, H.; Yamazaki, H.; Sato, H.; Sakaki, S. J. J. O. T. A. C. S., Iridium-catalyzed borylation of benzene with diboron. Theoretical elucidation of catalytic cycle including unusual iridium (V) intermediate. 2003, 125 (51), 16114-16126.

26. Boller, T. M.; Murphy, J. M.; Hapke, M.; Ishiyama, T.; Miyaura, N.; Hartwig, J. F. J. J. O. T. A. C. S., Mechanism of the mild functionalization of arenes by diboron reagents catalyzed by iridium complexes. Intermediacy and chemistry of bipyridine-ligated iridium trisboryl complexes. 2005, 127 (41), 14263-14278.

27. Chotana, G. A.; Rak, M. A.; Smith, M. R. J. J. O. T. A. C. S., Sterically directed functionalization of aromatic C− H bonds: selective borylation ortho to cyano groups in arenes and heterocycles. 2005, 127 (30), 10539-10544.

28. Vanchura, B. A.; Preshlock, S. M.; Roosen, P. C.; Kallepalli, V. A.; Staples, R. J.; Maleczka Jr, R. E.; Singleton, D. A.; Smith III, M. R. J. C. C., Electronic effects in iridium C–H borylations: insights from unencumbered substrates and variation of boryl ligand substituents. 2010, 46 (41), 7724-7726.

29. Ishiyama, T.; Isou, H.; Kikuchi, T.; Miyaura, N. J. C. C., Ortho-C–H borylation of benzoate esters with bis (pinacolato) diboron catalyzed by iridium–phosphine complexes. 2010, 46 (1), 159-161.

30. Kawamorita, S.; Ohmiya, H.; Hara, K.; Fukuoka, A.; Sawamura, M. J. J. O. T. A. C. S., Directed Ortho Borylation of Functionalized Arenes Catalyzed by a Silica-Supported Compact Phosphine− Iridium System. 2009, 131 (14), 5058-5059.

31. Su, B.; Hartwig, J. F. J. A. C., Iridium-Catalyzed, Silyl-Directed, peri-Borylation of C− H Bonds in Fused Polycyclic Arenes and Heteroarenes. 2018, 130 (32), 10320-10324.

32. Boebel, T. A.; Hartwig, J. F. J. J. O. T. A. C. S., Silyl-directed, iridium-catalyzed ortho-borylation of arenes. A one-pot ortho-borylation of phenols, arylamines, and alkylarenes. 2008, 130 (24), 7534-7535.

33. Takagi, J.; Sato, K.; Hartwig, J. F.; Ishiyama, T.; Miyaura, N. J. T. L., Iridium-catalyzed C–H coupling reaction of heteroaromatic compounds with bis (pinacolato) diboron: regioselective synthesis of heteroarylboronates. 2002, 43 (32), 5649-5651.

34. Robbins, D. W.; Boebel, T. A.; Hartwig, J. F. J. J. O. T. A. C. S., Iridium-catalyzed, silyl-directed borylation of nitrogen-containing heterocycles. 2010, 132 (12), 4068-4069.

35. Roosen, P. C.; Kallepalli, V. A.; Chattopadhyay, B.; Singleton, D. A.; Maleczka Jr, R. E.; Smith III, M. R. J. J. O. T. A. C. S., Outer-sphere direction in iridium C–H borylation. 2012, 134 (28), 11350-11353.

36. Kuninobu, Y.; Ida, H.; Nishi, M.; Kanai, M. J. N. C., A meta-selective C–H borylation directed by a secondary interaction between ligand and substrate. 2015, 7 (9), 712-717.

37. Ishiyama, T.; Takagi, J.; Yonekawa, Y.; Hartwig, J. F.; Miyaura, N. J. A. S.; Catalysis, Iridium-Catalyzed Direct Borylation of Five-Membered Heteroarenes by Bis (pinacolato) diboron: Regioselective, Stoichiometric, and Room Temperature Reactions. 2003, 345 (9-10), 1103-1106.

38. Paul, S.; Chotana, G. A.; Holmes, D.; Reichle, R. C.; Maleczka, R. E.; Smith, M. R. J. J. O. T. A. C. S., Ir-catalyzed functionalization of 2-substituted indoles at the 7-position: Nitrogen-directed aromatic borylation. 2006, 128 (49), 15552-15553.

39. Lo, W. F.; Kaiser, H. M.; Spannenberg, A.; Beller, M.; Tse, M. K. J. T. L., A highly selective Ir-catalyzed borylation of 2-substituted indoles: a new access to 2, 7-and 2, 4, 7-substituted indoles. 2007, 48 (3), 371-375.

40. Kawamorita, S.; Ohmiya, H.; Sawamura, M. J. T. J. O. O. C., Ester-directed regioselective borylation of heteroarenes catalyzed by a silica-supported iridium complex. 2010, 75 (11), 3855-3858.

41. Kong, D.; Han, S.; Zi, G.; Hou, G.; Zhang, J. J. T. J. O. O. C., Enantioselective synthesis of boryl tetrahydroquinolines via Cu-catalyzed hydroboration. 2018, 83 (4), 1924-1932.

42. Sadler, S. A.; Tajuddin, H.; Mkhalid, I. A.; Batsanov, A. S.; Albesa-Jove, D.; Cheung, M. S.; Maxwell, A. C.; Shukla, L.; Roberts, B.; Blakemore, D. C. J. O.; Chemistry, B., Iridium-catalyzed C–H borylation of pyridines. 2014, 12 (37), 7318-7327.

43. Yang, L.; Semba, K.; Nakao, Y. J. A. C., para-Selective C− H Borylation of (Hetero) Arenes by Cooperative Iridium/Aluminum Catalysis. 2017, 129 (17), 4931-4935.

44. Tajuddin, H.; Harrisson, P.; Bitterlich, B.; Collings, J. C.; Sim, N.; Batsanov, A. S.; Cheung, M. S.; Kawamorita, S.; Maxwell, A. C.; Shukla, L., Iridium-catalyzed C–H borylation of quinolines and unsymmetrical 1, 2-disubstituted benzenes: insights into steric and electronic effects on selectivity. Chemical Science 2012, 3 (12), 3505-3515.

45. Harrisson, P.; Morris, J.; Marder, T. B.; Steel, P. G., Microwave-accelerated iridium-catalyzed borylation of aromatic C− H bonds. Organic letters 2009, 11 (16), 3586-3589.

46. Konishi, S.; Kawamorita, S.; Iwai, T.; Steel, P. G.; Marder, T. B.; Sawamura, M. J. C. A. A. J., Site-Selective C□ H Borylation of Quinolines at the C8 Position Catalyzed by a Silica-Supported Phosphane–Iridium System. 2014, 9 (2), 434-438.

47. Ros, A.; Estepa, B.; López-Rodríguez, R.; Álvarez, E.; Fernández, R.; Lassaletta, J. M. J. A. C., Use of hemilabile N, N ligands in nitrogen-directed Iridium-catalyzed borylations of arenes. 2011, 123 (49), 11928-11932.

48. Jha, N.; Khot, N. P.; Kapur, M., Transition-Metal-Catalyzed C−H Bond Functionalization of Arenes/Heteroarenes via Tandem C−H Activation and Subsequent Carbene Migratory Insertion Strategy. 2021, 21 (12), 4088-4122.

49. Das, R.; Kapur, M., Transition-Metal-Catalyzed C−H Functionalization Reactions of π-Deficient Heterocycles. 2018, 7 (7), 1217-1235.

50. Chrzanowska, M.; Rozwadowska, M. D. J. C. R., Asymmetric synthesis of isoquinoline alkaloids. 2004, 104 (7), 3341-3370.

51. Chrzanowska, M.; Grajewska, A.; Rozwadowska, M. D. J. C. R., Asymmetric synthesis of isoquinoline alkaloids: 2004–2015. 2016, 116 (19), 12369-12465.

52. Wang, S.; Chai, Z.; Zhou, S.; Wang, S.; Zhu, X.; Wei, Y. J. O. L., A novel Lewis acid catalyzed [3+ 3]-annulation strategy for the syntheses of tetrahydro-β-carbolines and tetrahydroisoquinolines. 2013, 15 (11), 2628-2631.

53. Sridharan, V.; Suryavanshi, P. A.; Menendez, J. C. J. C. R., Advances in the chemistry of tetrahydroquinolines. 2011, 111 (11), 7157-7259.

54. Singh, K. N.; Singh, P.; Singh, P.; Deol, Y. S. J. O. L., Nucleophilic addition of β-amino carbanions to arynes: one-pot synthesis of 4-aryl-N-methyl-1, 2, 3, 4-tetrahydroisoquinolines. 2012, 14 (9), 2202-2205.

55. Gatland, A. E.; Pilgrim, B. S.; Procopiou, P. A.; Donohoe, T. J. J. A. C. I. E., Short and Efficient Syntheses of Protoberberine Alkaloids using Palladium-Catalyzed Enolate Arylation. 2014, 53 (52), 14555-14558.

56. Chaumontet, M.; Piccardi, R.; Baudoin, O. J. A. C., Synthesis of 3, 4-Dihydroisoquinolines by a C (sp3)□ H Activation/Electrocyclization Strategy: Total Synthesis of Coralydine. 2009, 121 (1), 185-188.

57. Tiwari, V. K.; Kapur, M. J. O.; Chemistry, B., Catalyst-controlled positional-selectivity in C–H functionalizations. 2019, 17 (5), 1007-1026.

58. Das, R.; Kapur, M. J. A. J. O. O. C., Transition-Metal-Catalyzed C− H Functionalization Reactions of π-Deficient Heterocycles. 2018, 7 (7), 1217-1235.

59. Seiple, I. B.; Su, S.; Rodriguez, R. A.; Gianatassio, R.; Fujiwara, Y.; Sobel, A. L.; Baran, P. S. J. J. O. T. A. C. S., Direct C− H arylation of electron-deficient heterocycles with arylboronic acids. 2010, 132 (38), 13194-13196.

60. Suresh, R.; Muthusubramanian, S.; Kumaran, R. S.; Manickam, G. J. A. J. O. O. C., C2-Arylation of Substituted Pyridine N-oxides with Heteroaryl Carboxylic Acids by Palladium-Catalyzed Decarboxylative Coupling. 2014, 3 (5), 604-608.

61. Xiao, B.; Liu, Z.-J.; Liu, L.; Fu, Y. J. J. O. T. A. C. S., Palladium-catalyzed C–H activation/cross-coupling of pyridine N-oxides with nonactivated secondary alkyl bromides. 2013, 135 (2), 616-619.

62. Leclerc, J. P.; Fagnou, K. J. A. C. I. E., Palladium-Catalyzed Cross-Coupling Reactions of Diazine N-Oxides with Aryl Chlorides, Bromides, and Iodides. 2006, 45 (46), 7781-7786.

63. Fagnou, K. J. C. A., Mechanistic considerations in the development and use of azine, diazine and azole N-oxides in palladium-catalyzed direct arylation. 2009, 35-56.

64. Das, R.; Khot, N. P.; Deshpande, A. S.; Kapur, M. J. S., Ruthenium-catalyzed directed C (3)–H olefination of N-acetyl-1, 2-dihydroisoquinolines: a method to achieve C3-olefinated isoquinolines. 2019, 51 (12), 2515-2522.

65. Jha, N.; Singh, R. P.; Saxena, P.; Kapur, M. J. O. L., Iridium (III)-Catalyzed C (3)–H Alkylation of Isoquinolines via Metal Carbene Migratory Insertion. 2021, 23 (22), 8694-8698.

66. Tiwari, V. K.; Pawar, G. G.; Jena, H. S.; Kapur, M. J. C. C., Palladium catalyzed, heteroatom-guided C–H functionalization in the synthesis of substituted isoquinolines and dihydroisoquinolines. 2014, 50 (55), 7322-7325.

67. Reddy, B. S.; Umadevi, N.; Narasimhulu, G.; Yadav, J. J. T. L., Oxidative C–H functionalization: a novel strategy for the acetoxylation/alkoxylation of arenes tethered to 3, 4-dihydroisoquinolines. 2012, 53 (45), 6091-6094.

68. Dang, X.; He, Y.; Liu, Y.; Chen, X.; Li, J.-L.; Zhou, X.-L.; Jiang, H.; Li, J. J. R. A., Rh (iii)-catalyzed synthesis of tetracyclic isoquinolinium salts via C–H activation and [4+ 2] annulation of 1-phenyl-3, 4-dihydroisoquinolines and alkynes in ethanol. 2018, 8 (52), 30050-30054.

69. Marigo, M.; Marsich, N.; Farnetti, E., Polymerization of phenylacetylene catalyzed by organoiridium compounds. Journal of Molecular Catalysis A: Chemical 2002, 187 (2), 169-177.

70. Iqbal, S. A.; Cid, J.; Procter, R. J.; Uzelac, M.; Yuan, K.; Ingleson, M. J. J. A. C., Acyl-Directed ortho-Borylation of Anilines and C7 Borylation of Indoles using just bbr3. 2019, 131 (43), 15525-15529.

71. Tiwari, V. K.; Kamal, N.; Kapur, M., One Substrate, Two Modes of C–H Functionalization: A Metal-Controlled Site-Selectivity Switch in C–H Arylation Reactions. Organic Letters 2017, 19 (1), 262-265.

72. Molander, G. A.; Cavalcanti, L. N. J. T. J. O. O. C., Oxidation of organotrifluoroborates via oxone. 2011, 76 (2), 623-630.

73. He, G.; Chen, S.; Wang, Q.; Huang, H.; Zhang, Q.; Zhang, D.; Zhang, R.; Zhu, H., Studies on copper(i)-catalyzed highly regio- and stereo-selective hydroboration of alkynamides. Organic & Biomolecular Chemistry 2014, 12 (31), 5945-5953.

74. Clentsmith, G. K.; Field, L. D.; Messerle, B. A.; Shasha, A.; Turner, P. J. T. L., Intramolecular cyclization of ortho-alkynylanilines by Rh (I)-catalyzed hydroamination to yield benzo (dipyrroles). 2009, 50 (13), 1469-1471.

75. Hiroshi, I.; Takao, K.; Tatsuo, I.; Norio, M., Iridium-catalyzed ortho-C–H Borylation of Aryl Ketones with Bis(pinacolato)diboron. 2011, 40 (9), 1007-1008.

76. Preshlock, S. M.; Ghaffari, B.; Maligres, P. E.; Krska, S. W.; Maleczka, R. E.; Smith, M. R., High-Throughput Optimization of Ir-Catalyzed C–H Borylation: A Tutorial for Practical Applications. Journal of the American Chemical Society 2013, 135 (20), 7572-7582.

77. Sasaki, I.; Doi, H.; Hashimoto, T.; Kikuchi, T.; Ito, H.; Ishiyama, T. J. C. C., Iridium (i)-catalyzed vinylic C–H borylation of 1-cycloalkenecarboxylates with bis (pinacolato) diboron. 2013, 49 (68), 7546-7548.

78. Itoh, H.; Kikuchi, T.; Ishiyama, T.; Miyaura, N. J. C. L., Iridium-catalyzed ortho-C–H borylation of aryl ketones with bis (pinacolato) diboron. 2011, 40 (9), 1007-1008.

79. Lv, J.; Zhang, X. J.; Wang, M.; Zhao, Y.; Shi, Z. J. C. A. E. J., bbr3-Mediated P (III)-Directed C− H Borylation of Phosphines. 2022, 28 (9), e202104100.

80. Légaré Lavergne, J.; Jayaraman, A.; Misal Castro, L. C.; Rochette, É.; Fontaine, F.-G. J. J. O. T. A. C. S., Metal-Free Borylation of Heteroarenes Using Ambiphilic Aminoboranes: On the Importance of Sterics in Frustrated Lewis Pair C–H Bond Activation. 2017, 139 (41), 14714-14723.

81. Toutov, A. A.; Liu, W.-B.; Betz, K. N.; Fedorov, A.; Stoltz, B. M.; Grubbs, R. H. J. N., Silylation of C–H bonds in aromatic heterocycles by an Earth-abundant metal catalyst. 2015, 518 (7537), 80-84.

82. Bose, S. K.; Marder, T. B. J. S., A leap ahead for activating CH bonds. 2015, 349 (6247), 473-474.

83. Légaré, M.-A.; Courtemanche, M.-A.; Rochette, É.; Fontaine, F.-G. J. S., Metal-free catalytic CH bond activation and borylation of heteroarenes. 2015, 349 (6247), 513-516.

84. Sun, C.-L.; Shi, Z.-J. J. C. R., Transition-metal-free coupling reactions. 2014, 114 (18), 9219-9280.

85. Miyaura, N. J. B. O. T. C. S. O. J., Metal-catalyzed reactions of organoboronic acids and esters. 2008, 81 (12), 1535-1553.

86. Leonori, D.; Aggarwal, V. K., Lithiation–Borylation Methodology and Its Application in Synthesis. Accounts of Chemical Research 2014, 47 (10), 3174-3183.

87. Darses, S.; Genet, J.-P., Potassium Organotrifluoroborates: New Perspectives in Organic Synthesis. Chemical Reviews 2008, 108 (1), 288-325.

88. Fyfe, J. W. B.; Watson, A. J. B., Recent Developments in Organoboron Chemistry: Old Dogs, New Tricks. Chem 2017, 3 (1), 31-55.

89. Namirembe, S.; Morken, J. P., Reactions of organoboron compounds enabled by catalyst-promoted metalate shifts. Chemical Society Reviews 2019, 48 (13), 3464-3474.

90. Qiao, J. X.; Lam, P. Y. S., Copper-Promoted Carbon-Heteroatom Bond Cross-Coupling with Boronic Acids and Derivatives. Synthesis 2011, 2011 (06), 829-856.

91. Louërat, F.; Fort, Y.; Mamane, V. J. T. L., Direct 1, 4-difunctionalization of isoquinoline. 2009, 50 (41), 5716-5718.

92. Le, T. N.; Cho, W.-J. J. B. O. T. K. C. S., A concise synthesis of 8-oxoberberine and oxychelerythrine, natural isoquinoline alkaloids through biomimetic synthetic way. 2006, 27 (12), 2093-2096.

93. Wada, Y.; Nishida, N.; Kurono, N.; Ohkuma, T.; Orito, K., Synthesis of a 3-Arylisoquinoline Alkaloid, Decumbenine B. Wiley Online Library: 2007.

APPENDIX A

^{1}H AND ^{13}C NMR SPECTRUMS OF REACTANTS

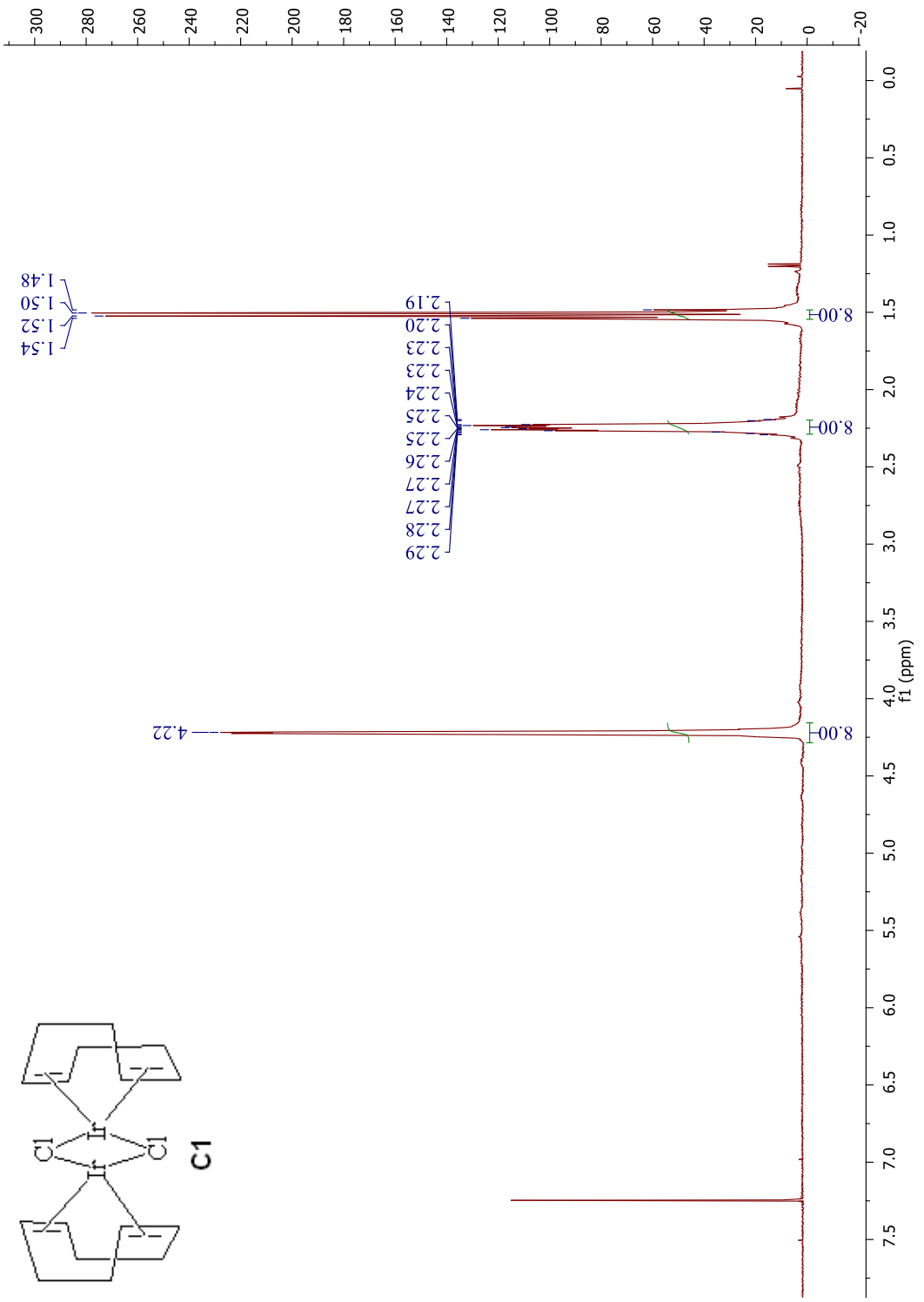
C1
f1 (ppm)
8.00
8.00
8.00
4.22
2.19
2.20
2.23
2.23
2.24
2.25
2.25
2.26
2.27
2.27
2.28
2.29
1.48
1.50
1.52
1.54

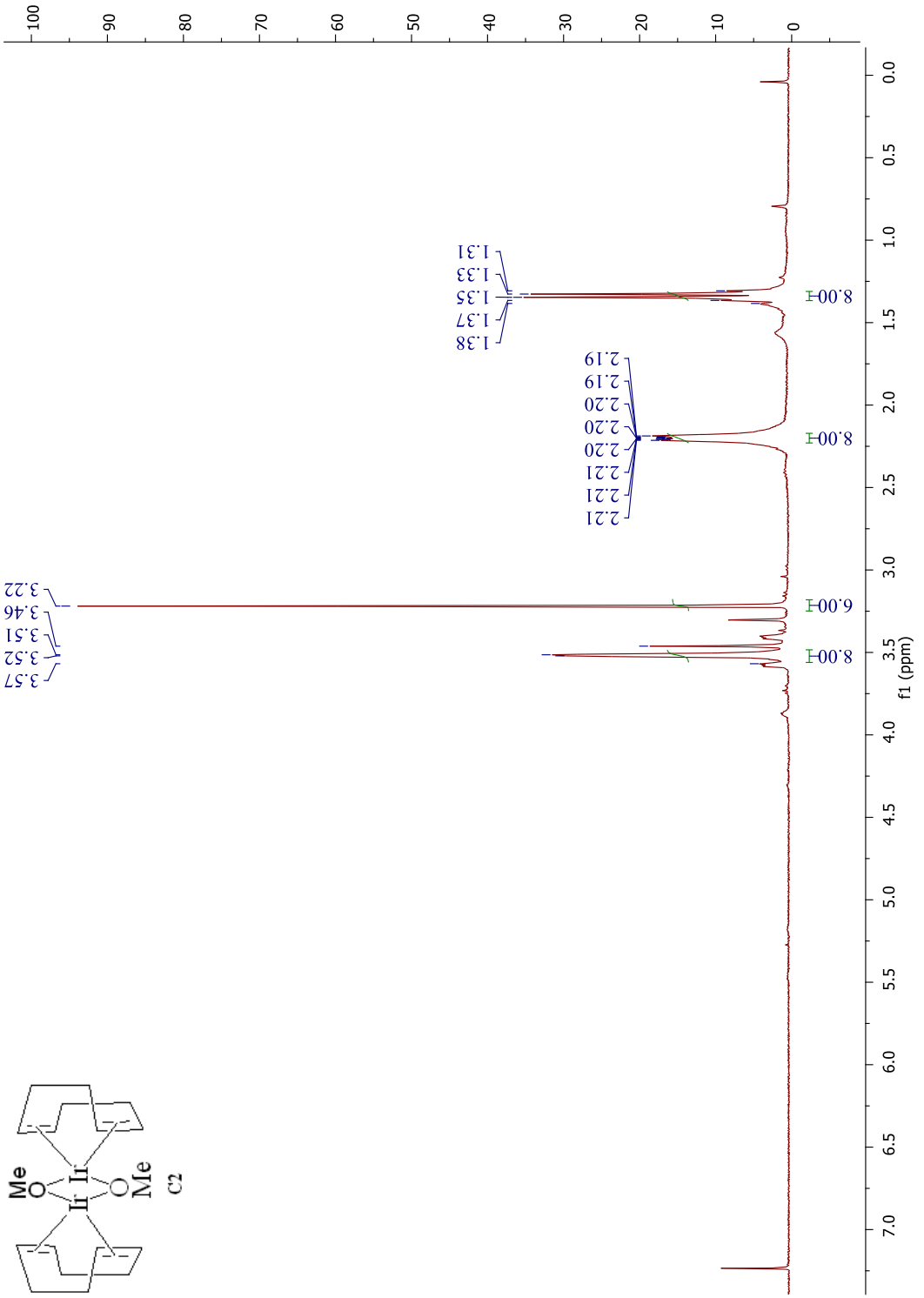
Me
O
Ir
Ir
O
Me
C2
3.57
3.52
3.51
3.46
3.22
2.21
2.21
2.20
2.20
2.20
2.21
2.21
2.19
2.19
1.38
1.37
1.35
1.33
1.31
8.00
6.00
8.00
8.00
f1 (ppm)

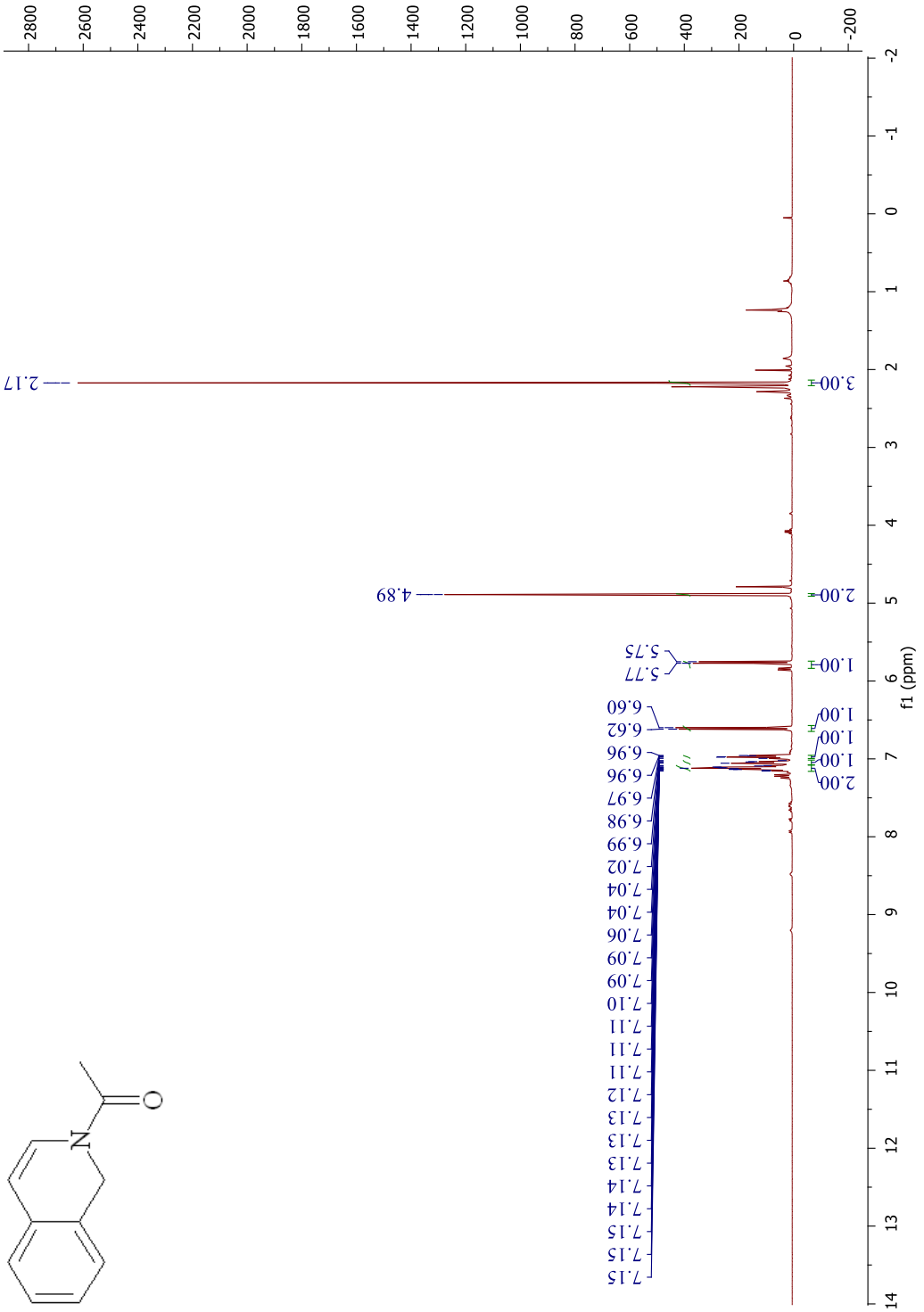
2.17
4.89
5.77
5.75
6.60
6.62
6.96
6.96
6.97
6.98
6.99
7.02
7.04
7.04
7.06
7.09
7.09
7.10
7.11
7.11
7.11
7.12
7.13
7.13
7.13
7.14
7.14
7.15
7.15
7.15
2.00
1.00
1.00
1.00
1.00
1.00
2.00
3.00
f1 (ppm)

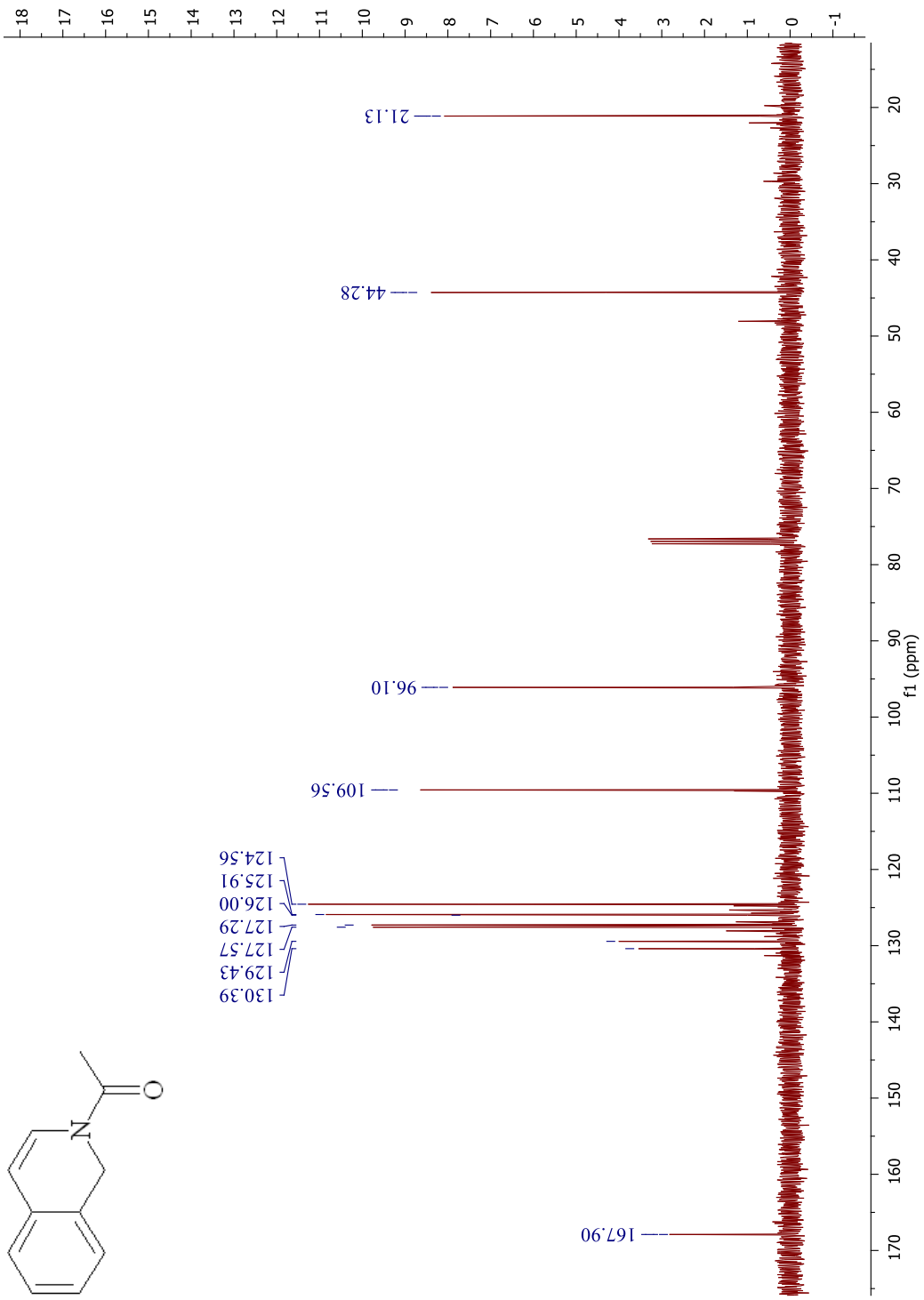
167.90
130.39
129.43
127.57
127.29
126.00
125.91
124.56
109.56
96.10
44.28
21.13
f1 (ppm)

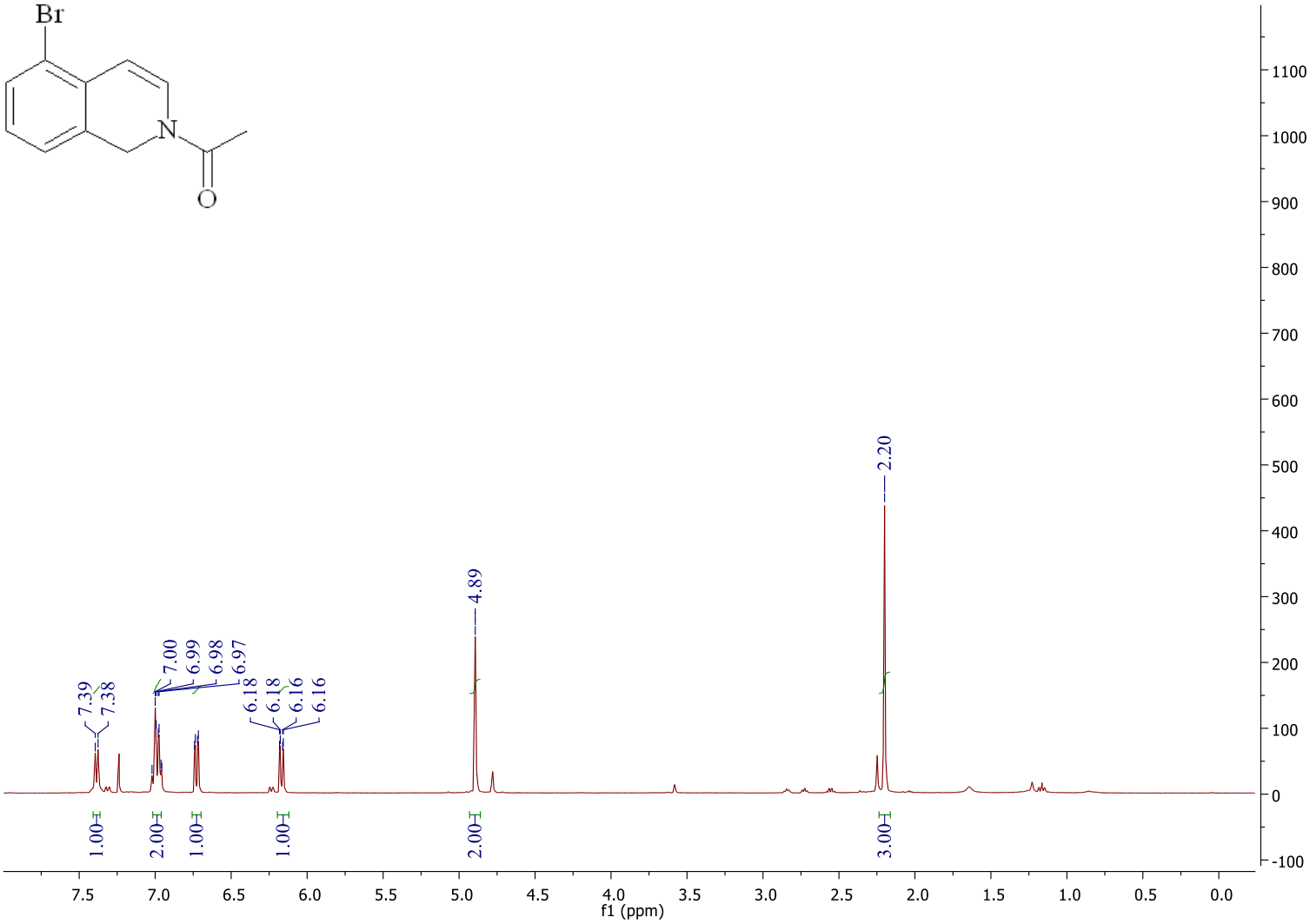
Br
N
O
7.39
7.38
7.00
6.99
6.98
6.97
6.18
6.18
6.16
6.16
4.89
2.20
1.00
2.00
1.00
1.00
2.00
3.00
f1 (ppm)

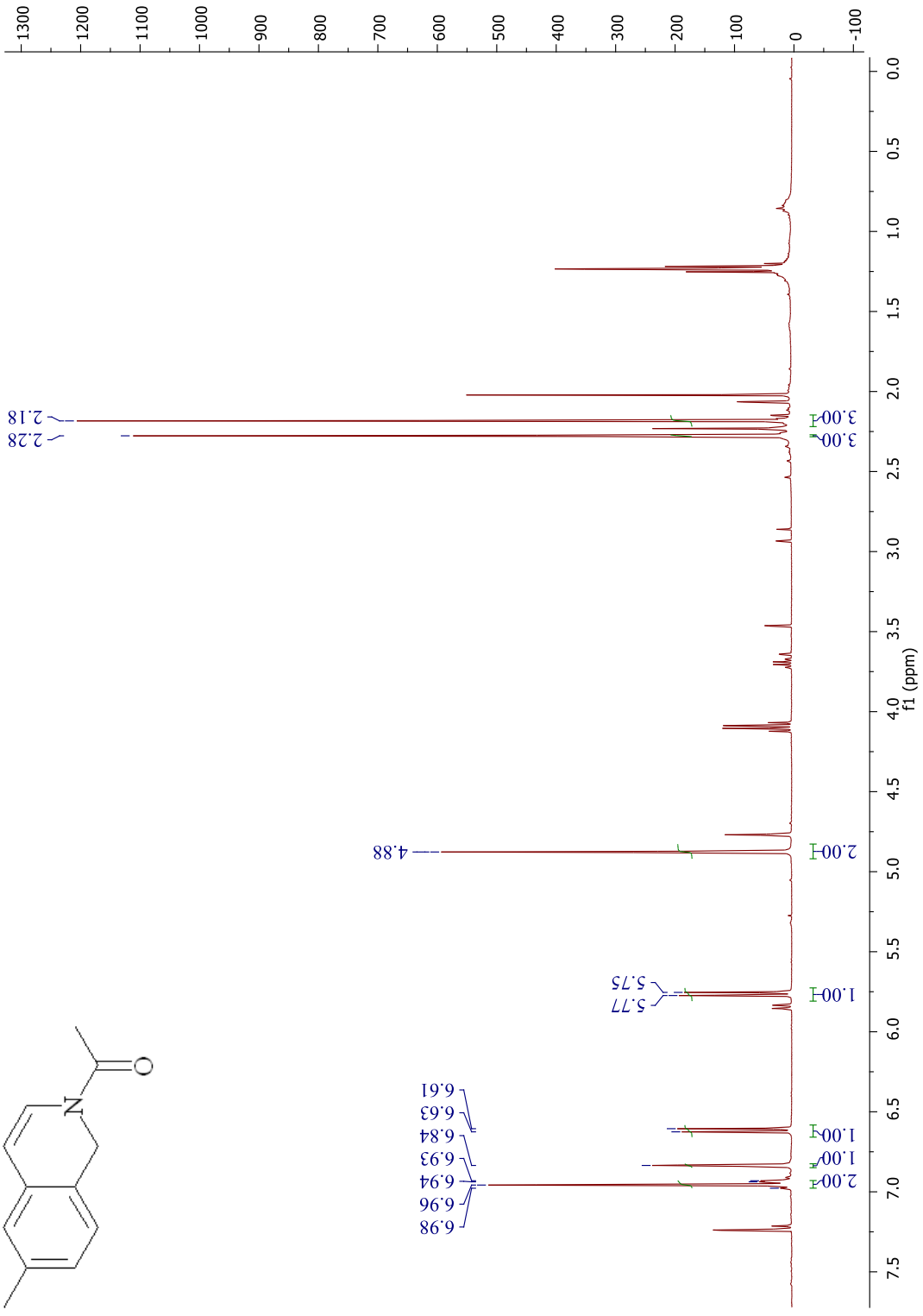
2.18
2.28
4.88
5.75
5.77
6.61
6.63
6.84
6.93
6.94
6.96
6.98
3.00
3.00
2.00
1.00
2.00
1.00
1.00
f1 (ppm)

168.47
137.26
130.21
127.96
126.55
126.01
125.81
125.34
109.75
44.14
21.05
f1 (ppm)
O
N

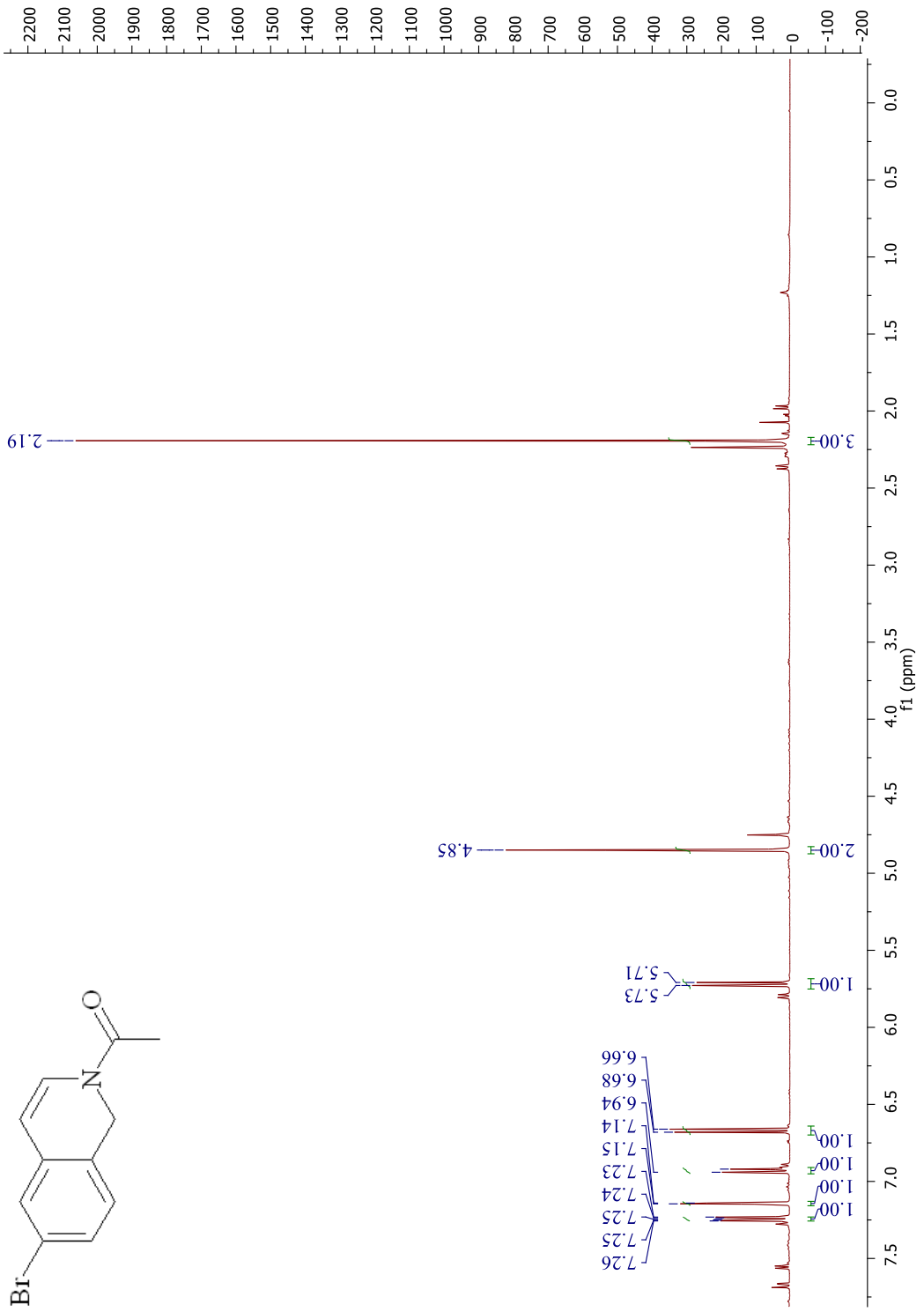
2.19
4.85
5.73
5.71
7.26
7.25
7.25
7.24
7.23
7.15
7.14
6.94
6.68
6.66
3.00
2.00
1.00
1.00
1.00
1.00
1.00
f1 (ppm)
Br
N
O

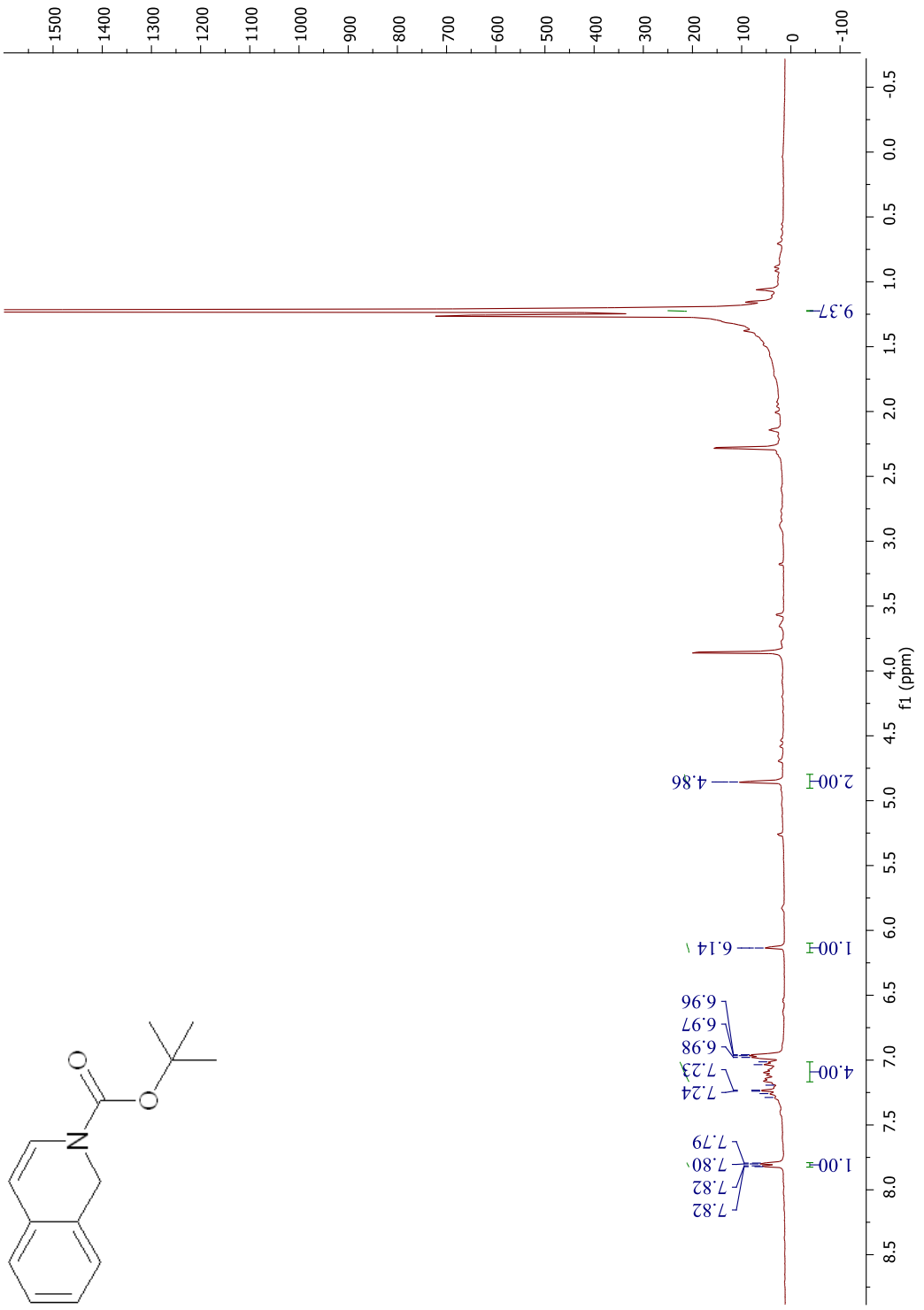
9.37
2.00
4.86
1.00
6.14
6.96
6.97
6.98
4.00
7.23
7.24
1.00
7.79
7.80
7.82
7.82
f1 (ppm)

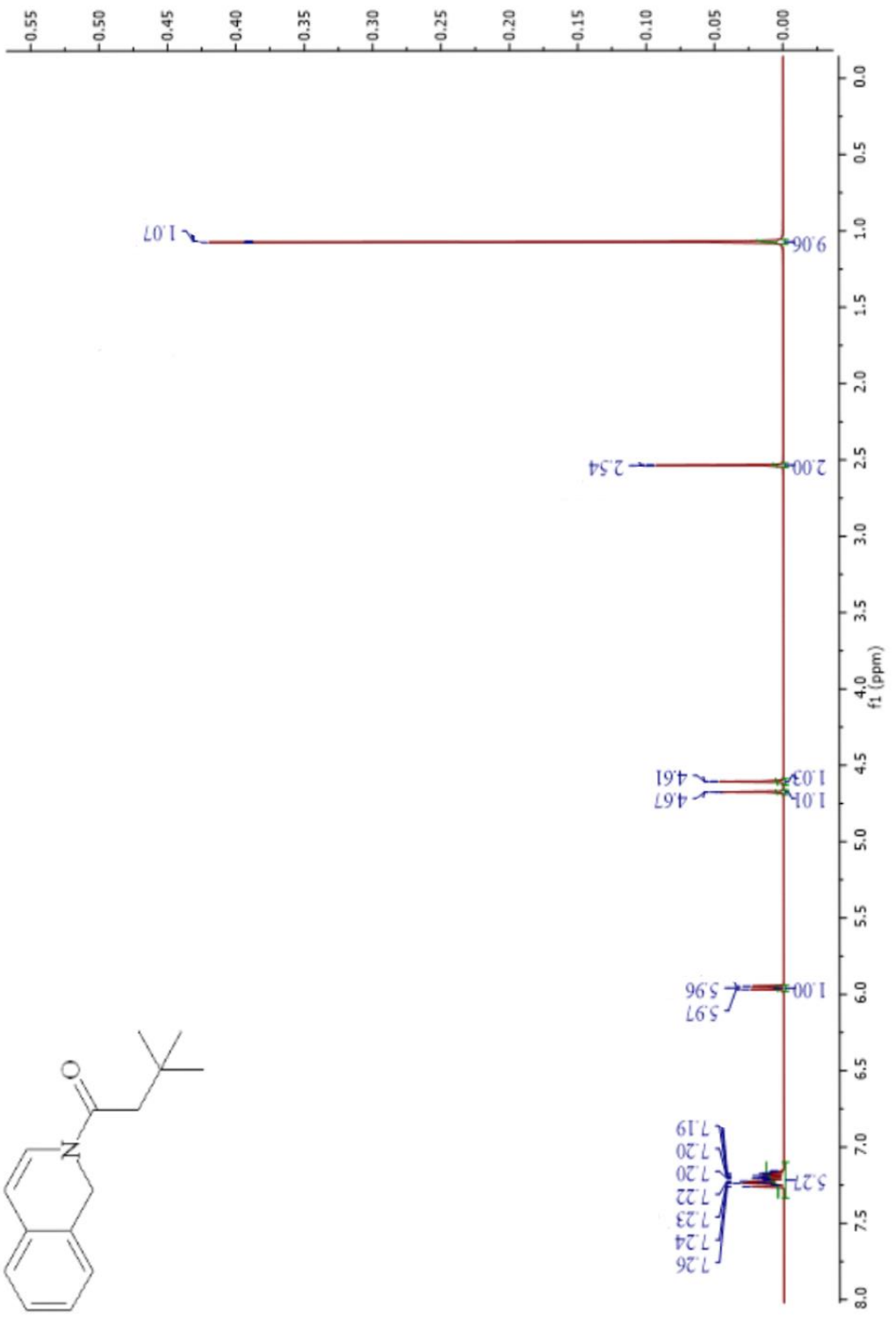
1.07
9.06
2.54
2.00
4.61
4.67
1.03
1.01
1.00
5.96
5.97
7.19
7.20
7.20
7.22
7.23
7.24
7.26
5.27
f1 (ppm)

APPENDIX B ^{1}H,

^{13}C, NOE, NOESY, COSY and HMBC NMR OF 2a

1.27
2.29
4.86
6.14
6.96
6.98
7.02
7.04
7.09
7.11
7.12
7.15
7.17
12.00
3.00
2.00
1.00
1.00
1.00
1.00
f1 (ppm)
O
B
O
O
N
O

172.87
130.20
128.41
127.16
126.41
125.48
115.67
80.85
45.58
29.69
25.25
16.74
f1 (ppm)

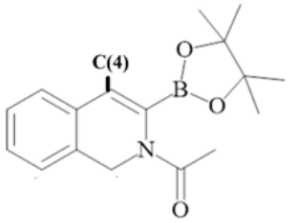

C(4)-H is irradiated

LA-EC-0903-NOE-3

Sample Name	LA-EC-0903-NOE-3	Pulse sequence	NOESY1D	Temperature	19	Study owner	vnmr1
Date collected	2021-03-09	Solvent	cdcl3	Spectrometer	vnmrj.iyte.edu.tr-vnmrs400	Operator	vnmr1

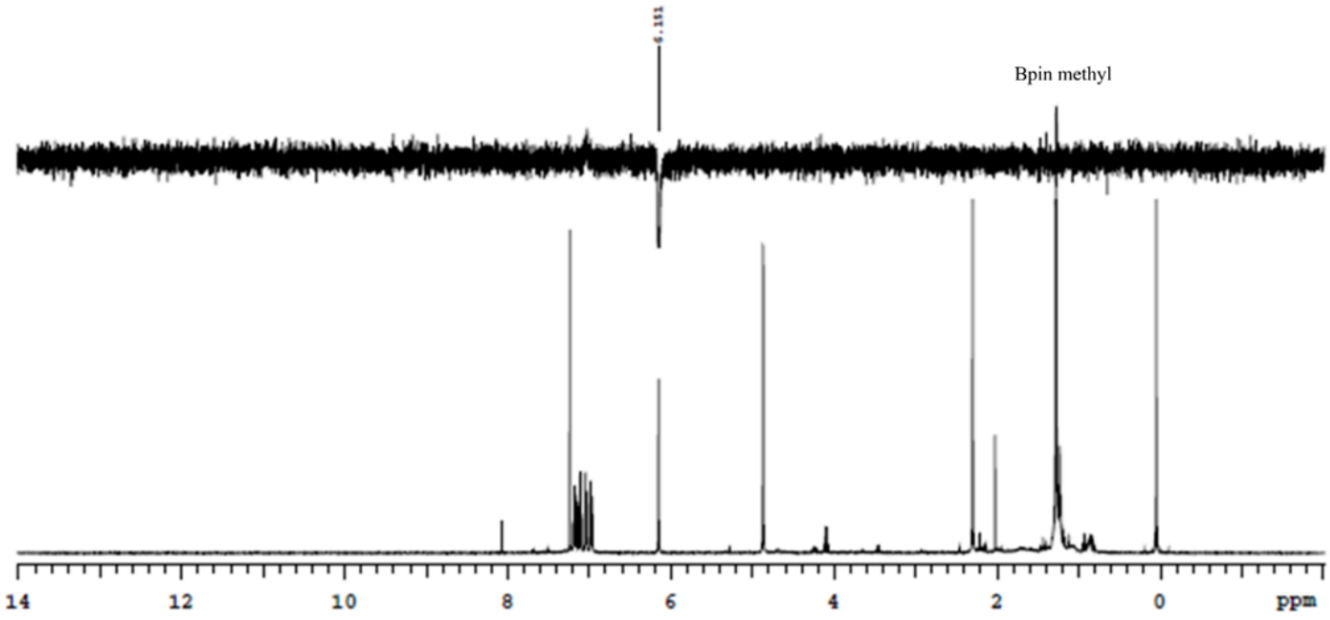

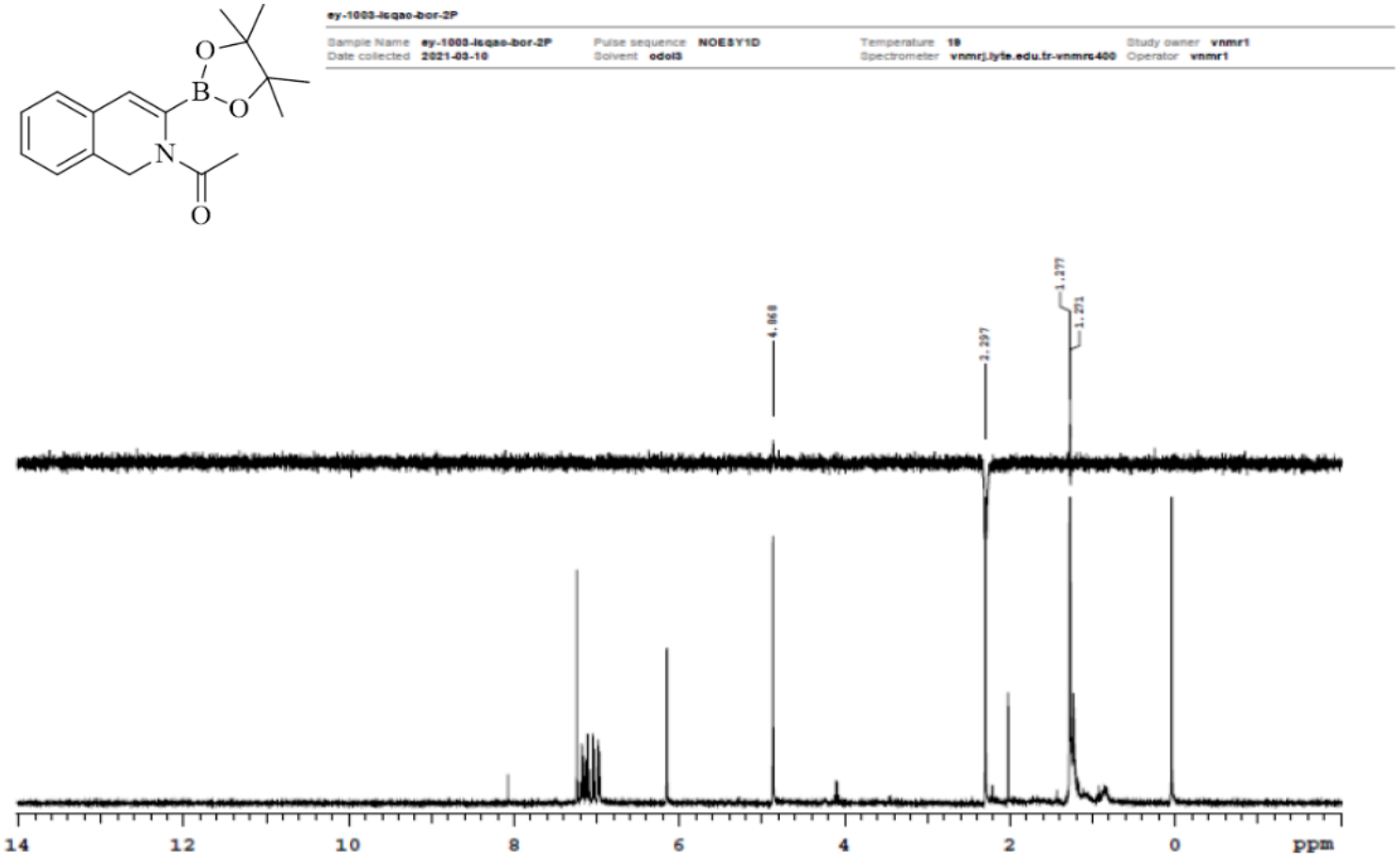
ey-1003-isqao-bor-2P
Sample Name ey-1003-isqao-bor-2P
Date collected 2021-03-10
Pulse sequence NOESY1D
Solvent odcl3
Temperature 19
Spectrometer vnmrj.lyte.edu.tr-vnmrs400
Study owner vnmr1
Operator vnmr1
O
B
O
N
O
4.868
2.297
1.277
1.271
14
12
10
8
6
4
2
0
ppm

ey-1003-isqac-bor-3P

Sample Name	ey-1003-isqac-bor-3P	Pulse sequence	NOESY1D	Temperature	19	Study owner	vnmr1
Date collected	2021-03-10	Solvent	cdcl3	Spectrometer	vnmrj.iyte.edu.tr-vnmrs400	Operator	vnmr1

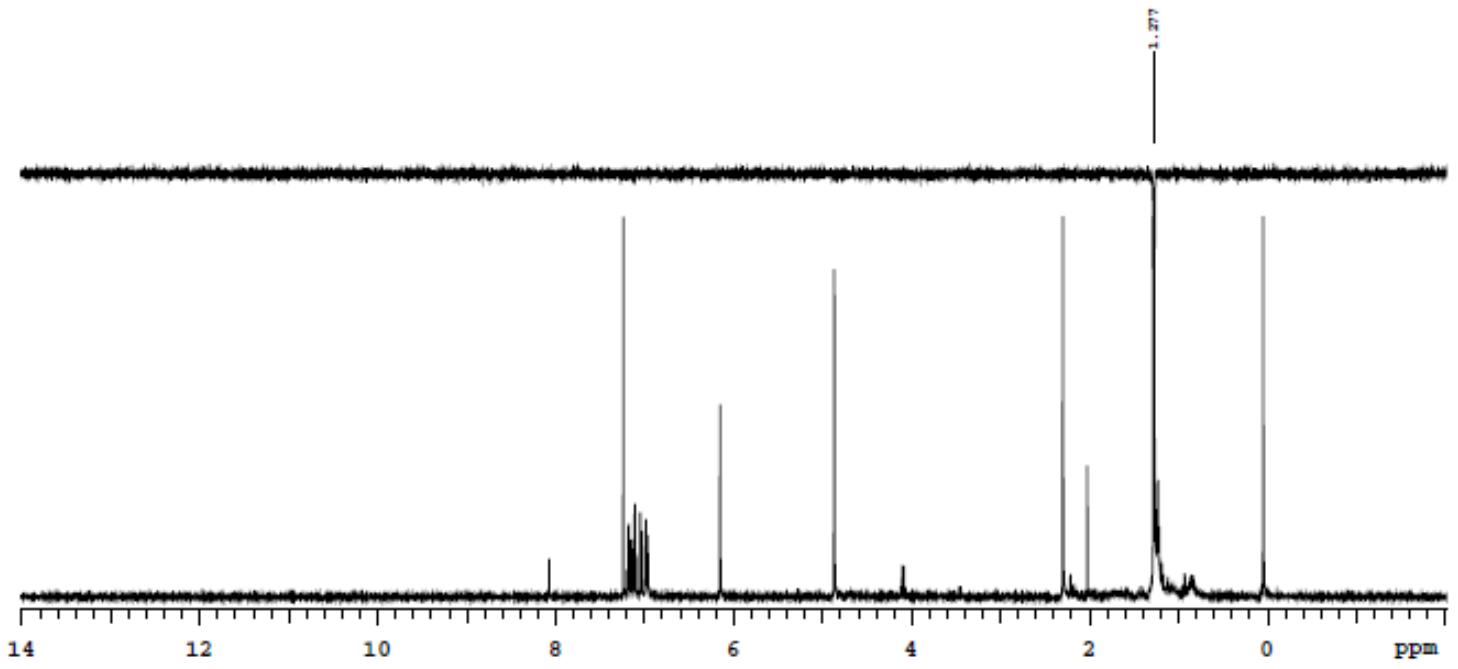

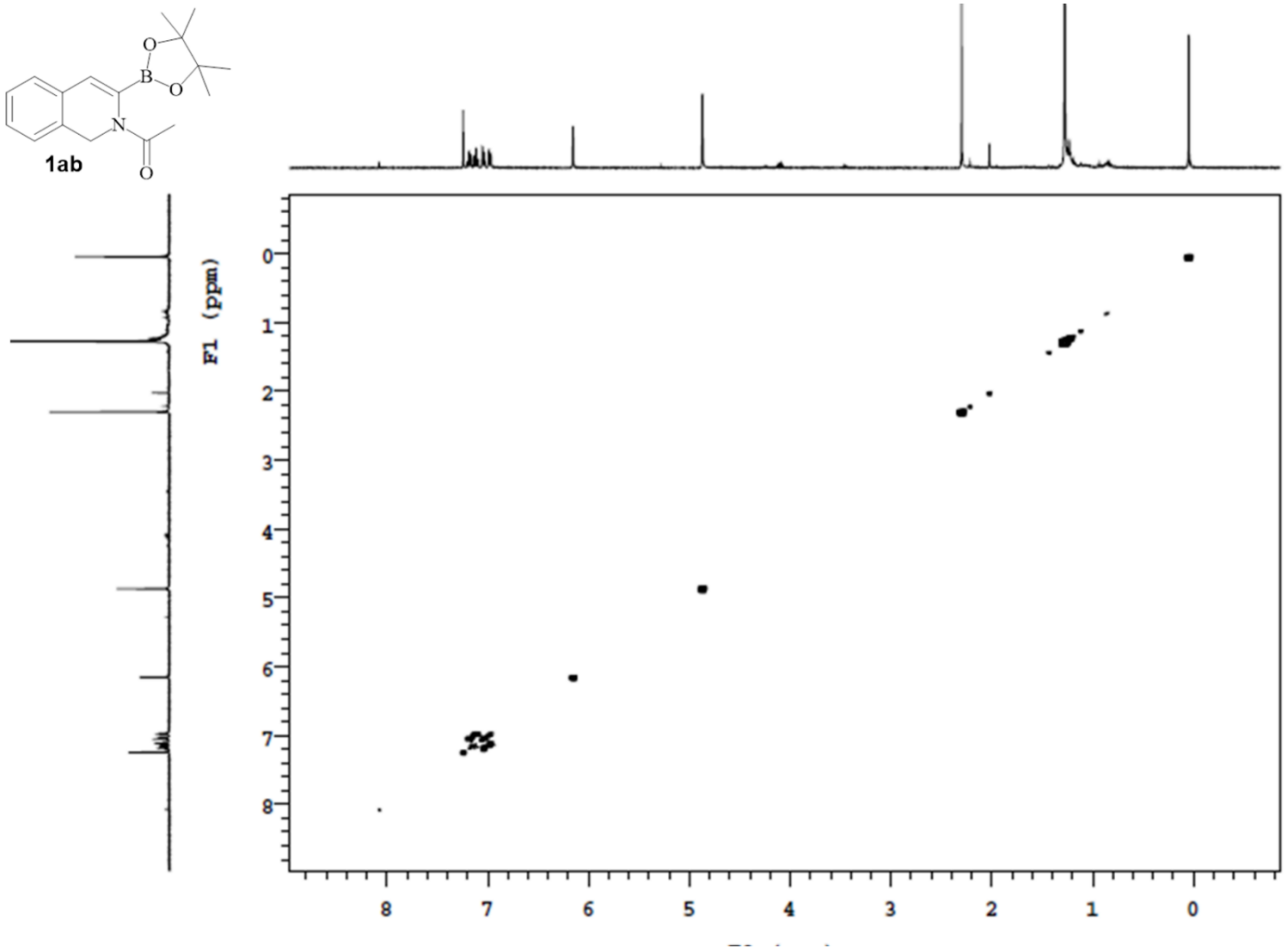
1ab
O
B
O
N
O
F1 (ppm)
0
1
2
3
4
5
6
7
8
8
7
6
5
4
3
2
1
0

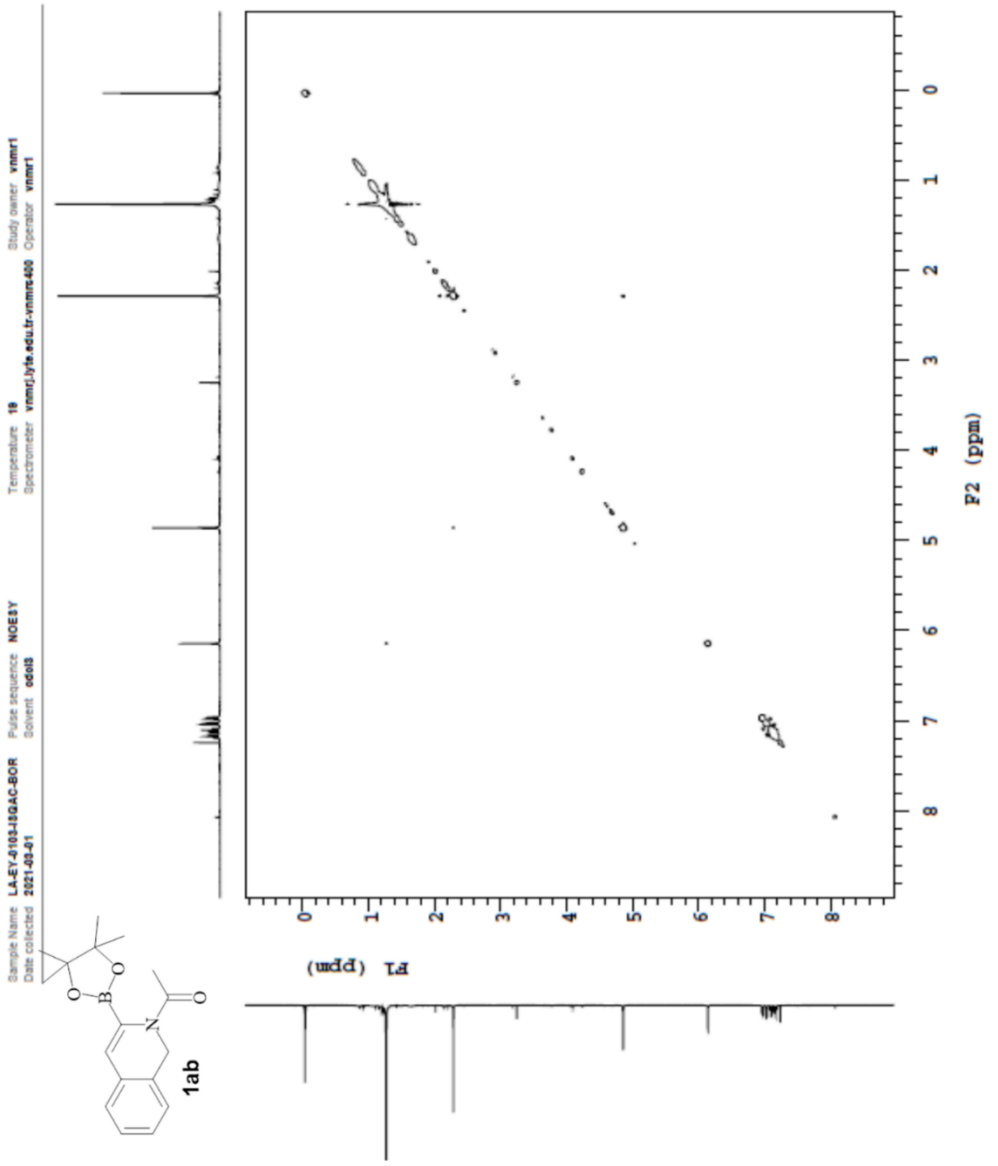
Sample Name LA-EY-0103-IBQAC-BOR
Date collected 2021-03-01
Pulse sequence NOESY
Solvent cdcl3
Temperature 19
Spectrometer vnmrj.lyte.edu.tr-vnmrs400
Study owner vnmr1
Operator vnmr1
1ab
F1 (ppm)
F2 (ppm)

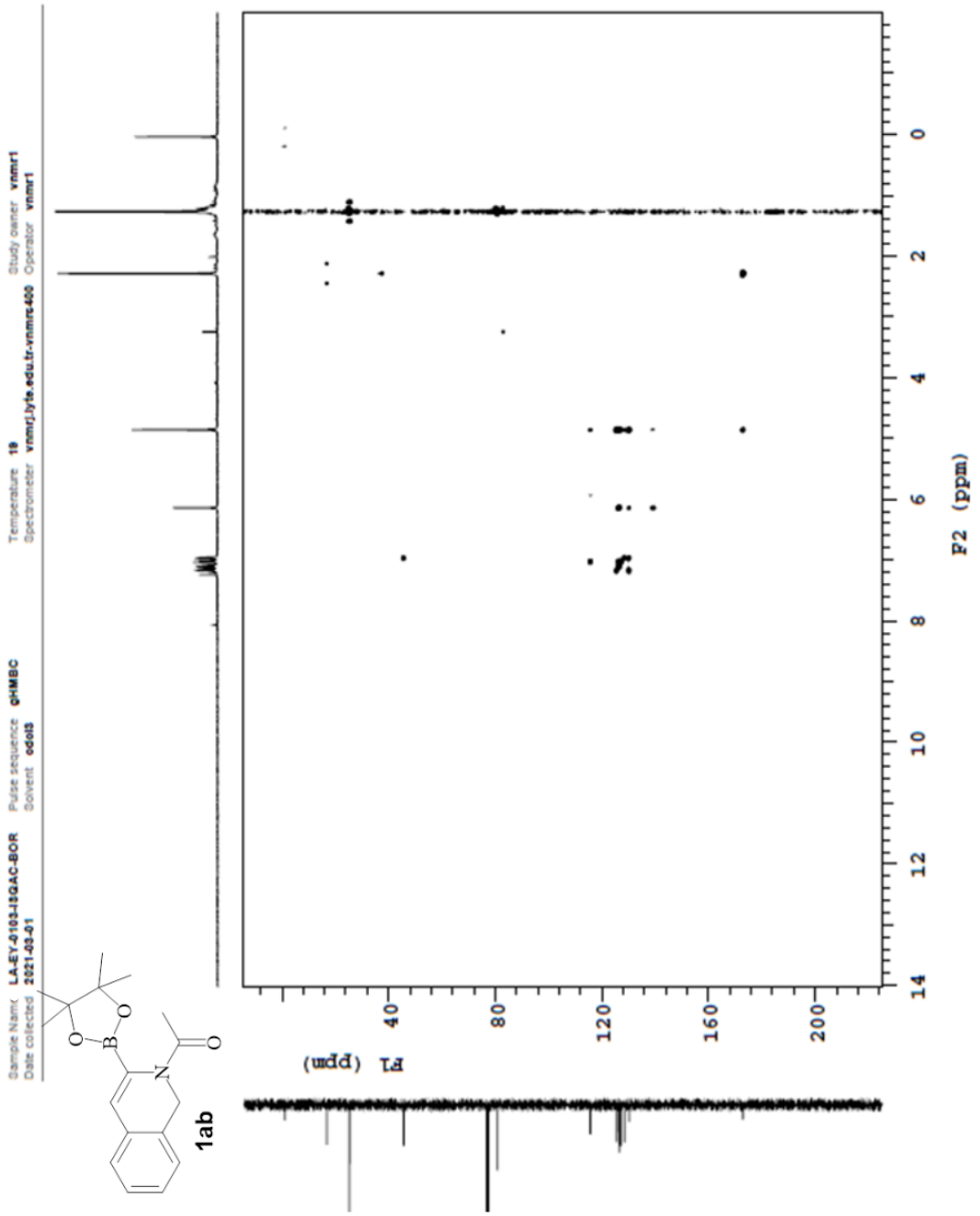
Sample Name LA-EY-0103-ISQAC-BOR
Date collected 2021-03-01
Pulse sequence gHMBC
Solvent cdcl3
Temperature 19
Spectrometer vnmrj.iyte.edu.tr-vnmrs400
Study owner vnmr1
Operator vnmr1
1ab
F1 (ppm)
F2 (ppm)

APPENDIX C

^{1}H, ^{13}C, NMR OF PRODUCTS

1000
900
800
700
600
500
400
300
200
100
0
0.0
0.5
1.0
1.5
2.0
2.5
3.0
3.5
4.0
4.5
5.0
5.5
6.0
6.5
7.0
7.5
8.0
8.5
f1 (ppm)
12.00
3.00
2.00
1.00
2.00
1.00
1.29
2.31
4.85
6.53
6.96
6.94
7.42
7.40
7.40
7.42
Br
B
O
O
N
O

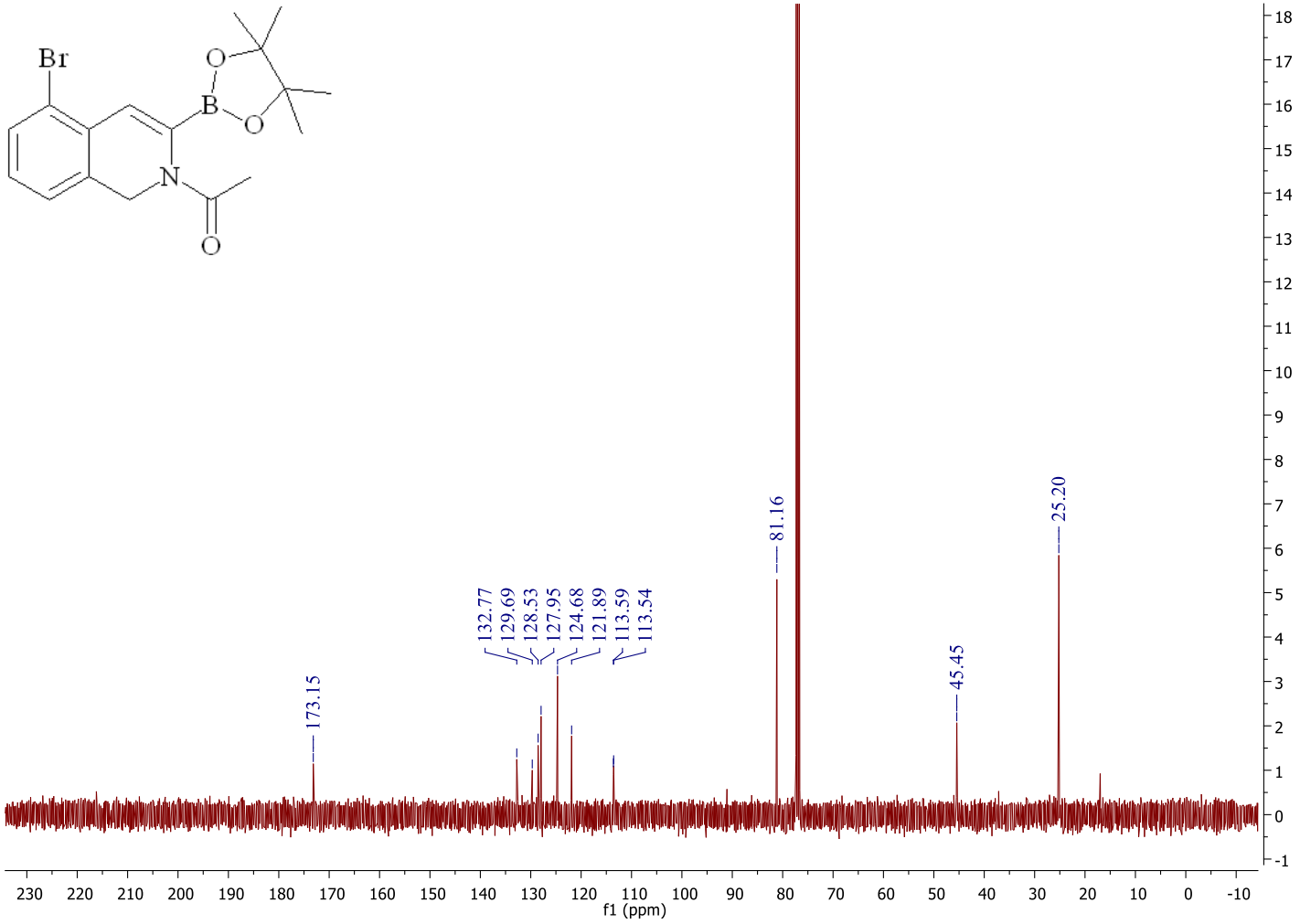
Br
O
B
O
N
O
173.15
132.77
129.69
128.53
127.95
124.68
121.89
113.59
113.54
81.16
45.45
25.20
f1 (ppm)

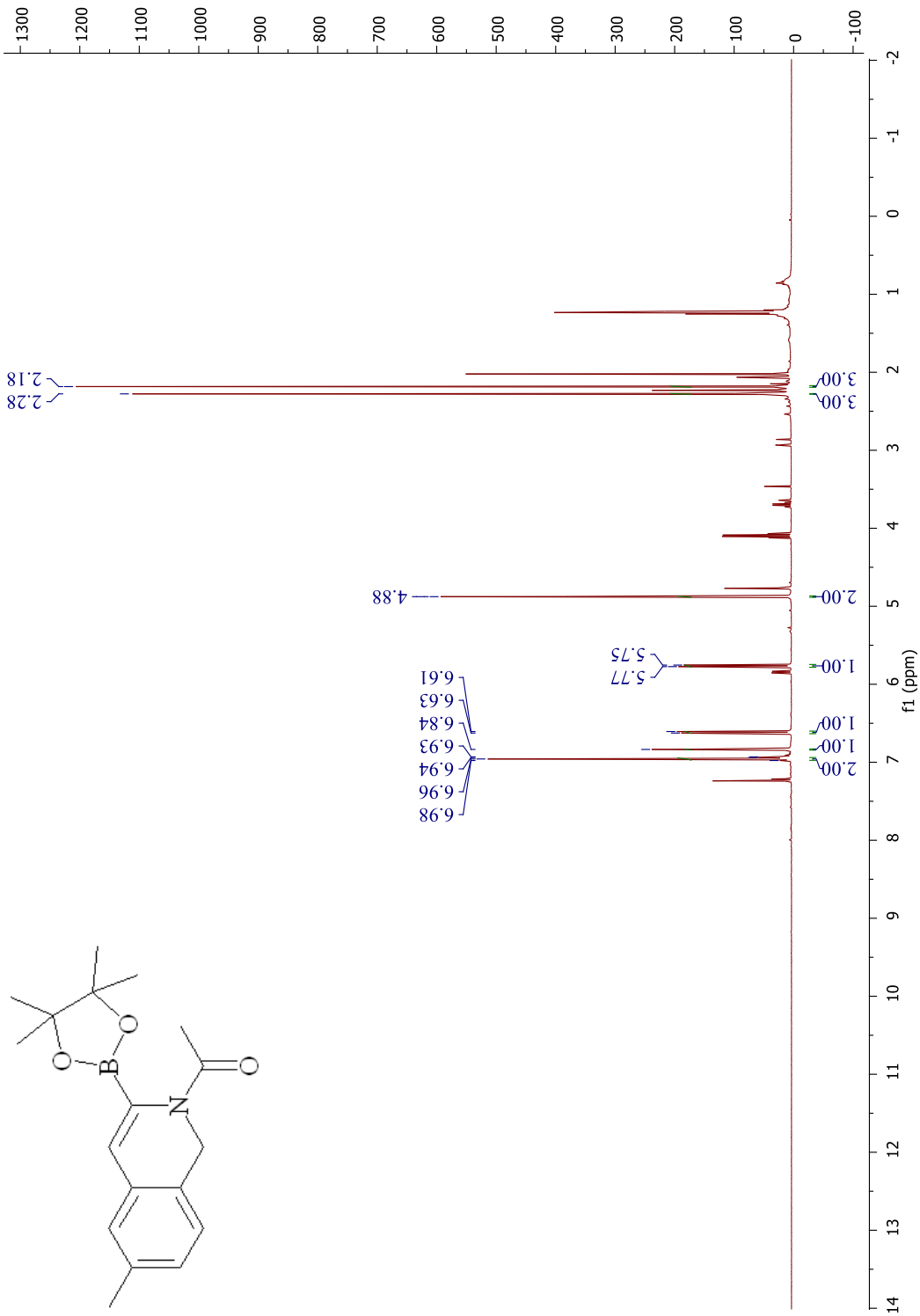
2.28
2.18
4.88
5.77
5.75
6.98
6.96
6.94
6.93
6.84
6.63
6.61
3.00
3.00
2.00
1.00
1.00
2.00
f1 (ppm)

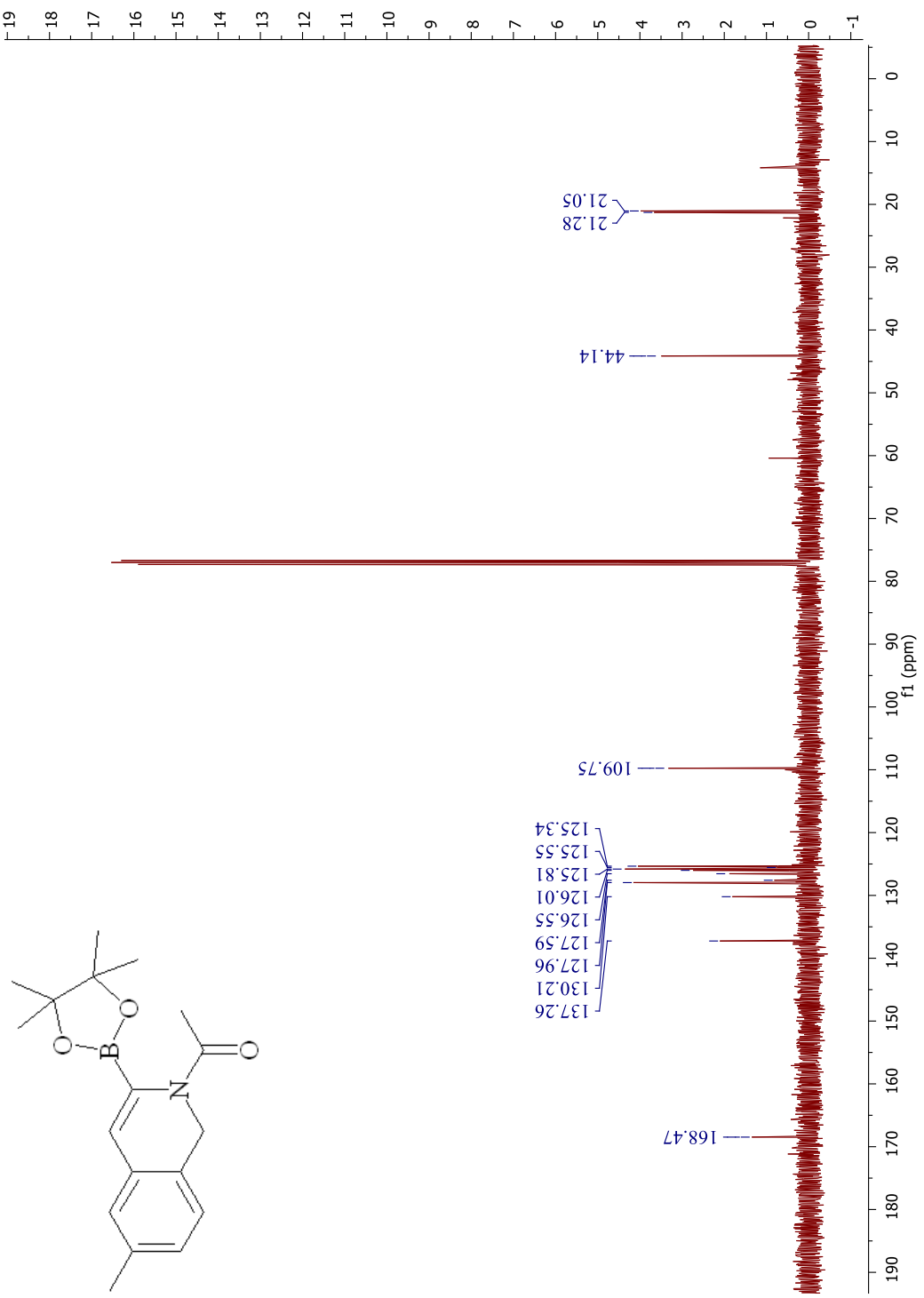
168.47
137.26
130.21
127.96
127.59
126.55
126.01
125.81
125.55
125.34
109.75
44.14
21.28
21.05
f1 (ppm)

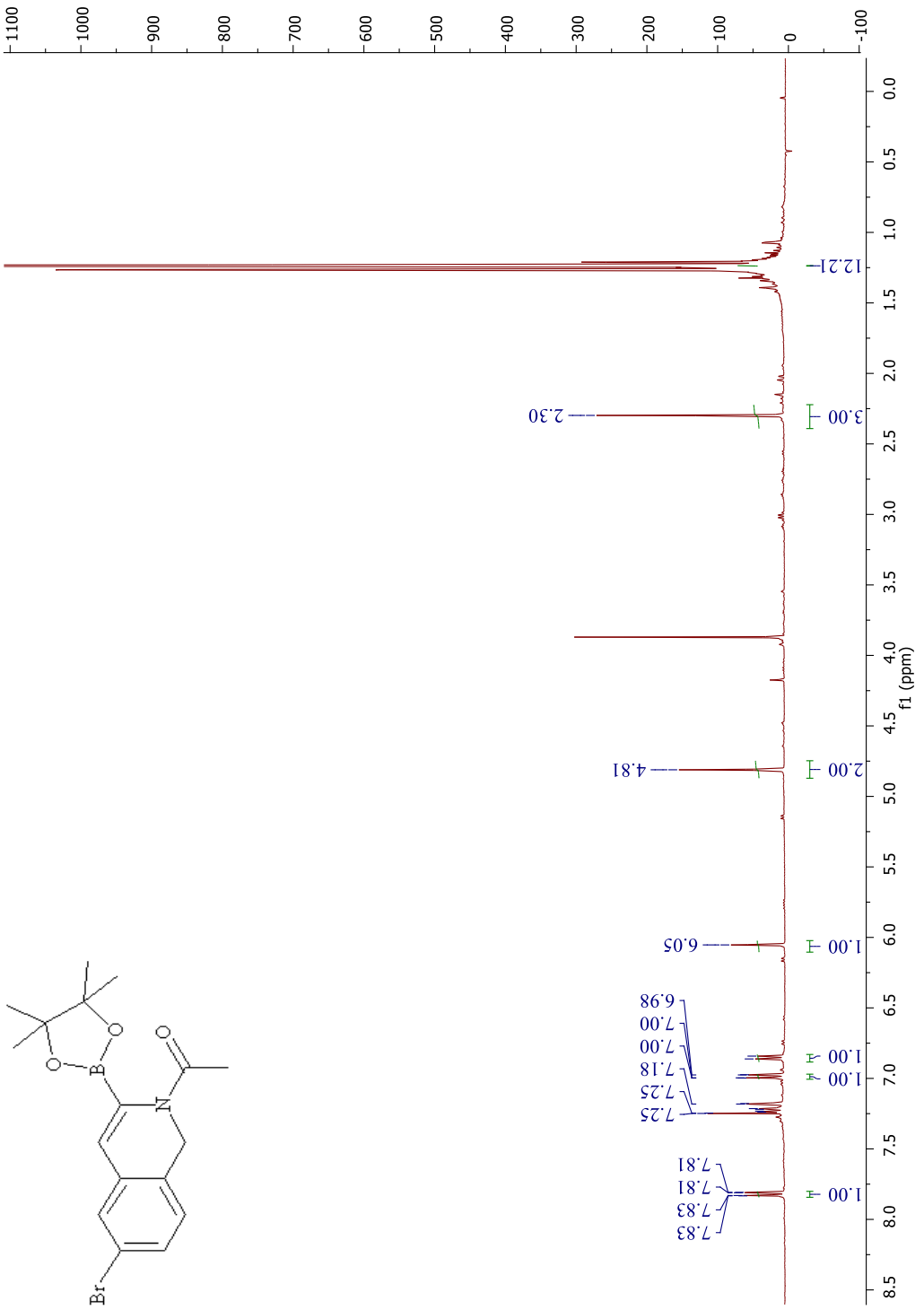
12.21
3.00
2.30
2.00
4.81
1.00
6.05
1.00
1.00
7.83
7.83
7.81
7.81
7.25
7.25
7.18
7.00
7.00
6.98
1.00
f1 (ppm)
Br
B
O
O
N
O

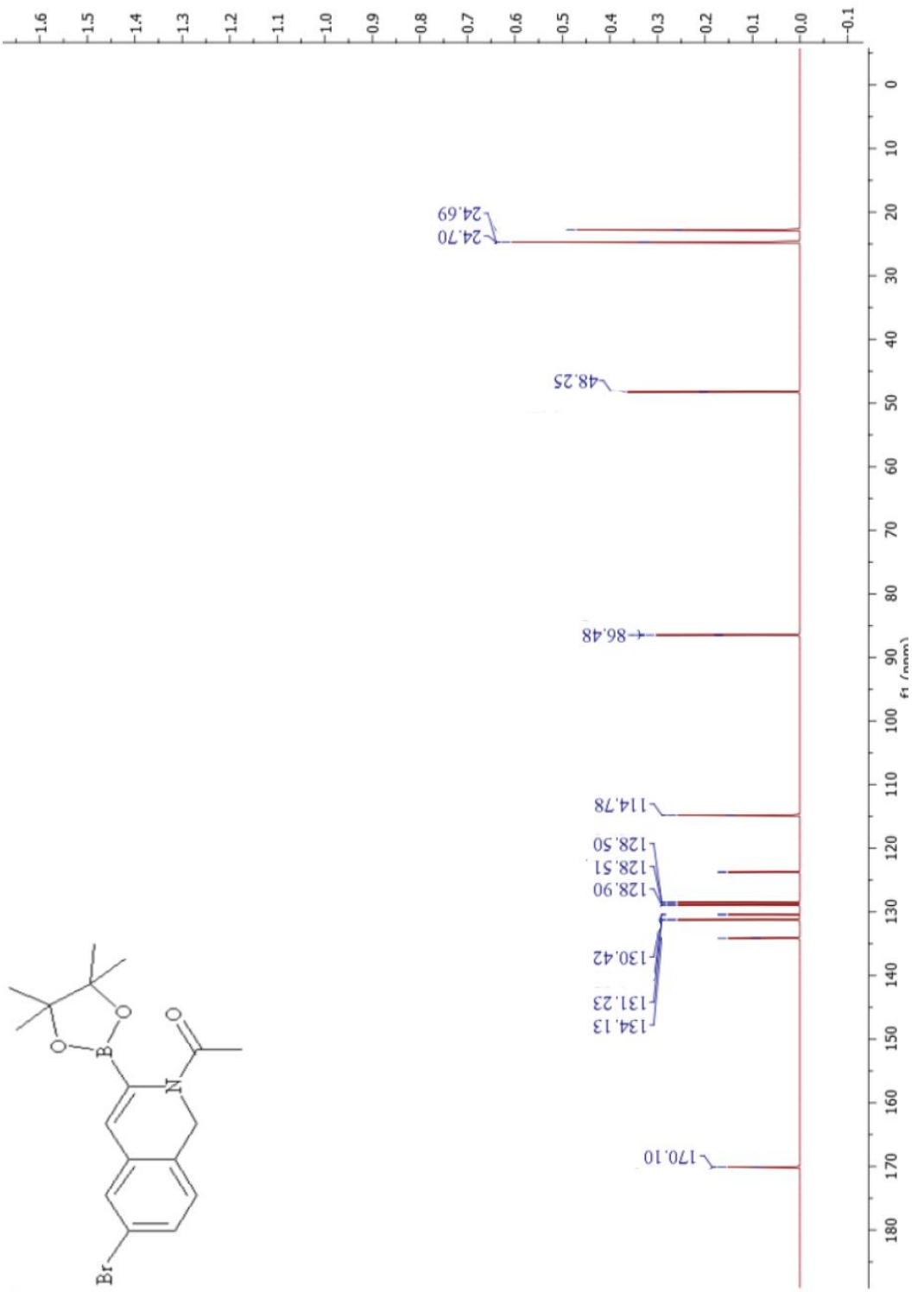
24.69
24.70
48.25
86.48
114.78
128.50
128.51
128.90
130.42
131.23
134.13
170.10
f1 (ppm)
Br
B
O
O
N
O

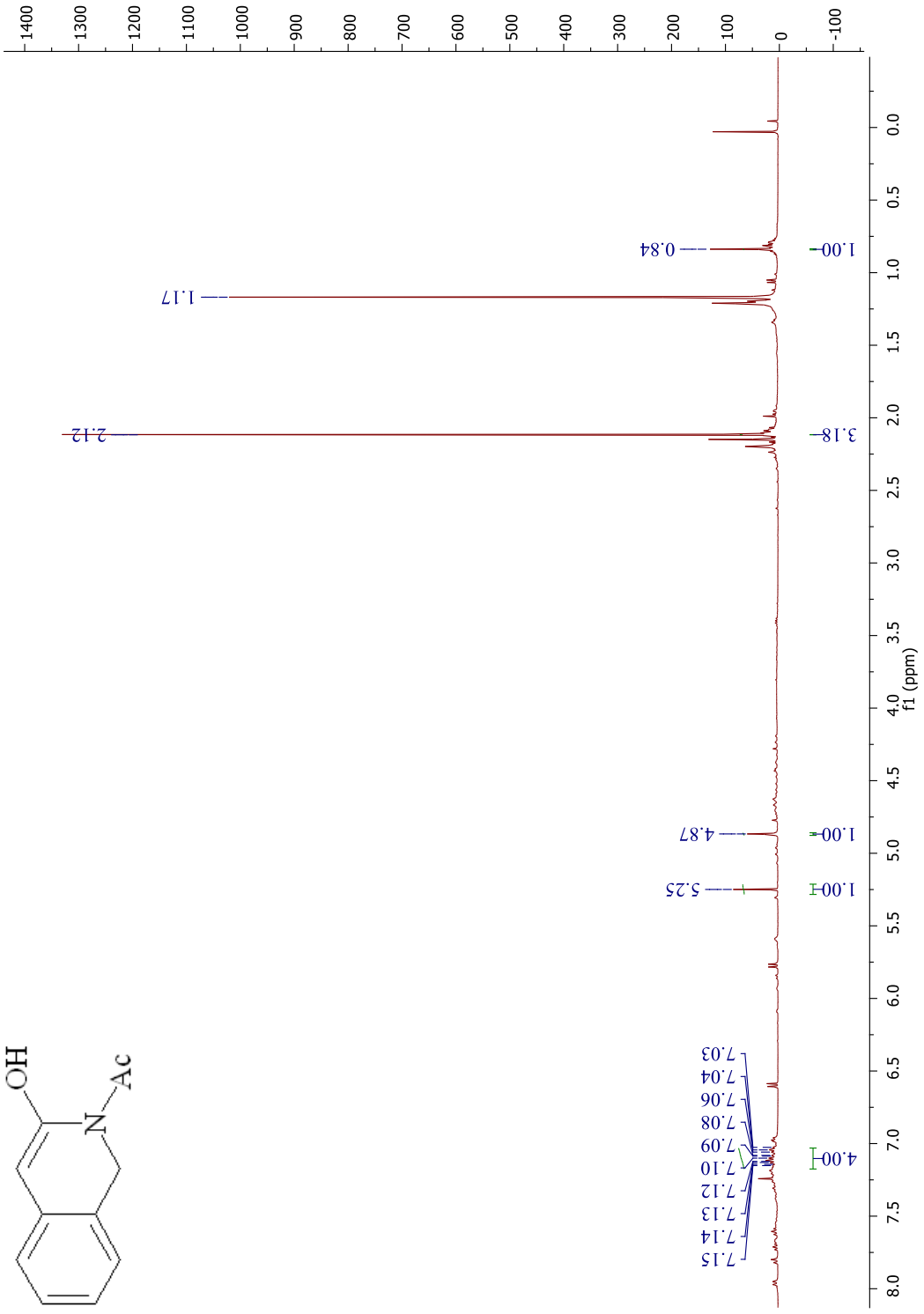
OH
N
Ac
7.15
7.14
7.13
7.12
7.10
7.09
7.08
7.06
7.04
7.03
5.25
4.87
2.12
1.17
0.84
4.00
1.00
1.00
1.00
3.18
1.00
f1 (ppm)

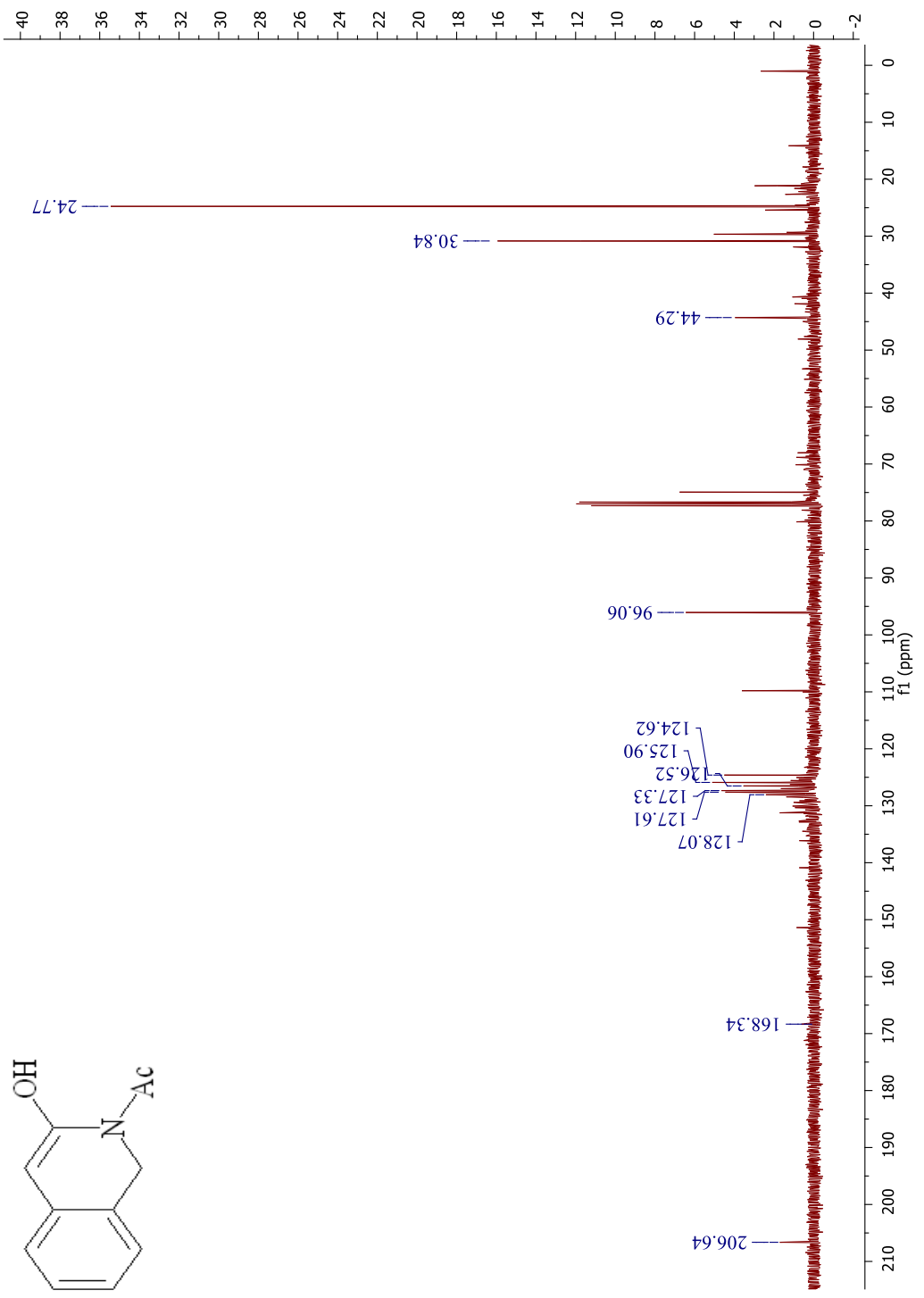
206.64
168.34
128.07
127.61
127.33
126.52
125.90
124.62
96.06
44.29
30.84
24.77
f1 (ppm)
OH
N
Ac

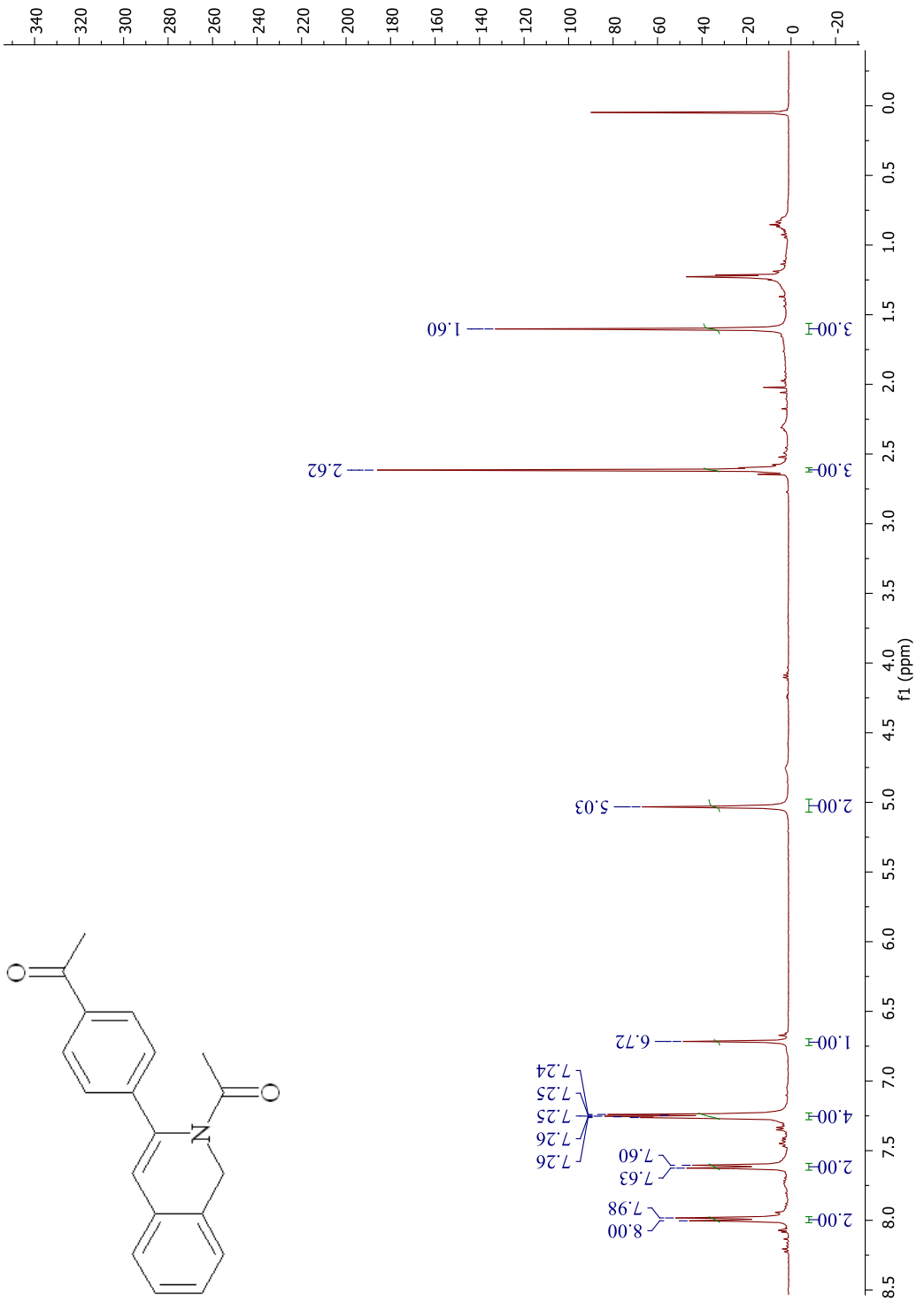
8.00
7.98
2.00
7.63
7.60
2.00
7.26
7.26
7.25
7.25
7.24
4.00
6.72
1.00
5.03
2.00
2.62
3.00
1.60
3.00
f1 (ppm)

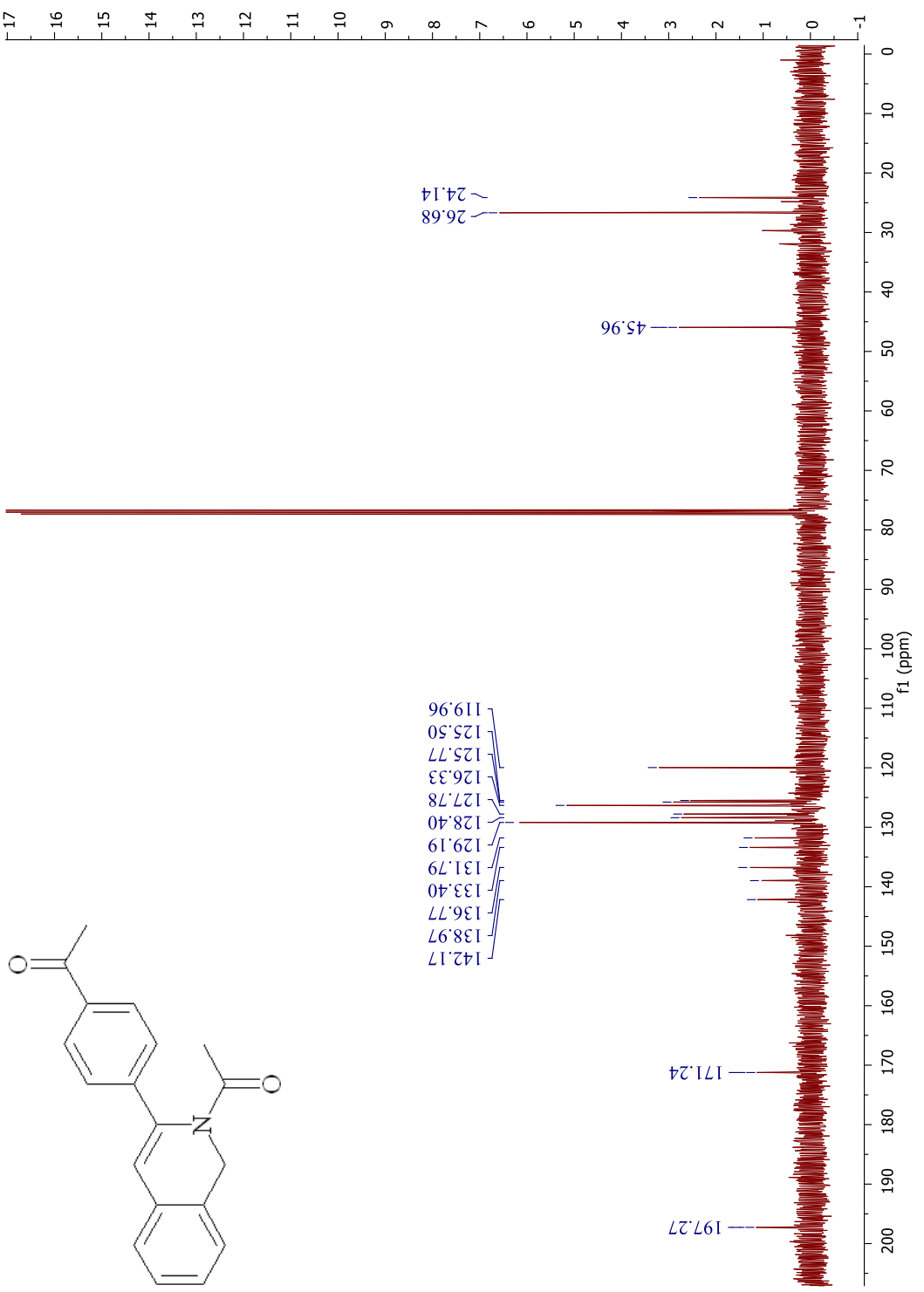
197.27
171.24
142.17
138.97
136.77
133.40
131.79
129.19
128.40
127.78
126.33
125.77
125.50
119.96
45.96
26.68
24.14
f1 (ppm)

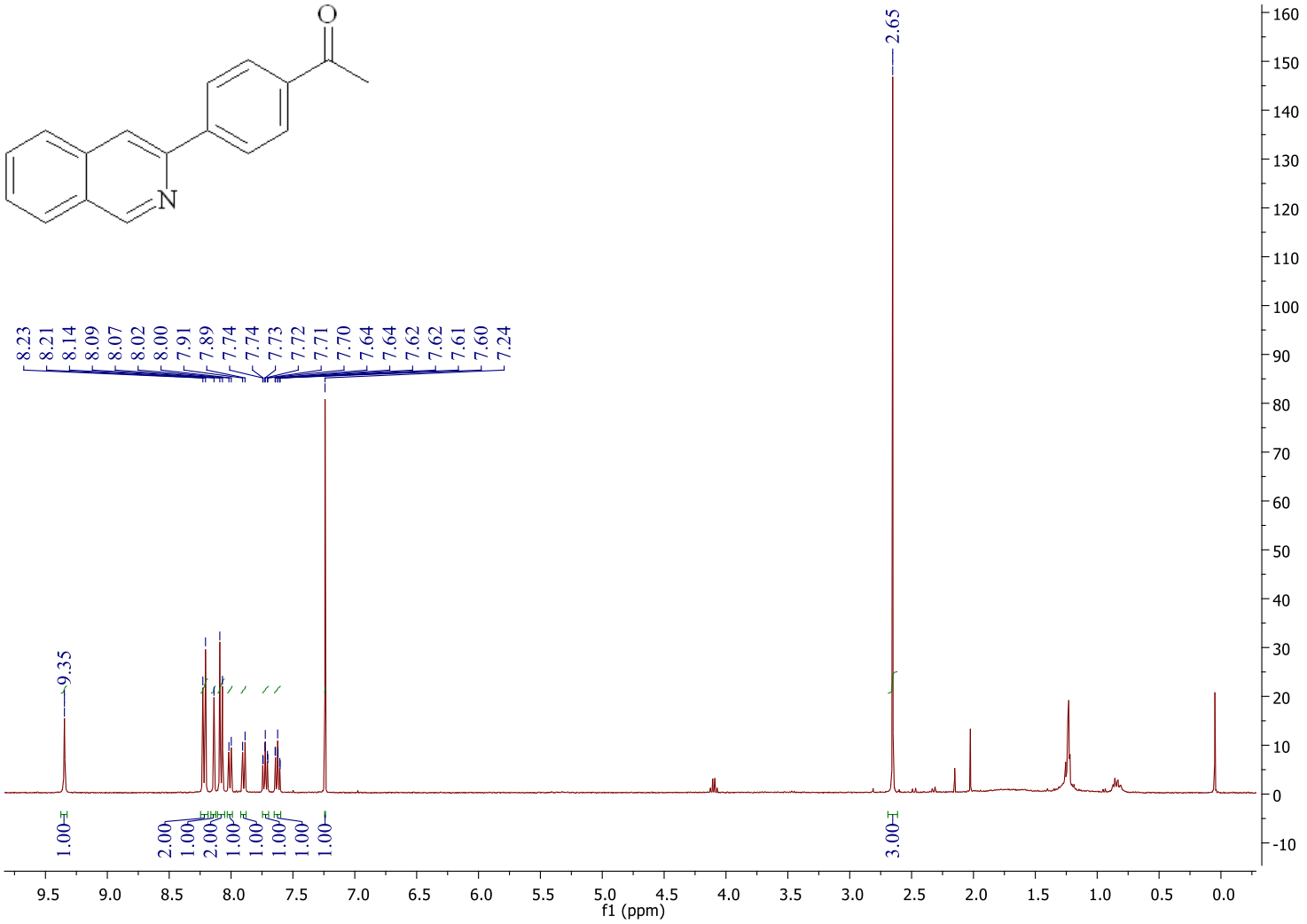
O
N
8.23
8.21
8.14
8.09
8.07
8.02
8.00
7.91
7.89
7.74
7.74
7.73
7.72
7.71
7.70
7.64
7.64
7.62
7.62
7.61
7.60
7.24
9.35
2.65
1.00
2.00
1.00
2.00
1.00
1.00
1.00
1.00
3.00
f1 (ppm)

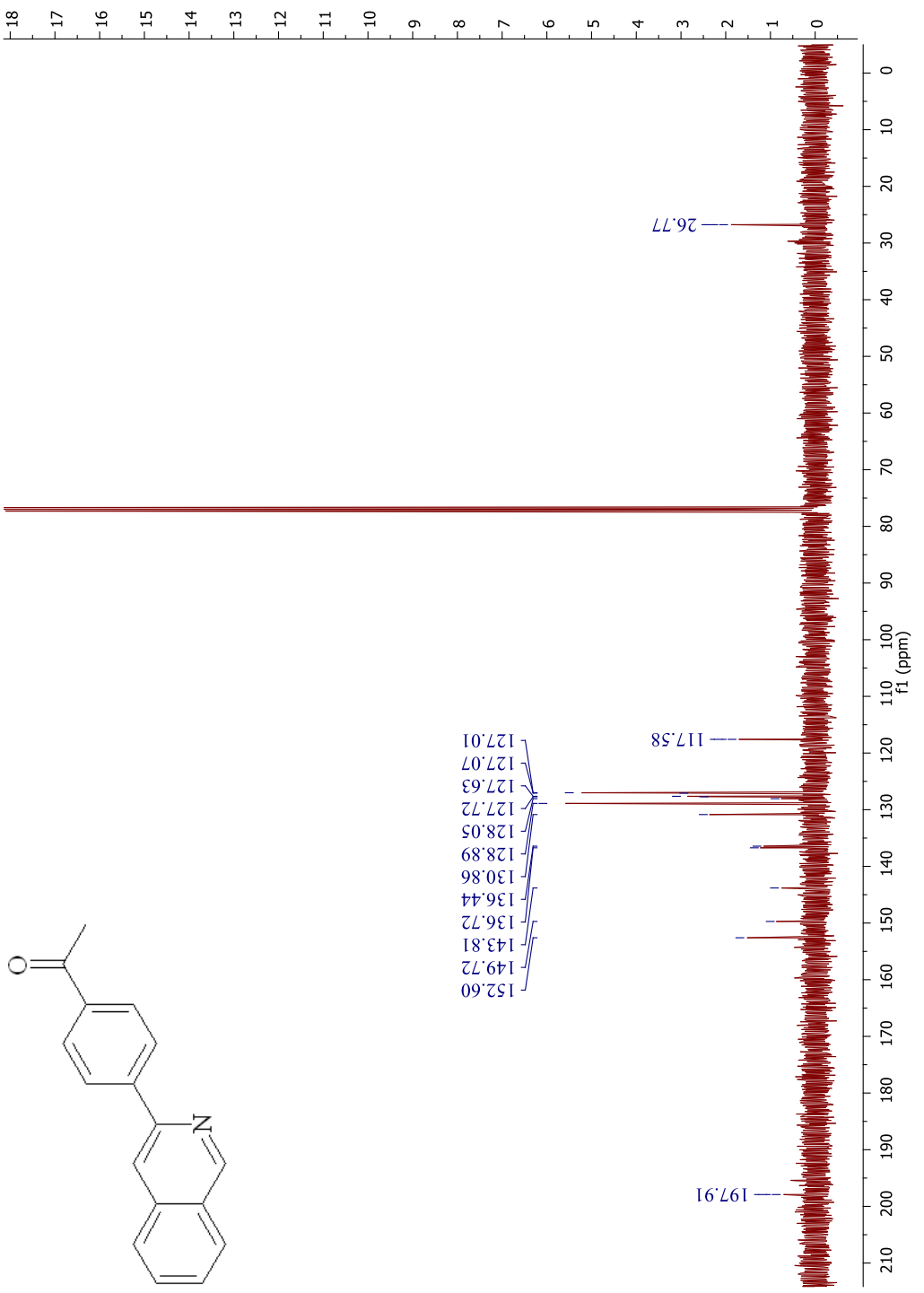
197.91
152.60
149.72
143.81
136.72
136.44
130.86
128.89
128.05
127.72
127.63
127.07
127.01
117.58
26.77
f1 (ppm)
O
N

APPENDIX D

MASS SPECTRUMS OF REACTANTS AND PRODUCTS

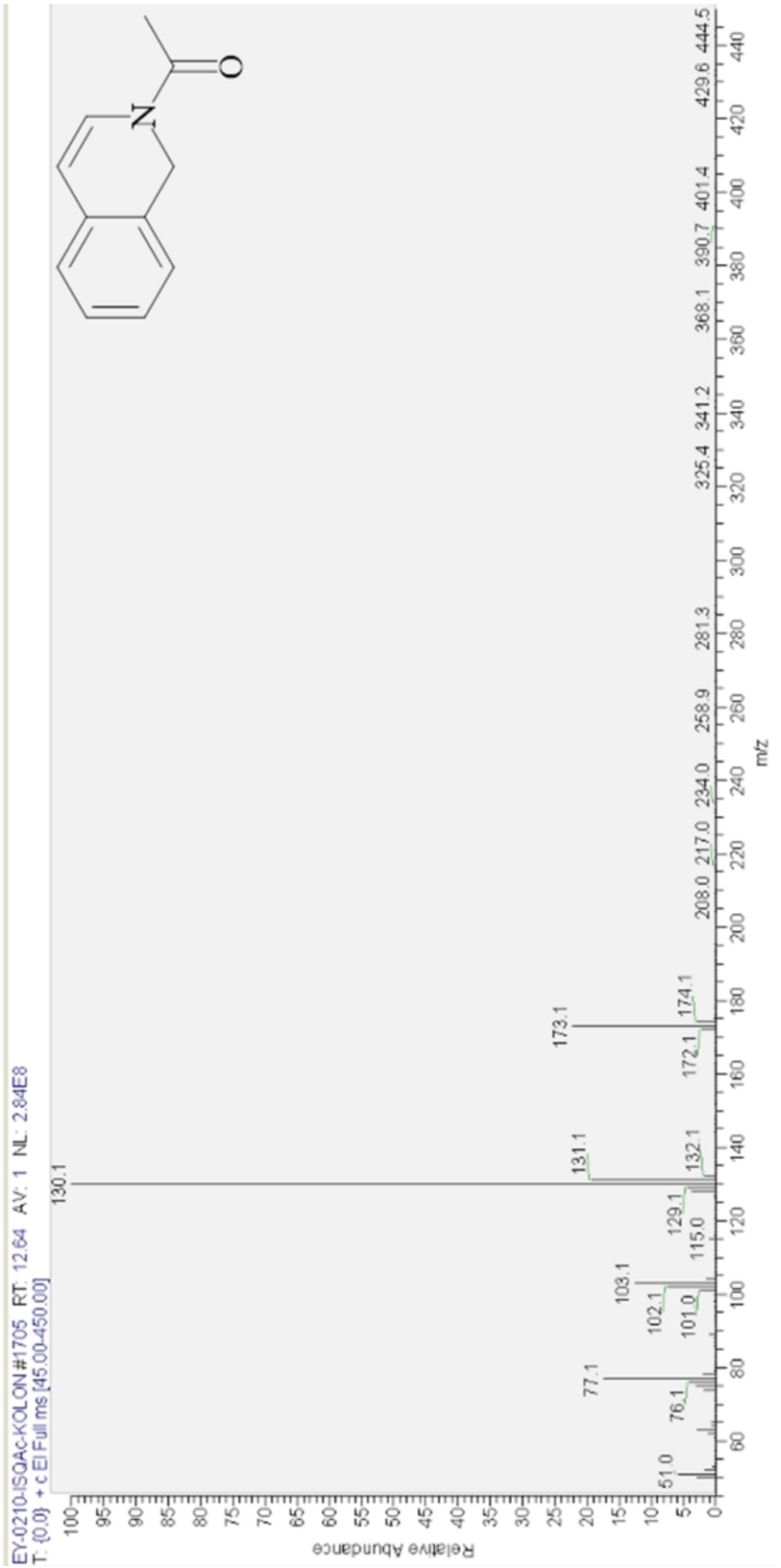
EY-0210-ISQAc-KOLON #1705 RT: 12.64 AV: 1 NL: 2.84E8
T: {0,0} + c EI Full ms [45.00-450.00]
Relative Abundance
m/z
130.1
131.1
173.1
77.1
103.1
102.1
101.0
129.1
115.0
132.1
172.1
174.1
76.1
51.0
O
N

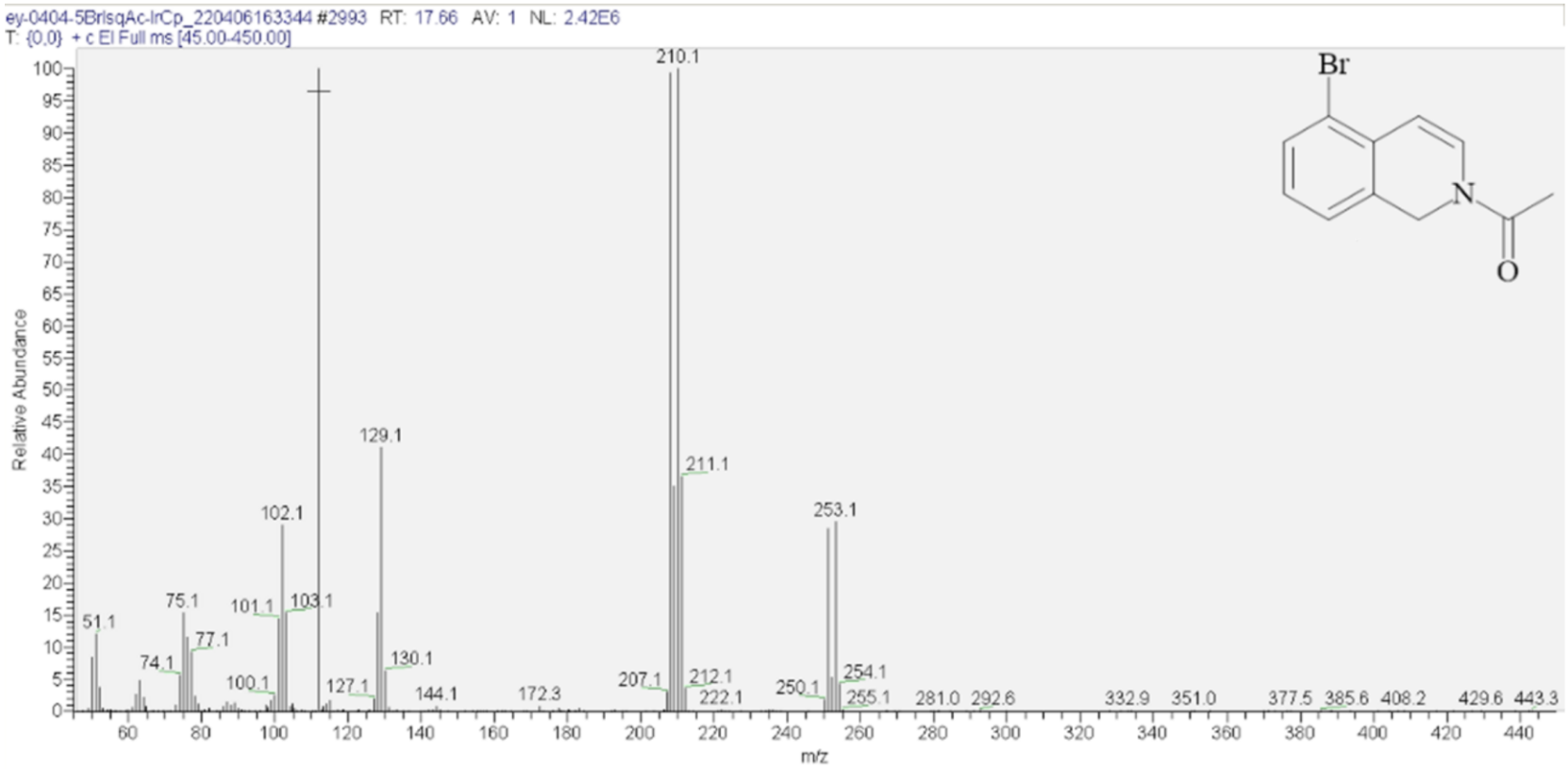
ey-0404-5BrisqAc-IrCp_220406163344 #2993 RT: 17.66 AV: 1 NL: 2.42E6
T: {0,0} + c EI Full ms [45.00-450.00]
Relative Abundance
m/z
Br
N
O
210.1
129.1
211.1
253.1
102.1
75.1
101.1
103.1
51.1
77.1
74.1
130.1
100.1
127.1
144.1
172.3
207.1
212.1
222.1
250.1
254.1
255.1
281.0
292.6
332.9
351.0
377.5
385.6
408.2
429.6
443.3

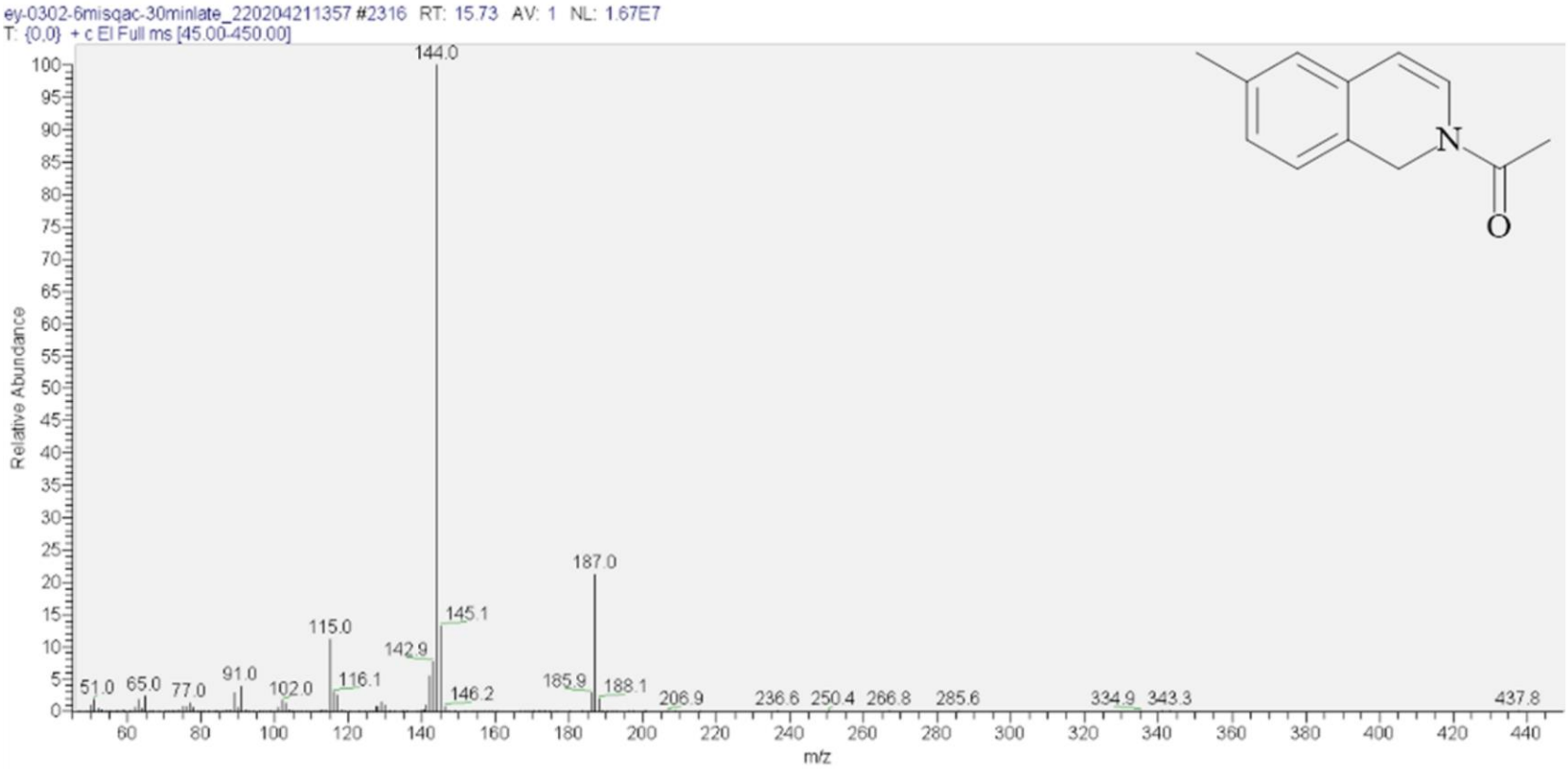
ey-0302-6misqac-30minlate_220204211357 #2316 RT: 15.73 AV: 1 NL: 1.67E7
T: {0,0} + c EI Full ms [45.00-450.00]
Relative Abundance
m/z
144.0
187.0
145.1
115.0
142.9
91.0
51.0
65.0
77.0
102.0
116.1
146.2
185.9
188.1
206.9
236.6
250.4
266.8
285.6
334.9
343.3
437.8
N
O

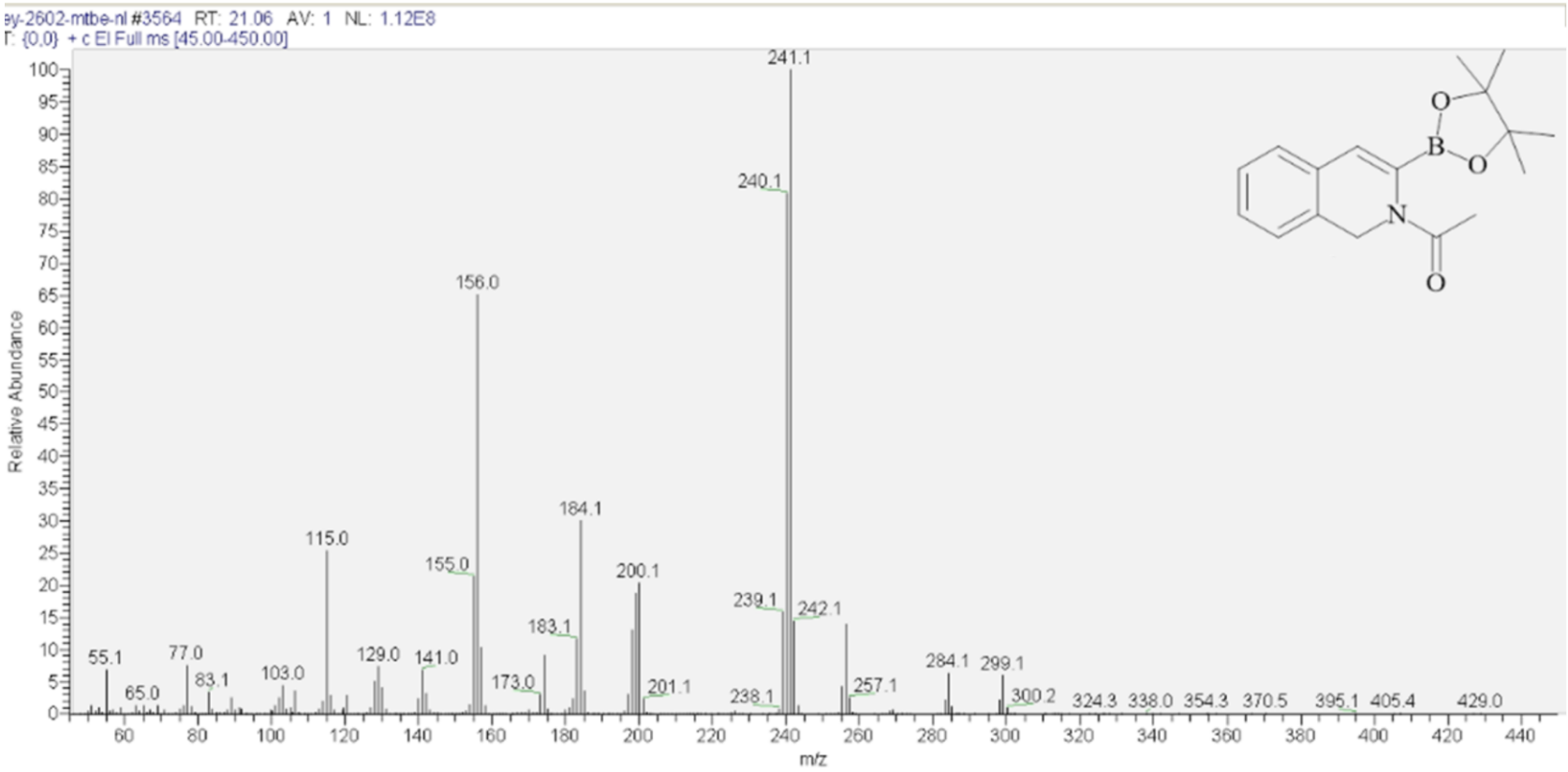
ey-2602-mtbe-nl #3564 RT: 21.06 AV: 1 NL: 1.12E8
T: {0,0} + c EI Full ms [45.00-450.00]
Relative Abundance
m/z
241.1
240.1
156.0
115.0
184.1
155.0
200.1
239.1
242.1
183.1
55.1
77.0
83.1
65.0
103.0
129.0
141.0
173.0
201.1
238.1
257.1
284.1
299.1
300.2
324.3
338.0
354.3
370.5
395.1
405.4
429.0
O
B
O
N
O

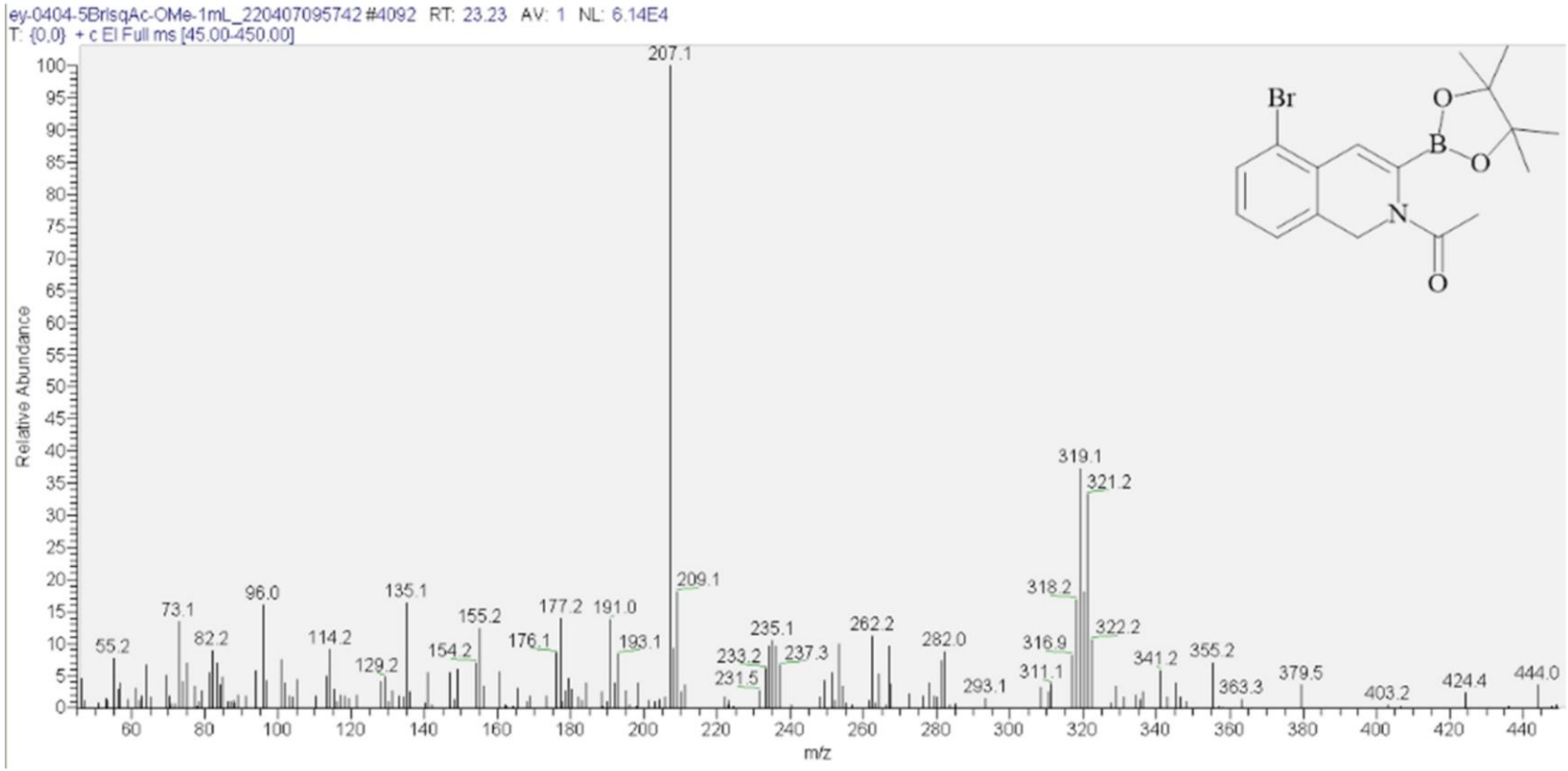
ey-0404-5BrisqAc-OMe-1mL_220407095742 #4092 RT: 23.23 AV: 1 NL: 6.14E4
T: {0,0} + c EI Full ms [45.00-450.00]
Relative Abundance
m/z
Br
O
B
O
N
O
207.1
319.1
321.2
209.1
318.2
322.2
96.0
73.1
135.1
155.2
177.2
191.0
82.2
114.2
176.1
193.1
235.1
262.2
282.0
55.2
154.2
129.2
233.2
237.3
316.9
341.2
355.2
231.5
311.1
293.1
363.3
379.5
403.2
424.4
444.0

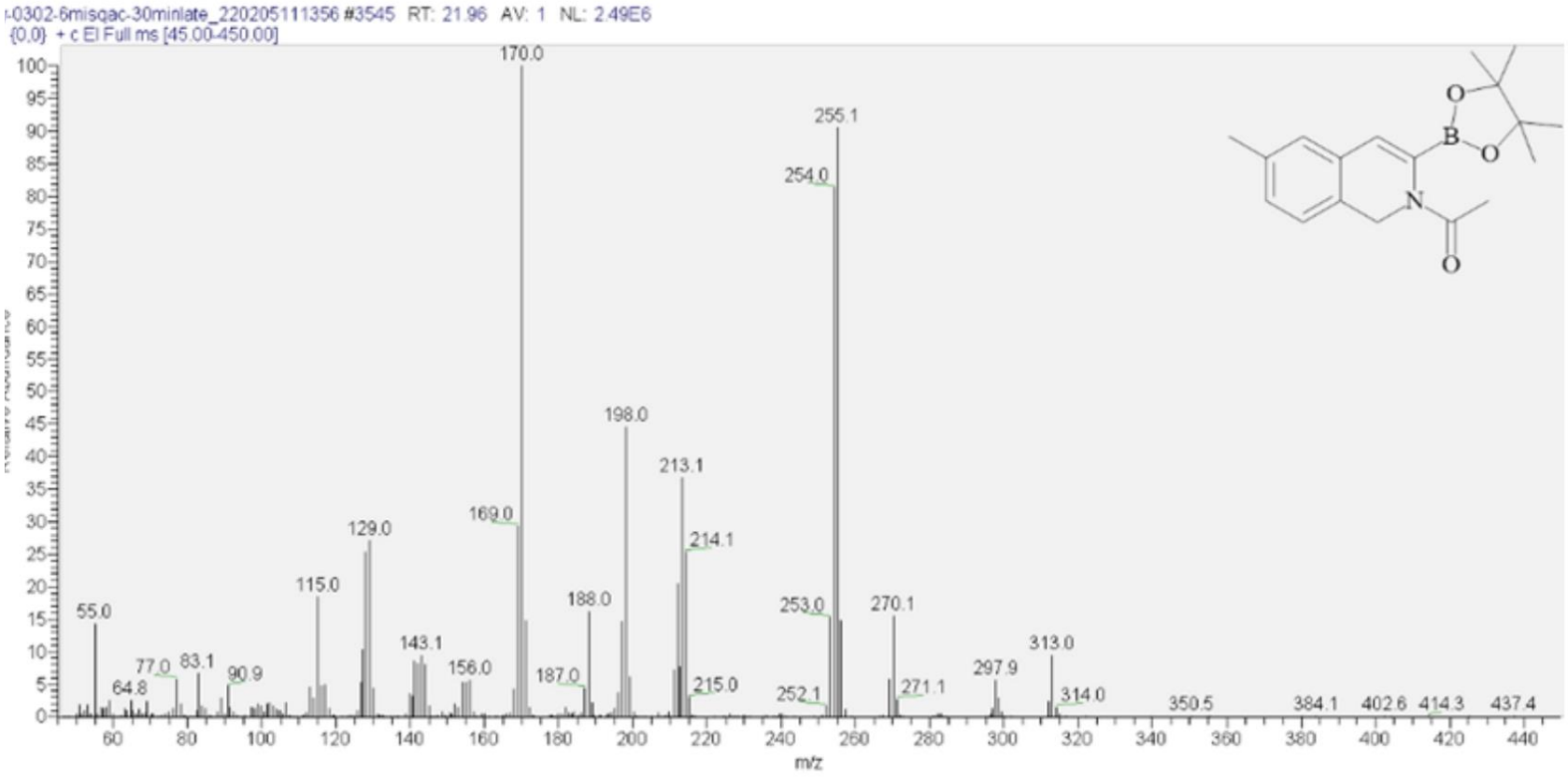
-0302-6misqac-30minlate_220205111356 #3545 RT: 21.96 AV: 1 NL: 2.49E6
{0,0} + c EI Full ms [45.00-450.00]
170.0
255.1
254.0
198.0
213.1
169.0
129.0
214.1
115.0
188.0
253.0
270.1
55.0
143.1
313.0
77.0
83.1
156.0
297.9
64.8
90.9
187.0
215.0
252.1
271.1
314.0
350.5
384.1
402.6
414.3
437.4
m/z
O
B
O
N
O

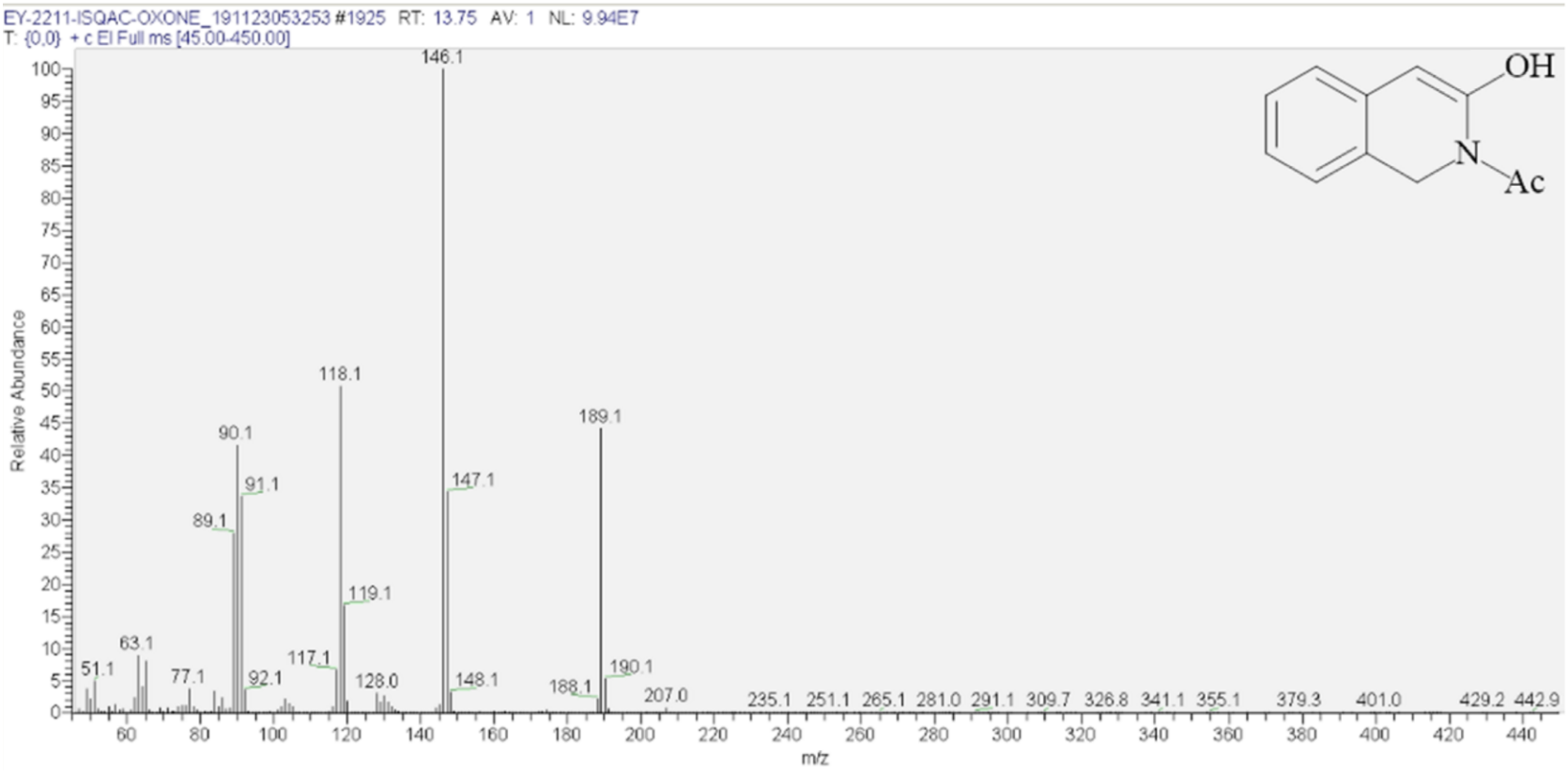
EY-2211-ISQAC-OXONE_191123053253 #1925 RT: 13.75 AV: 1 NL: 9.94E7
T: {0,0} + c EI Full ms [45.00-450.00]
Relative Abundance
m/z
146.1
118.1
189.1
90.1
91.1
147.1
89.1
119.1
63.1
51.1
77.1
92.1
117.1
128.0
148.1
188.1
190.1
207.0
235.1
251.1
265.1
281.0
291.1
309.7
326.8
341.1
355.1
379.3
401.0
429.2
442.9
OH
N
Ac

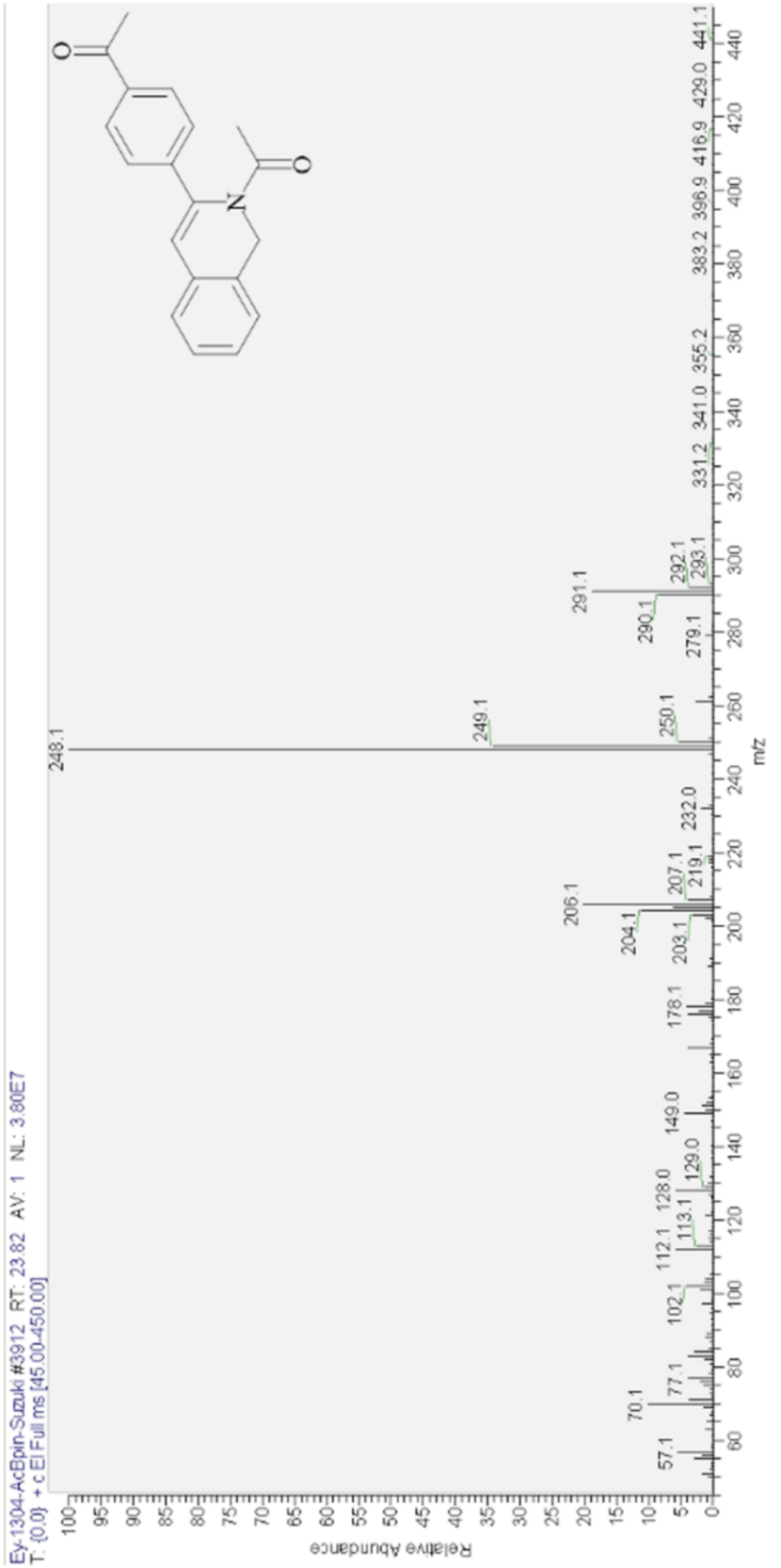
Ey-1304-AcBpin-Suzuki #3912 RT: 23.82 AV: 1 NL: 3.80E7
T: {0,0} + c EI Full ms [45.00-450.00]
Relative Abundance
m/z
248.1
249.1
250.1
291.1
206.1
204.1
70.1
77.1
102.1
112.1
128.0
149.0
178.1
O
N
O

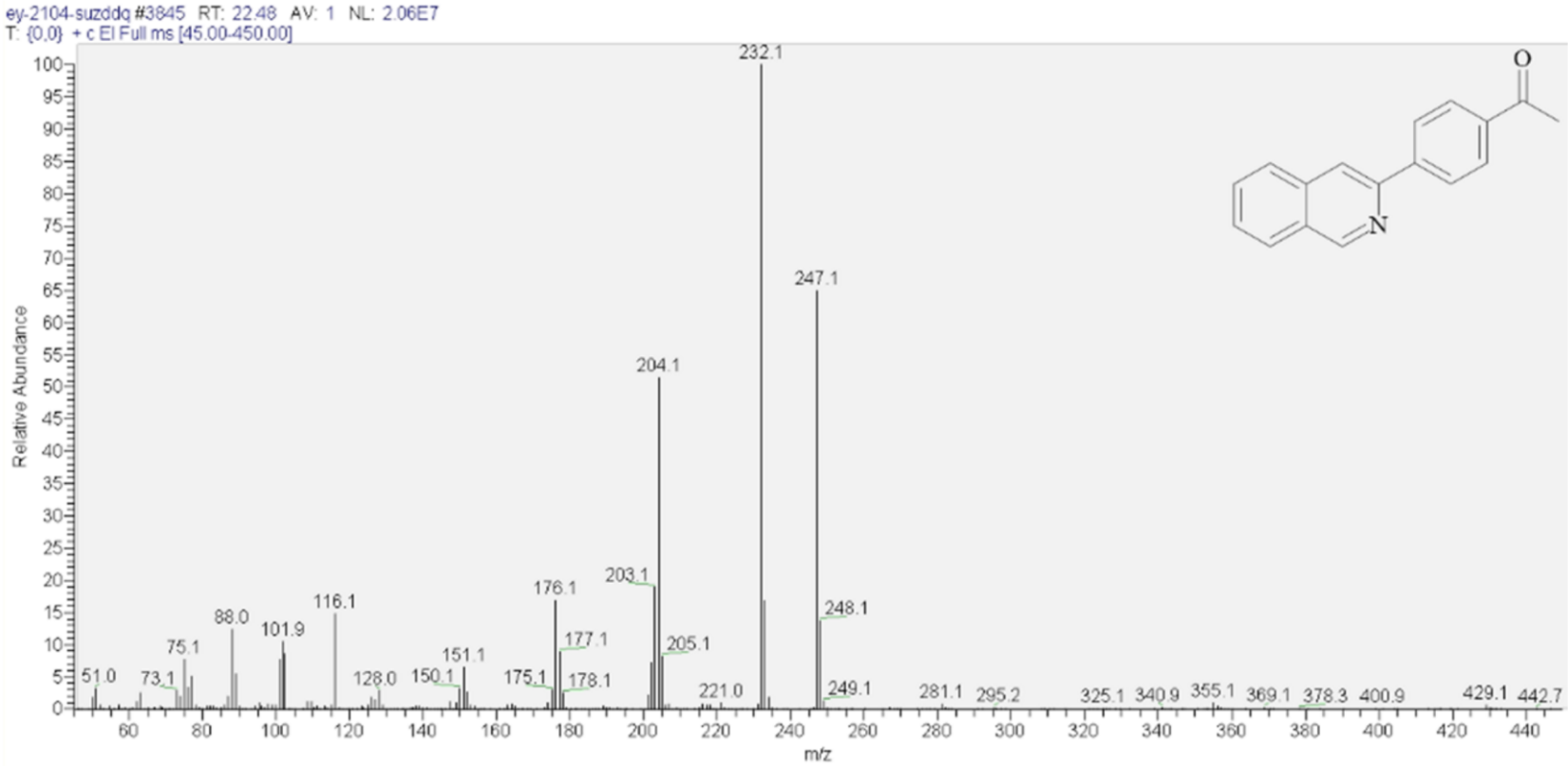
ey-2104-suzddq #3845 RT: 22.48 AV: 1 NL: 2.06E7
T: {0,0} + c EI Full ms [45.00-450.00]
Relative Abundance
m/z
232.1
247.1
204.1
203.1
176.1
116.1
88.0
101.9
75.1
151.1
248.1
205.1
177.1
51.0
73.1
128.0
150.1
175.1
178.1
221.0
249.1
281.1
295.2
325.1
340.9
355.1
369.1
378.3
400.9
429.1
442.7
O
N